Development of fluorescent sensors for reactive nitrogen species like nitric oxide and nitrite ion

A Dissertation submitted to the
Indian Institute of Technology Guwahati as
Partial fulfillment for the Degree of
Doctor of Philosophy in Chemistry

Submitted by

Kanhu Charan Rout
(Roll No. 10612216)

Supervisor

Prof. Biplab Mondal

Department of Chemistry
Indian Institute of Technology Guwahati

July, 2015

Dedicated to my family and friends

Statement

I hereby declare that this thesis entitled "**Development of fluorescent sensors for reactive nitrogen species like nitric oxide and nitrite ion**" is the outcome of research work carried out by me under the supervision of Prof. Biplab Mondal, in the Department of Chemistry, Indian Institute of Technology Guwahati, India.

In keeping with the general practice of reporting scientific observations, due acknowledgements have been made whenever work described here has been based on the findings of other investigators.

July, 2015 **Kanhu Charan Rout**

Certificate

This is to certify that Mr Kanhu Charan Rout has been working under my supervision since July, 2010 as a regular Ph. D. Student in the Department of Chemistry, Indian Institute of Technology, Guwahati. I am forwarding his thesis entitled **"Development of fluorescent sensors for reactive nitrogen species like nitric oxide and nitrite ion"** being submitted for the Ph. D. degree.

I certify that he has fulfilled all the requirements according to the rules of this institute regarding the investigations embodied in his thesis and this work has not been submitted elsewhere for a degree.

July, 2015 **Biplab Mondal**

Acknowledgements

I would like to thank my supervisor, Prof. Biplab Mondal for his continuous help and guidance during my research work. He provided me the opportunity and resources to work on one of the most interesting field of chemistry. He always helped me to learn the chemistry, inspiring me to do my best and making sure I am progressing along a forward path. It is those things that have given me the most confidence in my scientific abilities.

I would like to acknowledge my sincere gratitude to all my doctoral committe members Prof. Bhisma Kumar Patel, Dr. Debasis Manna, Prof. Aiyagari Ramesh for their insightful advice and valuable suggestions. I am also grateful to entire faculty and staff of the Department of Chemistry, Indian Institute of Technology Guwahati for providing a wonderful work atmosphere throughout this period.

I would like to thank my labmates Amardeep-da, Moushumi-didi, Pankaj-da, Apurba-da, Aswini-da, Vikash, Somnath, Hemanta, Kuldeep, Soumen, and Baisakhi for their support and help as well as for making a pleasant environment in the laboratory to work.

I thank all the masters and summer research fellows of my lab, Tulika, Pritam, Ivy, Narayani, Najmul, Soham, Sayantani, Arpan, Hemrupa, Tarali, Ayushree, Nimisha, Samarjit, Bhagyasmeeta, Arnab, Rini, Munmi, Dikshita, Banashree and Shyamalee to whom I have the opportunity to work.

I would like to give my special thanks to Mr Sumit Chaturvedi from Department of Biotechnology, Aligarh Muslim University for helping me in biological image study of my thesis.

The financial support from Indian Institute of Technology, Guwahati for the research fellowship is duly acknowledged.

Finally I would like to thank my family members, without their love and support this work would not have been completed.

July, 2015 **Kanhu Charan Rout**

Contents

Synopsis

The thesis entitled, "**Development of fluorescent sensors for reactive nitrogen species like nitric oxide and nitrite ion**" is divided into five chapters.

Chapter 1: **Introduction**

Nitric oxide (NO) is produced in biological systems by nitric oxide synthases (NOS).[1-3] It is now well-established that NO is an important signaling agent in the immune, cardiovascular, and nervous system.[4-6] However, the mechanisms by which NO performs its diverse biological roles remain elusive. To understand the origin, activities, and biological functions of NO there have been continuous search for methods and tools that can sensitively and selectively probe it in biological systems.[7-11] A NO sensor needs to have several requirements to be useful in biological systems, e.g. it should be biocompatible, non-toxic, specific, fast and can detect NO directly. Fluorescence techniques have been found as the most suitable one for sensing NO because of their sensitivity and high spatiotemporal resolution. [12-14] Since the early examples of fluorescence-based NO sensors such as *o*-diaminonaphthalene (DAN) and *o*-diaminofluoresceins (DAFs), a number of fluorescent probes have been reported till date.[15-28] Reduction of Cu(II) centre by NO has been utilized to develop fluorescent sensors. The quenched fluorescence intensity of a fluorescent ligand (FL) upon complexation with paramagnetic Cu(II), restoring back after the reduction of Cu(II) to Cu(I) by NO. The facile and faster reduction of Cu(II) to Cu(I) is one of the major criteria for this detection process. Hence the development of suitable Cu(II) complexes with fluorogenic ligand frameworks are very important. On the other hand, quantitative NO measurement via fluorimetry is a challenging task because of the lack of probes that display high specificity. A very high specificity for NO could be achieved if the chromophore/fluorophore of the probe is not assembled until the assembly process is triggered by the unique reactivity of NO. Moreover, an increase in conjugation would be expected to yield an advantageous red-shifted turn on

signal. In this direction second chapter of this thesis, describes a mechanism for NO detection with a framework, which displays a rapid and linear response to NO with turn on fluorescence signal from dark background. Chapter 3 describes the fluorescence based NO detection of a copper(II) complex of naphthol derivative. The development of a copper(II) complex as bio-compatible NO sensor has been described in chapter 4.

On the other hand, nitrite ions are not very well known to reduce Cu(II) to Cu(I). In Cu(II) complexes of ligands having α-β unsaturated ketone framework, it has been found that Cu(II) centre undergoes reduction by NO_2^-. This phenomenon may be utilized to develop selective sensor for NO_2^- like NO. Chapter 5 describes the examples of selective NO_2^- sensors based on the reduction of Cu(II) by NO_2^- ion methodology.

Chapter 2: **Selective chromogenic and fluorogenic probe for nitric oxide from dark background**

Sodium 5-aminonaphtalene-1-sulfonate (**ANS**) and Sodium 6-amino-4-hydroxynaphthalene-2-sulfonate (**AHS**) were found to undergo very fast reaction with NO in aerobic condition to produce **AZO-ANS** and **AHS-OH** respectively.

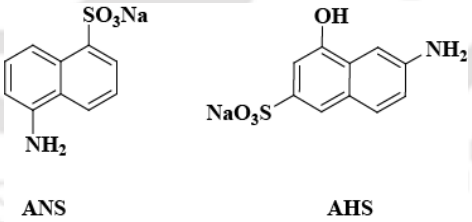

ANS AHS

Figure 2.1: Fluorophores used for the present study.

In UV-visible spectroscopy upon addition of NO with **ANS** in an aerobic condition, a new band around 480 nm slowly developed (Figure 2.2). The new band at 480 nm was attributed to the formation of new molecule **AZO-ANS**. The mechanism is shown in scheme 2.1.

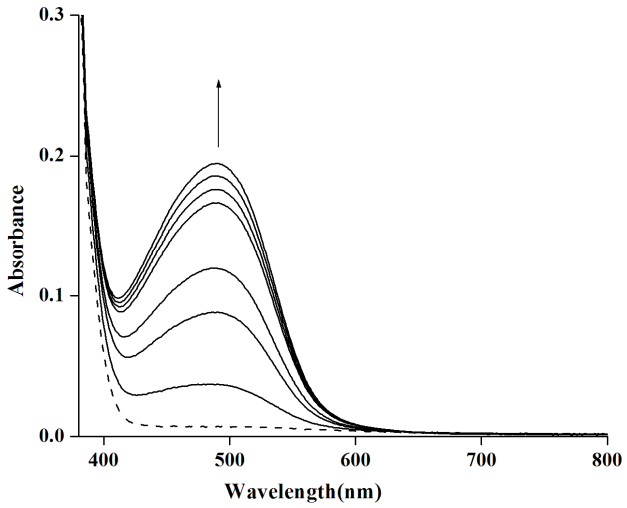

Figure 2.2: UV-visible spectra of **ANS** (dashed line) and after addition of NO (solid lines) in aerobic condition in methanol medium.

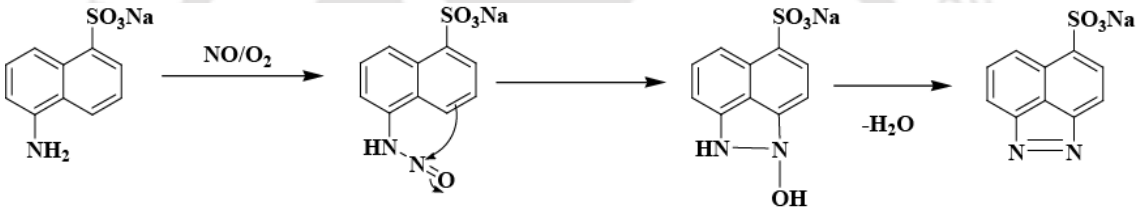

AZO-ANS

Scheme 2.1

ANS has an absorption band with λ_{max} at 335 nm in methanol solution. Upon excitation at 335 nm, it shows significant fluorescence emission centred at 475 nm in methanol at room temperature. The quantum yield was found to be 0.237 in methanol with respect to quinine sulphate. The fluorescence emission band of **ANS** centred at 475 nm was found to disappear upon addition of NO (Figure 2.3, a). When excited at 480 nm, a significant fluorescence enhancement of 8 fold at 580 nm was observed from the dark background (Figure 2.3, b). This was attributed to **AZO-ANS**. To study the selectivity of the probe with the other competitive reactive oxygen and nitrogen species, the fluorescence study has been done with ~ 100 fold excess of H_2O_2, KO_2, NO_2^-, NO_3^- however, no detectable fluorescence was observed in any case suggesting a high selectivity towards NO.

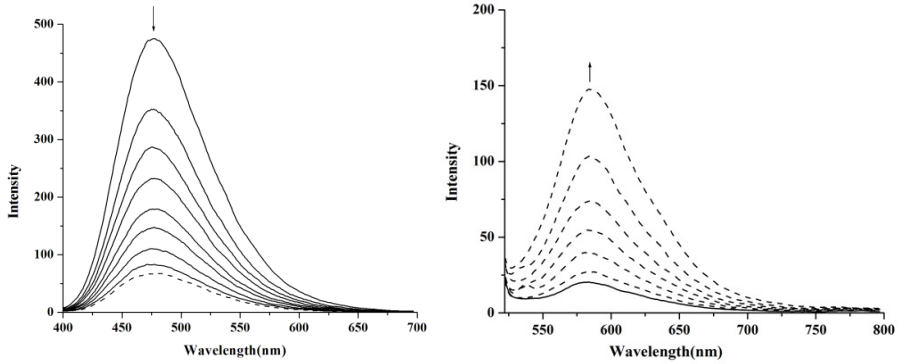

(**a**) (**b**)

Figure 2.3: (**a**) Fluorescence spectra of **ANS** (solid line) (λ_{ex}, 335 nm) and after addition of 1eq of NO (dashed line) in methanol medium. (**b**) Fluorescence enhancement (λ_{ex}, 480 nm) of **ANS** before (solid line) and after addition of NO (dashed lines) in aerobic condition in methanol medium.

On the other hand fluorophore **AHS** shows an absorption band at 320 nm in the UV-visible spectroscopy in methanol solution. A color change from light-yellow to deep-red was immediately observed after addition of NO gas into a solution of **AHS** in methanol. In UV-visible spectroscopy addition of NO in aerobic condition, developed a new band at 450 nm in methanol solution. This band was presumably due to the formation of N-nitrosamine intermediate. Immediately, the band at 450 nm disappeared and a new band around 530 nm slowly developed (Figure 2.4). The red shifting of the absorption wavelength was due to the formation of a new molecule as shown in scheme 2.2.

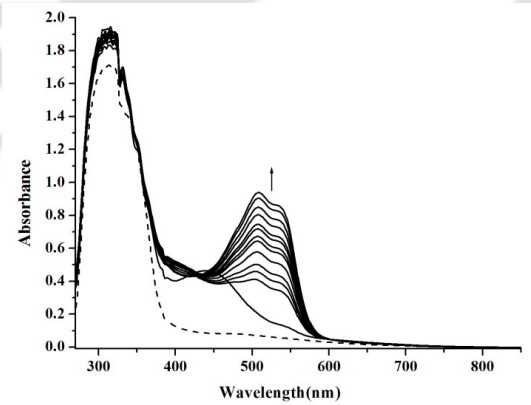

Figure 2.4: UV-visible spectra of **AHS** (dashed line) and after addition of NO in aerobic condition (solid lines) in methanol medium.

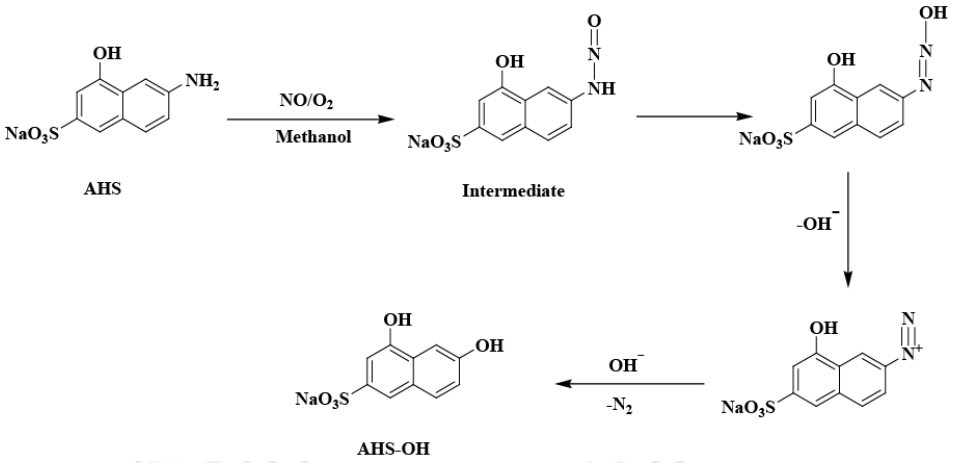

Scheme 2.2

AHS has an absorption wavelength at 320 nm. Upon excitation at 320 nm, it shows significant fluorescence emission centred at 410 nm in methanol or water at room temperature. The quantum yield was found to be 0.207 and 0.254, in methanol and water respectively. The fluorescence emission band of **AHS** centred at 410 nm was found to disappear upon addition of NO (Figure 2.5, a). But immediately fluorescence starts appearing from a dark background at 350 nm (Figure 2.5, b).

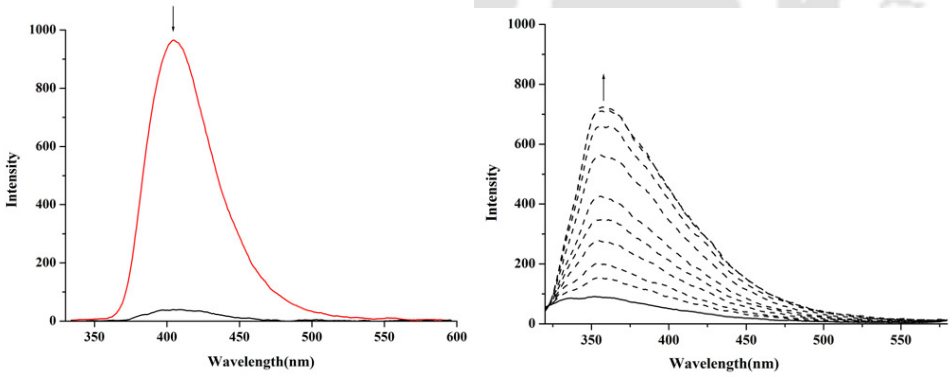

(**a**) (**b**)

Figure 2.5: (**a**) Fluorescence spectra of **AHS** (λ_{ex}, 320 nm) (red line) and after addition of 1eq of NO (black line) in methanol medium. (**b**) Fluorescence enhancement (λ_{ex}, 320 nm) of **AHS** before (solid line) and after addition of NO (dashed lines) in aerobic condition in methanol medium.

Thus, **ANS** and **AHS** selectively detect NO in an aerobic condition to form two new products which are characterized by different spectroscopic techniques. The fluorescence and UV-visible absorbance come from a dark background due to the formation of new molecules.

Chapter 3: **Fluorescence based nitric oxide detection of a copper(II) complex of naphthol derivative**

Cu(II) complex of 4-amino-3-hydroxy-1-naphthalene sulphonic acid (**AHNS**) was synthesized (Scheme 3.1). The complex was characterized by various spectroscopic analyses as well as by elemental analysis.

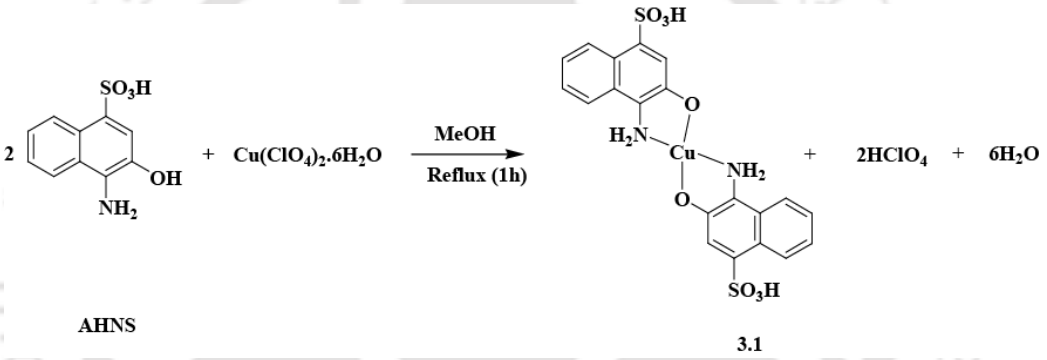

AHNS 3.1

Scheme 3.1

Solution conductivity measurement in methanol indicates the neutral nature of the complex **3.1**. The absence of perchlorate vibration in the FT-IR spectrum of complex **3.1** is also in accord with the phenolate binding of the ligand to metal center. Complex **3.1** in methanol shows an absorption at 480 nm (ε, 1016 M^{-1} cm^{-1}) in the UV-visible spectroscopy with strong intra-ligand transitions in the UV region. This 480 nm band is attributed to the phenolate → Cu^{II} charge transfer transition.

Addition of NO gas to a degassed methanol solution of complex **3.1** resulted in the shift of the band at 480 nm to 440 nm with the concomitant formation of other band at 617 nm, (Figure 3.1, a). The intensity of the band at 617 nm was found to decrease with time, indicating the presence of an unstable intermediate (Figure 3.1, b). Presumably, the

intermediate corresponds to [Cu^{II}-NO] species which decomposes to result in Cu(I) with simultaneous nitrosation of a substrate (e.g. solvent or ligand).

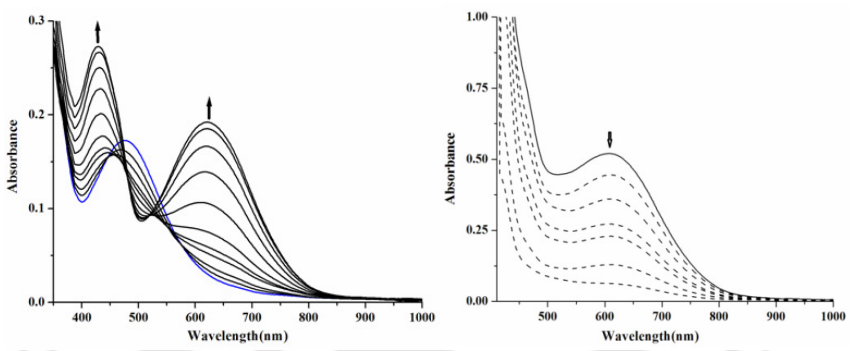

(**a**) (**b**)

Figure 3.1: (**a**) UV-visible spectra of complex **3.1** before (blue line) and after (black lines) purging NO in methanol. (**b**) UV-visible spectra of intermediate [Cu^{II}-NO] species (solid line) and it's decay (dashed lines) in methanol**.**

The formation of the [Cu^{II}-NO] intermediate was further supported from the solution FT-IR spectroscopic studies. In FT-IR spectroscopy, upon addition of NO to the methanol solution of complex **3.1,** a new strong frequency at 1650 cm^{-1} appeared which attributed to the coordinated NO stretching in the corresponding [Cu^{II}-NO] species (Figure 3.2).

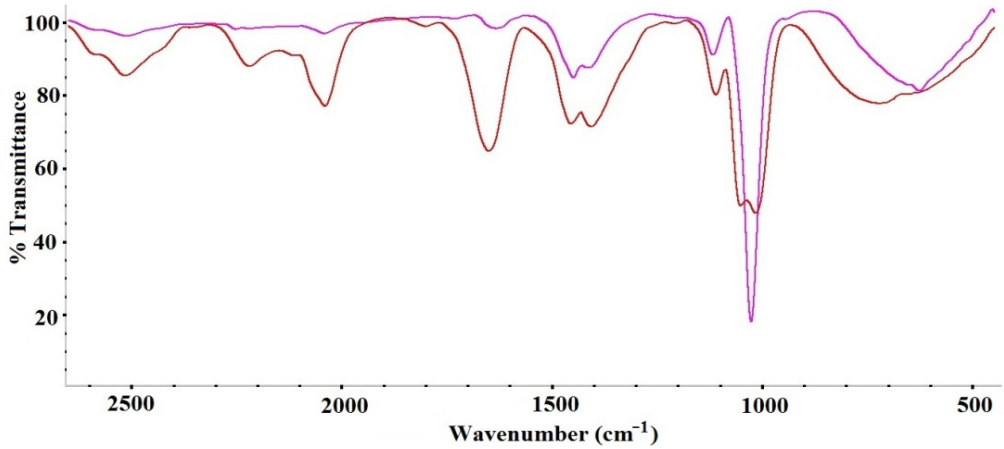

Figure 3.2: Solution FT-IR spectra of complex **3.1** before (magenta) and immediately after (red) purging NO gas in methanol.

This band disappeared with time indicating the unstable nature of the intermediate. It should be noted that NO in methanol gives band at 1610 cm^{-1} in solution FT-IR spectrum. The reduction was further confirmed by X-band EPR studies.

Removal of copper ion from the reaction mixture followed by isolation and characterization of the modified ligand suggests the formation of 4-amino-3-hydroxy-1-nitrosonaphthalene (Scheme 3.2).

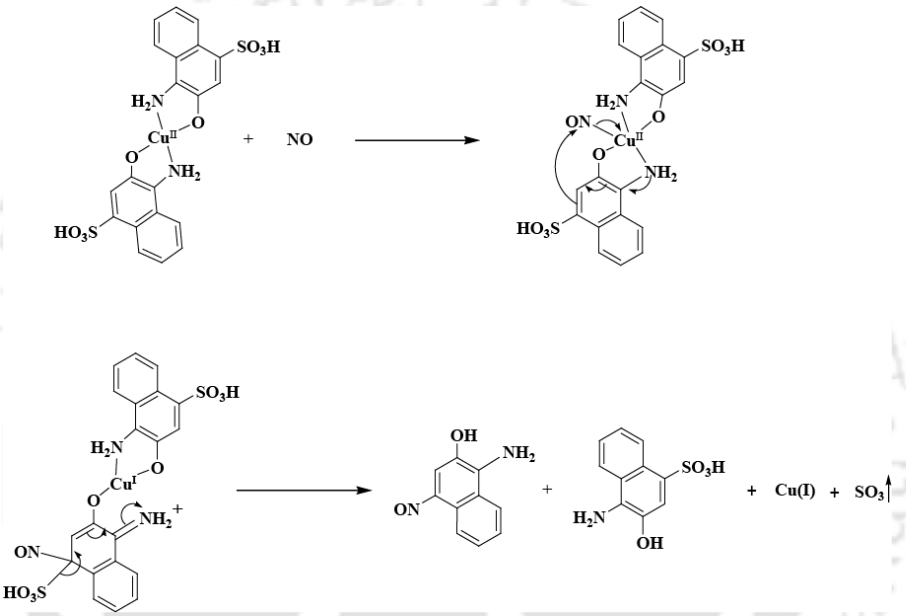

Scheme 3.2. Probable mechanism of the reaction

The formation of SO_3 in the reaction mixture was confirmed by trapping it in $BaCl_2$ solution. The free ligand was found to be fluorescent. Since the free ligand was not highly soluble in methanol, for fluorescence study the mono-sodium salt of the ligand (**NaAHNS**) was used. The fluorescence emission band of **NaAHNS** centered at 435 nm was found to disappear upon addition of equivalent amount of Cu(II) ion (Figure 3.3, a). Addition of NO gas to this solution restored the emission; however, much less intense. This is because of the formation of 4-amino-3-hydroxy-1-nitrosonaphthalene (Figure 3.3, b).

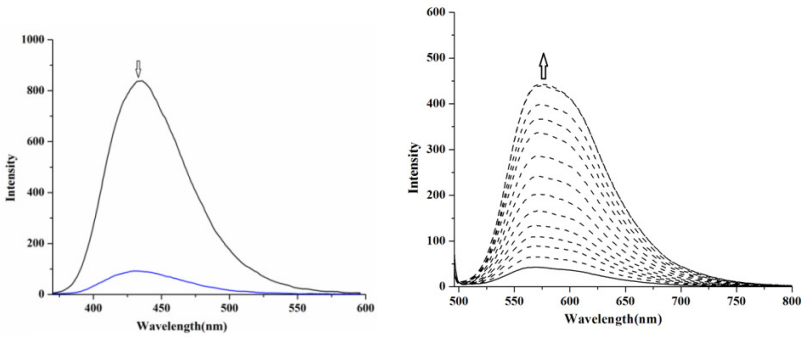

(**a**) (**b**)

Figure 3.3: (**a**) Fluorescence responses upon excitation at 350 nm for 20 μM solution of free ligand (black line) and after addition of 10 μM of $Cu(ClO_4)_2.6H_2O$ (blue line) in methanol. (**b**) Fluorescence enhancement upon excitation at 440 nm of 20 μM solution of complex **3.1** (solid line) and after addition of 1 equivalent of NO (dashed lines) in methanol with time.

Complex **3.1** reacts with NO in methanol solution to form [Cu^{II}-NO] intermediate species. This intermediate decomposes rapidly to offer Cu(I) and aromatic C-nitrosation reaction through desulphonation of the ligand. The C-nitroso product is responsible for fluorescence enhancement. Hence complex **3.1** can be used as a fluorescence based NO sensor.

Chapter 4: **Copper(II) complex as a selective turn on fluorosensor for nitric oxide and its intracellular application**

In this chapter a highly water soluble Cu(II) complex of a fluorophore ligand 4-(2-hydroxybenzylamino)-5-hydroxynaphthalene-2,7-disulfonic acid (**HBNS**) was synthesized and characterized.

The complex **4.1** was characterized by various spectroscopic analyses as well as by elemental analysis. Complex **4.1** in methanol shows an absorption at 460 nm (ε, 2,500 $M^{-1}cm^{-1}$) in UV-

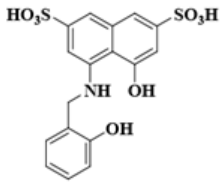

Figure 4.1: Ligand **HBNS** used for the present study.

visible spectroscopy with strong intra-ligand charge transfer bands. The 460 nm band is due to the phenolate-Cu(II) charge transfer transition. Solution conductivity shows the neutral nature of the complex. The absence of perchlorate vibration in the FT-IR spectrum also supports the phenolate binding of the ligand to copper center. The X-band EPR spectrum of the complex was recorded in methanol at 77 K and the calculated values are, $g_{\parallel}$, 2.402, $g_{\perp}$, 2.100 and $A_{\parallel}$, 122 × 10^{-4} cm^{-1} . The values confirm that Cu(II) is in square planar geometry. Addition of NO was found to induce reduction of Cu(II) to Cu(I). This has been evidenced by UV-visible and X-band EPR spectroscopic techniques (Figure 4.2, a and 4.2, b).

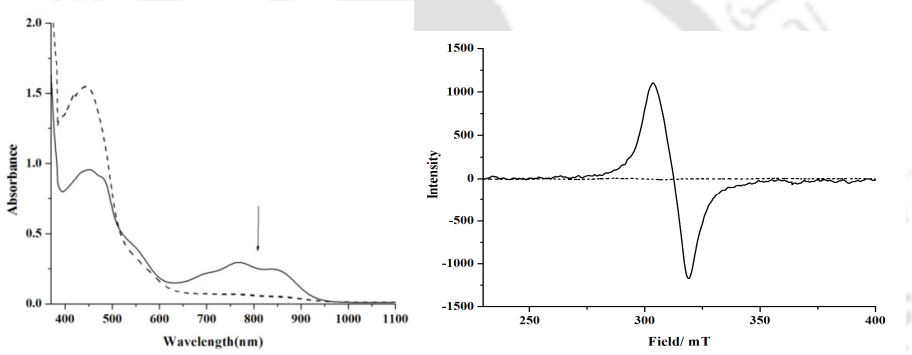

(**a**) (**b**)

Figure 4.2: (**a**) UV-visible spectra of complex **4.1** before (solid line) and after addition of NO (dashed line) in methanol. (**b**) X-band EPR spectra of complex **4.1** in methanol before (solid line) and after (dotted line) addition of NO at 298 K.

Ligand **HBNS** shows fluorescence emission centred at 410 nm upon excitation at 320 nm in methanol solution at room temperature. The quantum yield was found to be 0.21 in methanol with respect to quinine sulphate. The fluorescence emission of **HBNS** centred at 410 nm was found to quench significantly (90%) upon the addition of equivalent amount of Cu(II) ion in methanol medium (Figure 4.3, a). Addition of NO gas to this solution restored the emission intensity from a dark background (Figure 4.3, b). The blue shifting of the emission wave length was attributed to the modification of the ligand framework after reaction of the complex with NO gas. The restored intensity in the complex **4.1** starts appearing within 10

seconds of NO addition and becomes (9±1) fold increment of fluorescence intensity in 10 minutes.

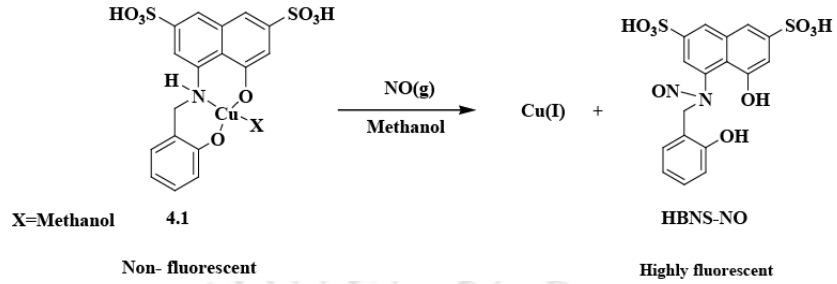

Scheme 4.1

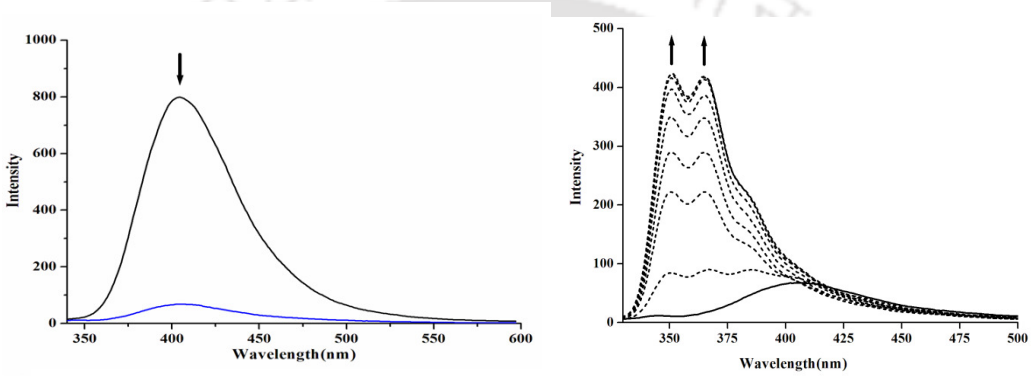

(**a**) (**b**)

Figure 4.3: (**a**) Fluorescence responses (λ_{ex}, 320 nm) for 20 µM solution of free ligand, (black line) and after addition of 20 µM of $Cu(ClO_4)_2.6H_2O$ in methanol (blue line). (**b**) Fluorescence responses (λ_{ex}, 320 nm) of deoxygenated methanol solution of complex **4.1** (20 µM) before (solid line) and after (dashed lines) purging of 1 equivalent of NO at 2, 4, 6, 8 and 10 minutes at 298 K.

The ability of complex **4.1** to detect NO encourages to study in *vitro*. SK-N-SH human neuroblastoma cell line was used for the present study as in this cell line cNOS can be activated by estrogen to produce NO. 17-*β* estradiol activated SK-N-SH cells were incubated with 10 µM complex **4.1**. On excitation at 320 nm, the activated cells without complex **4.1** did not show any fluorescence (Figure 4.4, A bottom); whereas the complex **4.1** incubated cells, after washing with cold PBS for three times, displayed significant fluorescence (Figures 4.4, B and 4.4, C).

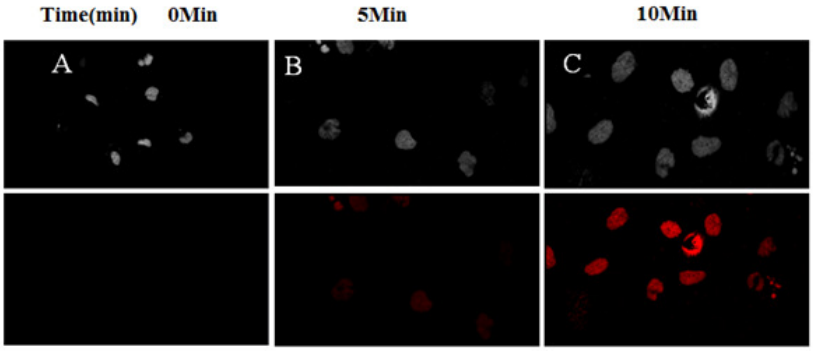

Figure 4.4: NO detection produced by cNOS. NO detection in SK-N- SH cells by complex **4.1**. Left to right, 10-min incubation of complex **4.1** (10 μM) and 0, 5, 10 min after co-treatment of complex **4.1** (10 μM) and 17-*β* estradiol (100 nM). Images were taken with a fluorescent microscope (Axio, HBU 50/ AC; Zeiss, Gottingen, Germany). (Top, phase contrast images; bottom, fluorescence images).

Thus complex **4.1** can be used as a fluorescence based NO sensor in methanol and water medium. The NO-triggered fluorescence enhancement of complex **4.1** arises by reduction of Cu(II) to Cu(I) with subsequent dissociation of the N-nitrosated fluorophore ligand from copper. The selective turn on fluorogenic nature of the complex is used to visualize endogenously produced NO in living cells.

Chapter 5: **Copper(II) complex as selective turn-on fluorescent probe for nitrite ion**

In this chapter Cu(II) complex, **5.1** with 3-(pyren-8-yl)-1-(pyridine-2-yl)prop-2-en-1-one (**PYAC**) was synthesized. The ligand **PYAC** was prepared by stirring a mixture of acetyl pyridine with 1-pyrenecarbaldehyde in presence of sodium hydroxide in ethanol. It was characterized by various spectral and elemental analyses. The X-ray single crystal structure of **PYAC** was determined (Figure 5.1).

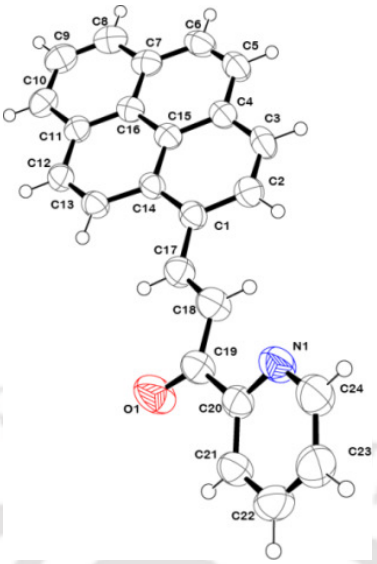

Figure 5.1: ORTEP diagram of ligand **PYAC** (50% thermal ellipsoid plot).

Complex **5.1** was prepared by stirring copper(II) perchlorate hexahydrate with equivalent amount of the ligand **PYAC** in acetonitrile (Scheme 5.1). The complex was characterized by spectroscopic and elemental analyses. Even after several attempts the X-ray quality crystals were not obtained.

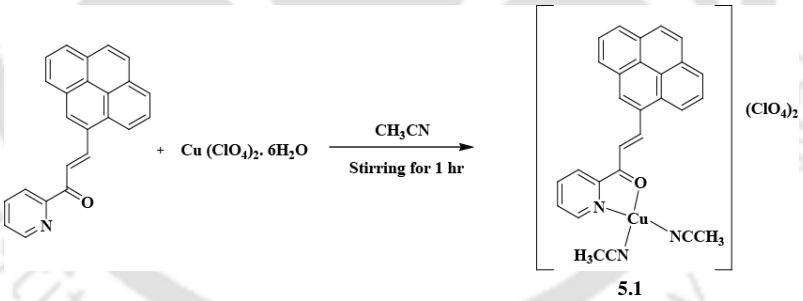

5.1

Scheme 5.1

Complex **5.1**, in acetonitrile solution displays absorption at 555 nm due to MLCT transition from the filled up *d*-orbital of the metal ion to the low lying π* orbital of the ligand. The absorptions at 425 and 377 nm were attributed to ligand based charge transfer transitions which were clear from the spectrum of the free ligand. In methanol, the MLCT band appeared at 530 nm. In FT-IR spectrum of complex **5.1**, the stretching frequency for C=O group appeared at 1596 cm^{-1} indicating that the C=O group is bonded to the metal ion. In X-

band EPR spectroscopy, the complex **5.1** displays signals at 77 K which are characteristic of square planar Cu(II). The calculated parameters are $g_{\parallel}$, 2.2555, $g_{\perp}$, 2.0842 and A, 124×10^{-4} cm^{-1}. Addition of aqueous nitrite solution to the acetonitrile solution of complex **5.1** was found to result in the immediate decrease of the intensity of 555 nm band in UV-visible spectrum (Figure 5.2).

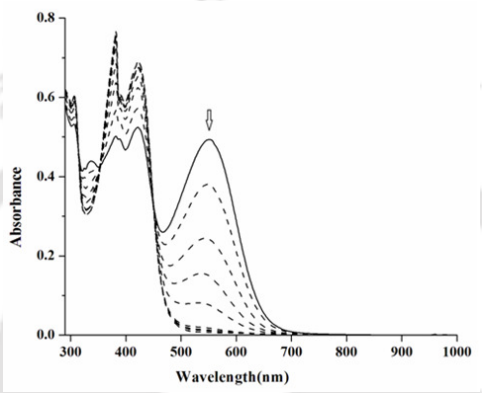

Figure 5.2: UV-visible spectra of complex **5.1** (solid line) and after addition of 0.5 equivalent of aqueous $NaNO_2$ (dashed lines) at 0-10 minutes time interval in acetonitrile.

In the FT-IR spectrum of complex **5.1**, a new stretching band at ~1384 cm^{-1} appeared after addition of nitrite (Figure 5.3). This has been assigned as the nitrate stretching frequency.

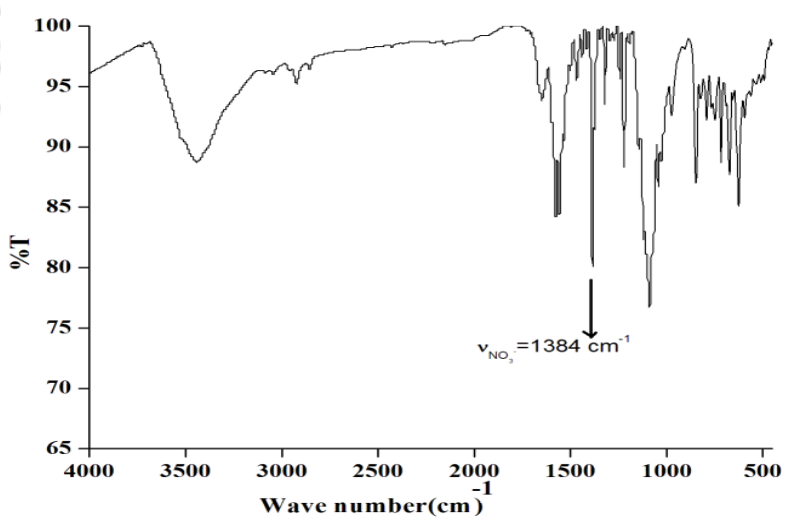

Figure 5.3: FT-IR spectrum of the crude product from the reaction of complex **5.1** with $NaNO_2$ in KBr pellet.

During the reaction Cu(II) is reduced to Cu(I) and nitrite ion (NO_2^-) ion is oxidized to nitrate (NO_3^-). Analysis of the reaction mixture revealed the formation of NO_3^- ion as the oxidation product. It should be noted that the reduction of Cu(II) to Cu(I) is one electron transfer process, whereas the oxidation of NO_2^- to NO_3^- involves two electron transfer. Thus, only 0.5 equivalent of nitrite ion is required for the reduction of Cu(II) center (eq. 5.1). This has been confirmed by titrating the solution of complex **5.1** with sodium nitrite (Figure 5.4).

$$2\,[LCu^{II}(CH_3CN)_2]^{2+} + NO_2^- + H_2O \longrightarrow 2\,[LCu^{I}(CH_3CN)_2]^{+} + NO_3^- + 2H^+ \quad \text{..... eq (5.1)}$$

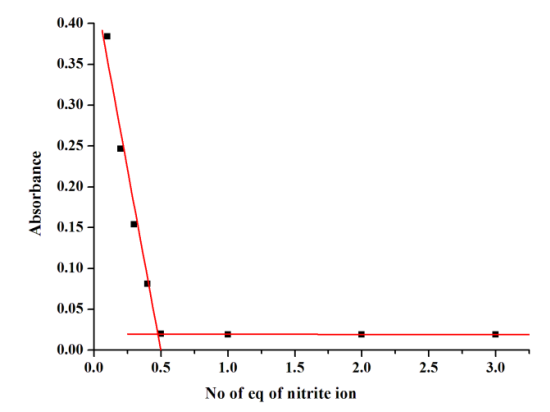

Figure 5.4: UV-visible titration plot for complex **5.1** with $NaNO_2$ in acetonitrile (considering the band at 555 nm).

Fluorescence spectroscopic study at 298 K suggested the significant quenching (> 90%) of fluorescence intensity of **PYAC** in presence of equivalent amount of Cu(II) owing to paramagnetic effect in acetonitrile or methanol solution (Figure 5.5, a).

Addition of 0.5 equivalent of NO_2^- solution to the complex was found to restore the quenched intensity instanteneously (Figure 5.5, b). This is attributed to the reduction of Cu(II) center by NO_2^-.

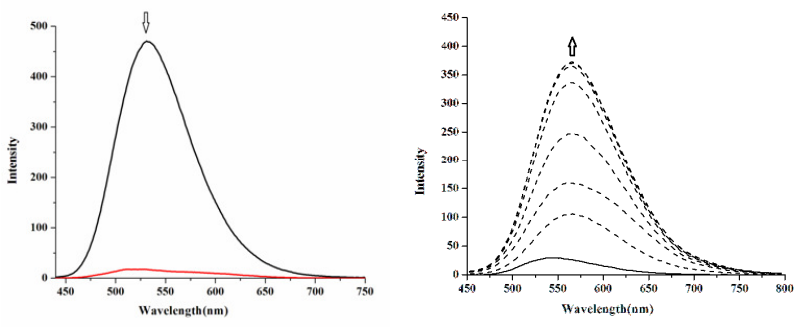

(**a**) (**b**)

Figure 5.5: (**a**) Fluorescence responses ($\lambda_{ex,}$ 425 nm) for 20 µM solution of **PYAC** (black line) and after addition of 20 µM $Cu(ClO_4)_2.6H_2O$ (red line) in acetonitrile. (**b**) Fluorescence enhancement ($\lambda_{ex,}$ 425 nm) by addition of $NaNO_2$ (0.5eq) with 10 µM complex **5.1** in acetonitrile.

Thus Cu(II) centre in the complex of **5.1** was found to be reduced by aqueous nitrite solution in acetonitrile solution. Simultaneous oxidation of the nitrite to nitrate was observed and water was found as the source of oxygen. This reduction methodology was utilized to develop fluorescence based selective sensor for nitrite ion.

References

1. Murad, F. *Angew. Chem. Int. Ed.* **1999**, *38*, 1856.

2. Moncada, S.; Palmer, R. M. J.; Higgs, E. A. *Pharmacol. Rev*. **1991**, *43*, 109.

3. Conner, E. M.; Grisham, M. B. Nitric Oxide: Biochemistry, Physiology, and Pathophysiology. *Methods Enzymol* **1995**, *7*, 3.

4. Ignarro, L. J. *Nitric Oxide Biology and Pathobiology,* 1st ed.; Academic Press: San Diego, 2000.

5. Garthwaite, J. E. *J. Neurosci.* **2008**, *27*, 2783.

6. Pluth, M. D.; Tomat E.; Lippard, S. J. *Annu. Rev. Biochem*. **2011**, *80*, 333.

7. Ye, X.; Rubakhin, S. S.; Sweedler, J. V. *Analyst* **2008**, *133*, 423.

8. Ghafourifar, P.; Parihar, M. S.; Nazarewicz, R..; Zenebe, W. J.; Parihar, A. In Nitric Oxide, Part F: Oxidative and Nitrosative Stress in Redox Regulation of Cell Signaling; Academic Press: New York, 2008, *440*, 317.

9. Hetrick, E. M.; Schoenfisch, M. H. *Annu. Rev. Anal. Chem.* **2009**, *2*, 409.

10. McQuade, L. E.; Lippard, S. J. *Curr. Opin. Chem. Biol.* **2010**, *14,* 43.

11. Nagano, T. J. *Clin. Biochem. Nutr.* **2009**, *45*, 111.

12. (a) Nagano, T.; Yoshimura, T. *Chem. Rev*. **2002**, *102*, 1235. (b) Hilderbrand, S. A.; Lim, M. H.; Lippard, S. J. *Topics in Fluorescence Spectroscopy*, Geddes, C. D.; Lakowicz, J. R.; Eds. Spinger: Berlin, 2005; pp 163.

13. Sasaki, E.; Kojima, H.; Nishimatsu, H.; Urano, Y.; Kikuchi, K.; Hirata, Y.; Nagano, T. J. Am. Chem. Soc. **2005**, 127, 3684.

14. Lim, M. H.; Lippard, S. J. *Acc. Chem. Res.* **2007**, *40*, 41.

15. Kojima, H.; Nakatsubo, N.; Kikuchi, K.; Kawahara, S.; Kirino, Y.; Nagoshi, H.; Hirata, Y.; Nagano, T. *Anal. Chem.* **1998**, *70*, 2446.

16. Heiduschka, P.; Thanos, S. *NeuroReport* **1998**, *9*, 4051.

17. Meineke, P.; Rauen, U.; de Groot, H.; Korth, H.-G.; Sustmann, R., *Chem. Eur. J.* **1999**, *5*, 1738.

18. Kojima, H.; Hirotani, M.; Nakatsubo, N.; Kikuchi, K.; Urano, Y.; Higuchi, T.; Hirata, Y.; Nagano, T. *Anal. Chem.* **2001**, *73,* 1967.

19. Gabe, Y.; Urano, Y.; Kikuchi, K.; Kojima, H.; Nagano, T. *J. Am. Chem. Soc.* **2004**, *126*, 3357.

20. Lim, M. H.; Xu, D.; Lippard, S. J. *Nat. Chem. Biol.* **2006**, *2*, 375.

21. Lim, M. H.; Wong, B. A.; Pitcock, Jr., W. H.; Mokshagundam, D.; Baik, M.-H.; Lippard, S. J. *J. Am. Chem. Soc.* **2006**, *128*, 14363.

22. Zheng, H.; Shang, G.-Q.; Yang, S.-Y.; Gao, X.; Xu, J.-G. *Org. Lett.* **2008**, *10*, 2357.

23. Wang, S.; Han, M.-Y.; Huang, D. *J. Am. Chem. Soc.* **2009**, *131*, 11692.

24. Kim, J.-H.; Heller, D. A.; Barone, P. W.; Song, C.; Zhang, J.; Trudel, L. J.; Wogan, G. N.; Tannenbaum, S. R.; Strano, M. S. *Nat. Chem.* **2009**, *1*, 473.

25. Jourd'heuil, D. *Free Radical Biol. Med.* **2002**, *33*, 676.

26. Wardman, P. *Free Radical Biol. Med.* **2007**, *43*, 995.

27. Zhang, X.; Kim, W. S.; Hatcher, N.; Potgieter, K.; Moroz, L. L.; Gillette R.; Sweedler, J. V. *J. Biol. Chem.* **2002**, *277*, 48472.

28. Ye, X.; Rubakhin, S. S.; Sweedler, J. V. *J. Neurosci. Methods* **2008**, *168*, 373.

Chapter 1

Introduction

Nitric oxide (NO) has attracted enormous interest from chemists and biochemists since it has been discovered as a signalling agent in humans.[1] It is also known that NO plays diverse roles in biological processes, for instance, when produced in low concentration it regulates vasodilatation, defence against pathogens and long-lasting enhancement in signal transmission, however in micro molar concentration, it stimulates the reactive nitrogen species (RNS) and causes carcinogenesis and neurodegenerative disorders.[2]

Most of these activities are attributed to the formation of nitrosyl complexes with metallo-proteins, primarily iron or copper-proteins.[3] For example, in soluble guanylyl cyclase (sGC),[4] the formation of a nitrosyl complex with Fe^{II} leads to labialization of a *trans* axial (proximal) histidine ligand in the protein backbone, and the resulting change in the protein conformation is believed to activate the enzyme for catalytic formation of the secondary messenger cyclic-guanylyl monophosphate (Cgmp) from guanylyl triphosphate (GTP). The reduction of Cu(II) centres in some proteins, such as cytochrome *c* oxidase and laccase, to Cu(I) on exposure to NO has also been known for a long time.[3,4] In cytochrome *c* oxidase, the NO mediated reduction of Cu(II) to Cu(I) is believed to regulate the electron transport activity of this protein.[5] These essentially inspired a wide range of research to identify the precise roles of nitric oxide in biology. Since NO is a reactive free radical and easily diffuses through most cells and tissues, it is difficult to have methods to follow NO immediately after production. Such methods can enhance the understanding of the various biological pathways of NO in *vivo*. Thus, a selective probe to detect the formation and migration of nitric oxide with spatiotemporal resolution directly from living cells is highly desirable compare to other methods such as spectroscopy, chemoluminscence, EPR and amperometry.[6-8]

In this aspect, the fluorescence-based detection technique is found to satisfy almost all the requirements.[7-9] Starting from the early examples of fluorescence-based sensors such as *o*-diaminonaphthalene (DAN) and *o*-diaminofluoresceins (DAFs), a number of fluorescent probes have been reported to date.[10] However, they are unable to detect or monitor NO itself as their fluorescence response depends on the formation of a triazole species by oxidized NO products such as N_2O_3. Thus, the NO related bio-events would not be detected in real time. Recently, a highly selective fluorescent imaging agent, NO_{550}, for NO has been reported which displays a rapid and linear response with a red-shifted turn-on signal.[11]

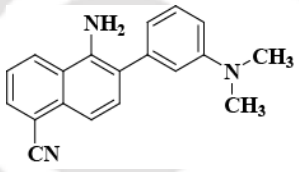

Figure 1.1: Structure of NO_{550}

1.1 Early fluorometric imaging of NO

The first fluorescence-based NO sensors were originally prepared for the measurement of nitrite (NO_2^-) ion in solution. The sensor molecule, 2, 3-diaminonaphthalene (DAN) undergoes diazotization at one of the amines under acidic conditions in the presence of nitrite. Following the diazotization, 2, 3-naphthotriazole is formed (Scheme 1.1).

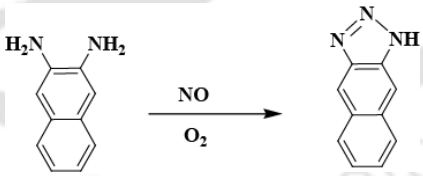

Scheme 1.1

It was also observed that formation of 2, 3-naphthotriazole is pH dependent, presumably a result of the pH dependence for the formation of the nitrosamine intermediate.[12] Hirobe proposed mechanism for triazole formation with N_2O_3 and N_2O_4, formed by the reaction of NO with O_2 (Scheme 1.2).[13]

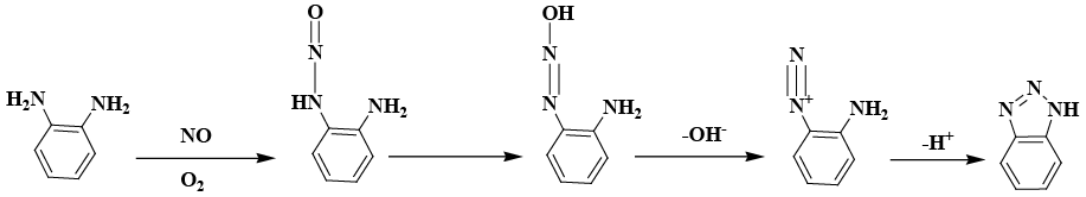

Scheme 1.2

Accordingly a number of fluorescent probes for NO have been reported, examples using fluoresceins (such as DAF-2 DA, Scheme 1.3), anthraquinones, rhodamines, BODIPYs and cyanines. [14-17]

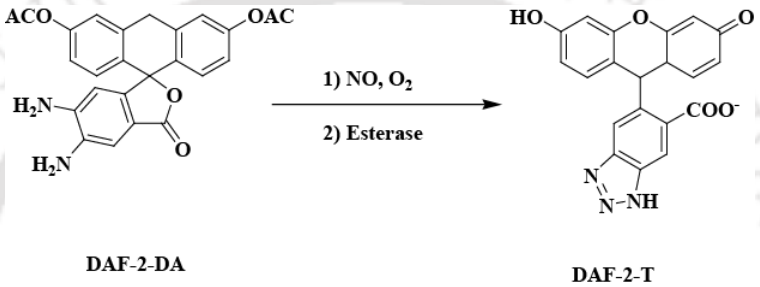

Scheme 1.3

But there are some limitations. In the presence of H_2O_2/peroxidase, $OONO^-$, OH or NO_2, the intrinsically electron-rich diamino benzene moiety is oxidized to an arylaminyl radical, which combines with NO and leads to triazole.[18-20] In addition dehydroascorbic acid (DHA) condenses with ortho diamino aromatics and turns on the fluorescence of such probes.[21] Eric V. Anslyn et al sought to overcome the limitations of the ortho diamino aromatics by creating a chemical mechanism for NO detection that eliminates the possibility of interferences. They designed a highly selective NO responsive fluorescent probe based on this new strategy and demonstrated its application in cellular imaging. The increase in conjugation of the probe was to yield an advantageous red-shifted turn on signal. They avoided the highly electron rich o-diamino aromatics in order to impede general oxidation by other reactive oxygen/nitrogen species. Their strategy involves a cascade of reactions that commence from air oxidation of NO. Their first embodiment of the strategy was the probe NO_{550}, which upon reaction with NO was predicted to generate a diazo ring system (AZO_{550}, Scheme 1.4). The dimethyl

amino and cyano groups were judiciously positioned to allow internal charge transfer upon photo excitation.

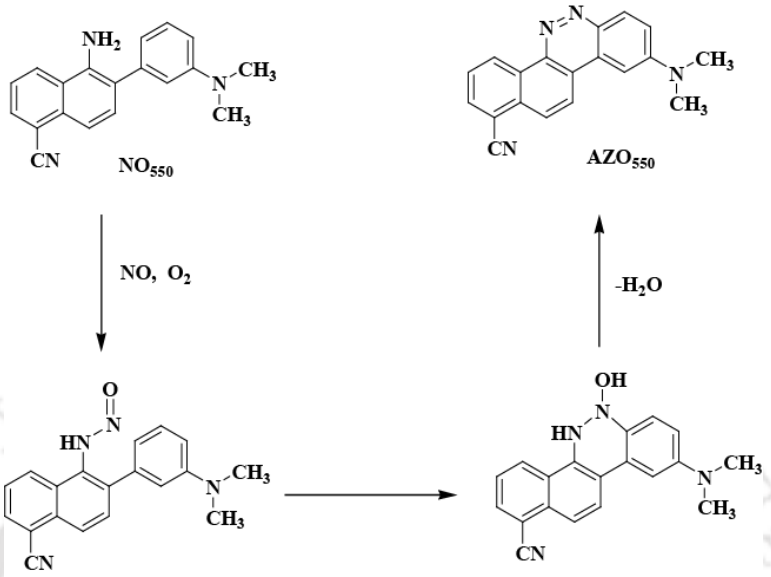

Scheme 1.4

Recently, Yun-Ming Wang and his group synthesized some NO fluorescent sensors based on deamination of aromatic primary monoamines.[22] The water soluble and nonfluorescent FA-OMe can sense NO and form the intensely fluorescent product dA-FA-OMe *via* reductive deamination of the aromatic primary mono amine (Scheme 1.5). The turn on fluorescence signals were performed by suppression of photoinduced electron transfer (PeT).

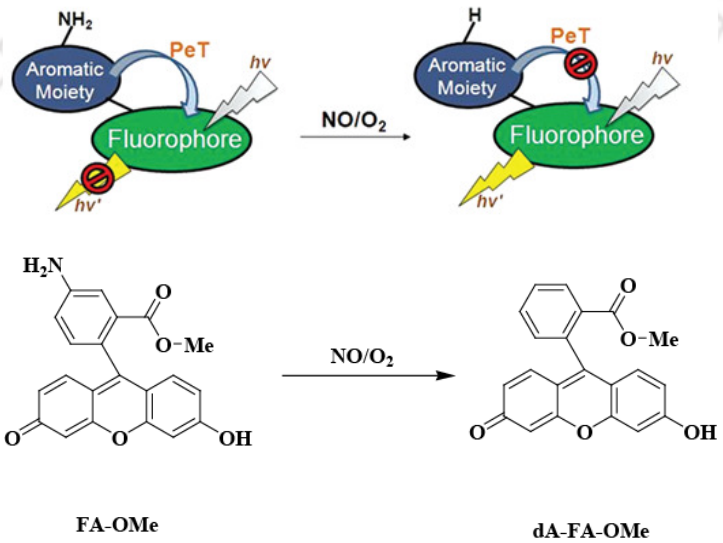

Scheme 1.5

There are several requirements for fluorescent NO sensors to be useful in biology. Probes should be nontoxic and afford direct, fast, reversible, specific and selective NO detection. It is preferable that they contain fluorophores that excite and emit in the visible or near infrared region in order to avoid interference or cellular damage by UV- light. Real time imaging with spatial resolution is desirable. The exploration of the reaction between NO and transition-metal complexes to devise metal-based fluorescent sensors that satisfy the aforementioned criteria.

.

1.2 Strategies for metal-based fluorescent NO sensors

First example of metal based fluorescent sensor was an iron complex showing the diminished fluorescence intensity when interact with NO.[23] There is another iron dithiocarbamate complex of acridine-TEMPO ligand which also showed decrease in the fluorescence intensity when allowed to come in contact with NO.[24] In both examples there is a decrease in the fluorescence intensity but in biological systems enhancement in the fluorescence intensity always preferred over quenching of fluorescence intensity. This approaches to develop metal-based fluorescent NO sensors which can be categorized into the following classes:

a) Fluorophore Displacement without Metal Reduction

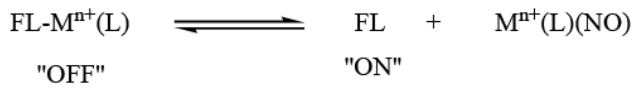

b) Metal Reduction without Fluorophore Displacement

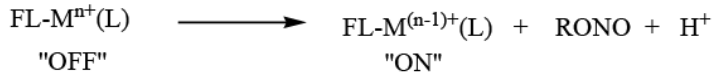

c) Metal Reduction with Fluorophore Displacement

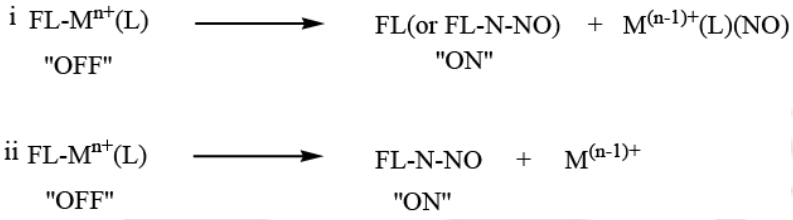

Scheme 1.6 Strategies adopted for fluorescent NO sensing.

The general strategy for NO sensing is to coordinate a fluorophore ligand to a metal ion to quench the fluorescence, which is restored by the interaction of NO with the metal center, sometimes with the release of the fluorophore and concomitant emission turn on. During metal reduction by NO, a species with NO^+ character can react with an amine functionality to produce an N-nitrosamine. If the fluorophore contains a coordinated amine, it can become N-nitrosated by an intramolecular pathway with concomitant dissociation and fluorescence enhancement. Utilizing this strategy, Lippard and his group constructed fluorescent probe families for imaging endogenous NO in live cells and tissue; these sensors employ Cu(II) to modulate NO reactivity. [25-29]

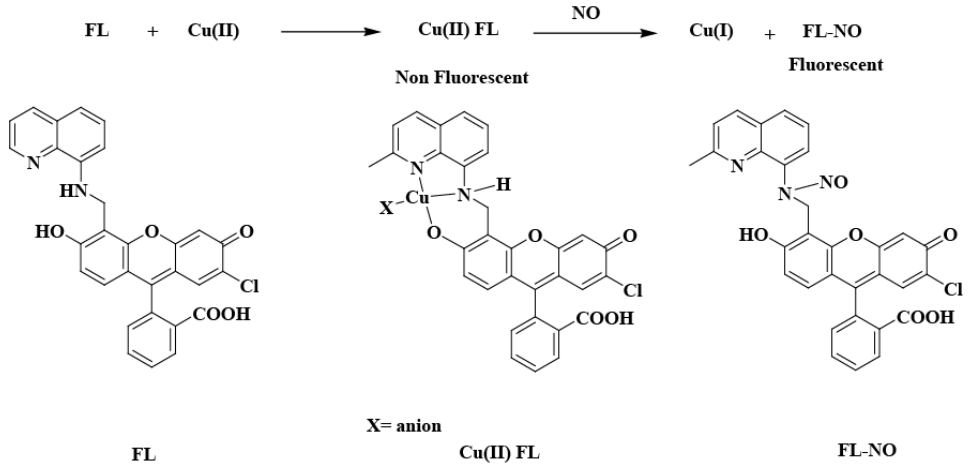

Scheme 1.7

To appreciate the diverse biological actions of NO, it is essential to understand not only the biosynthesis but also the metabolism of NO and the chemistry of NO in aqueous solution. NO in aqueous solution containing oxygen is oxidized primarily to Nitrite.

$$4NO + O_2 + 2H_2O \longrightarrow 4NO_2^- + 4H^+ \quad \text{..... eq (1.1)}$$

While nitrite (NO_2^-) was for decades considered to be physiologically inert, it is now accepted that NO_2^- represents a stable reservoir that can be reduced to bioactive NO and other reactive nitrogen species during hypoxia to mediate physiological signalling.[30] Concentrations of the anion are maintained at low micromolar levels in tissues (1-20 μM) and nanomolar levels in blood (100-200 nM).

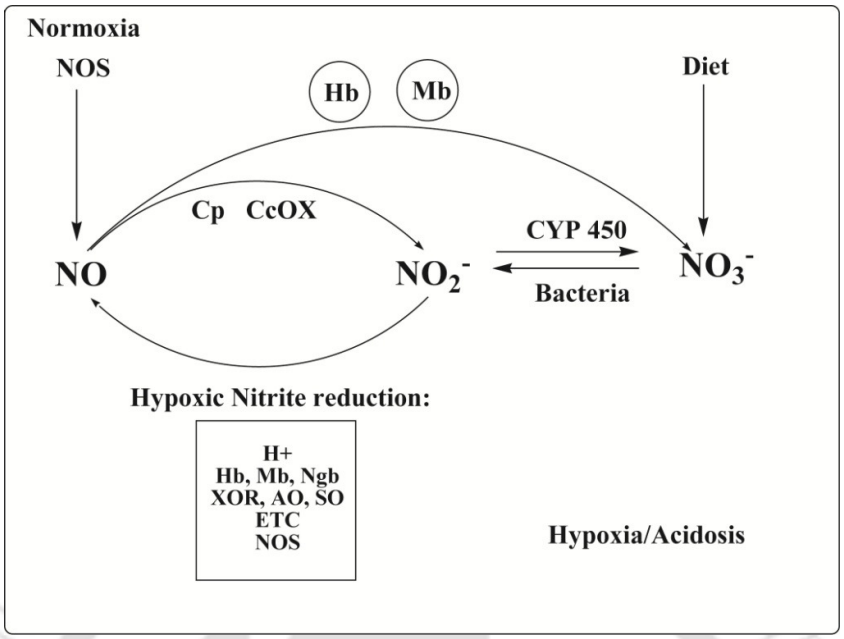

Figure 1.2: The nitrite-NO cycle.

In normoxia, NOS is functional and generates NO, which is oxidized by Mb and Hb to NO_3^- and by cytochrome c oxidase and ceruloplasmin to NO_2^-. NO_2^- is also derived from the diet. In hypoxia, nitrate is reduced to nitrite by anaerobic commensal bacteria and nitrite is reduced to bioactive NO by a number of mammalian nitrite reductase enzymes including Hb, Mb, neuroglobin (Ngb), xanthine oxidoreductase (XOR), aldehyde oxidase (AO), sulfite oxidase (SO), components of the mitochondrial electron transport chain (ETC) and NOS.

Nitrite is harmful to health because of possible carcinogenic effects,[31] its detection and quantification have become crucial in diverse fields,[32-35] including food, environmental, medicinal and biological analytes. While colorimetric and fluorometric detection methods play a pivotal role in modern sensing [36,37] because they often allow for a rapid qualitative and quantitative assessment, few reports deal with nitrite sensing. The most common colorimetric method for nitrite detection still involves the reaction of nitrite with aromatic amines to yield an azo dye via the intermediate diazonium salt, [38,39] but the intricacy of the approach precludes a fast and easy quantification. Very recently, (2-arylethynyl) anilines were shown

to react with nitrite in aqueous acidic media to produce yellow 4(1H)-cinnolones, thus setting up a rapid (5 min) chemodosimeter.[40]

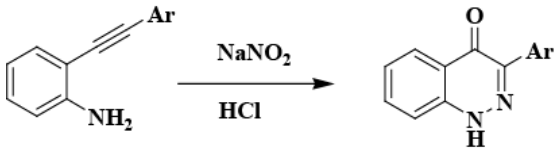

Scheme 1.8

In literature, a number of electrochemical and colorimetric sensors have been reported.[41,42] However, all these processes have some drawbacks and one method which satisfies almost all the requirement is a fluoremetric one.

1.3 References

1. (a) Furchgott, R. F. *Angew. Chem. Int. Ed.* **1999**, *38*, 1870. (b) Ignarro, J. *Angew. Chem. Int. Ed.* **1999**, *38*, 1882. (c) Murad, F. *Angew. Chem. Int. Ed.* **1999**, *38*, 1856. (d) Bon, C. L. M.; Garthwaite, J. *J. Neurosci.* **2003**, *23*, 1941. (e) Pepicelli, O.; Raiteri, M.; Fedele, E. *Neurochem. Int.* **2004**, *45*, 787. (f) Bonomo, R. P.; Pappalardo, G.; Rizzarelli, E.; Santoro, A. M.; Tabbi, G.; Vagliasindi, L. I. *Dalton Trans.* **2007**, 1400. (g) Bonomo, R. P.; Castronovo B. M. G.; Santoro, A. M. *Dalton Trans.* **2004**, 104. (h) Bonomo, R. P.; Pappalardo, G.; Rizzarelli, E.; Vagliasindi, L. I. *Dalton Trans.* **2008**, 3805. (i) Bonomo, R. P.; Di Natale, G.; Rizzarelli, E.; Tabbi, G.; Vagliasindi, L. I. *Dalton Trans.* **2009**, 2637.
2. (a) Ricciardolo, E. L. M.; Sterk, P. J.; Gaston, B.; Folkerts, G. *Phsiol. Rev.* **2004**, *84*, 731. (b) Wink, D. A.; Vodovotz, Y.; Laval, J.; Laval, F.; Dewhirst, M. W.; Mitchell, J. B. *Carcinogenesis* **1998**, *19*, 711. (c) Calabrese, V.; Bates, T. E; Stella, A. M. G. *Neurochem. Res.* **2000**, *25*, 1315.
3. (a) *Nitric Oxide: Biology and Pathobiology*, ed. Ignarro, L. J., Academic Press, San Diego, 2000. (b) Torres, J.; Svinstunenko, D.; Karlsson, B.; Cooper, C. E.; Wilson, M. T. *J. Am. Chem. Soc.* **2002**, *124*, 963. (c) Radi, R. *Chem. Res. Toxicol.* **1996**, *9*, 828.

4. (a) Kim, S.; Deinum, G.; Gardner, M. T.; Marletta, M. A.; Babcock, G. T. *J. Am. Chem. Soc.* **1996**, *118*, 8769. (b) Torres, J.; Cooper, C. E.; Wilson, M. T. *J. Biol. Chem.* **1998**, *273*, 8756.

5. Schopfer, M. P.; Mondal, B.; Lee, D.-H.; Sarjeant, A. A. N.; Karlin, K. D. *J. Am. Chem. Soc*. **2009**, *131*, 11304.

6. Nagano, T.; Yoshimura, T. *Chem. Rev*. **2002**, *102*, 1235.

7. Hilderbrand, S. A.; Lim, M. H.; Lippard, S. J. *In Topics in Fluorescence Spectroscopy*, Geddes, C. D.; Lakowicz, J. R. Eds. Springer: 2005; pp 163.

8. Maliniski, T.; Mesaros, S.; Tomboulian, P. *Methods Enzymol* **1998**, *170*, 31.

9. Sasaki, E.; Kojima, H.; Nishimatsu, H.; Urano, Y.; Kikuchi, K.; Hirata, Y.; Nagano, T. *J. Am. Chem. Soc.* **2005**, *127*, 3684.

10. (a) Meineke, P.; Rauen, U.; de Groot, H.; Korth, H.-G.; Sustmann, R. *Chem. Eur. J.* **1999**, *5*, 1738. (b) Lim, M. H.; Xu, D.; Lippard, S. J. *Nat. Chem. Biol.* **2006**, *2*, 375. (c) Zheng, H.; Shang, G.-Q.; Yang, S.-Y.; Gao, X.; Xu, J.-G. *Org. Lett.* **2008**, *10*, 2357. (d) Wang, S.; Han, M.-Y.; Huang, D. *J. Am. Chem. Soc.* **2009**, *131*, 11692. (e) Kim, J.-H.; Heller, D. A.; Barone, P. W.; Song, C.; Zhang, J.; Trudel, L. J.; Wogan, G. N.; Tannenbaum, S. R.; Strano, M. S. *Nat. Chem.* **2009**, *1*, 473. (f) Ye, X.; Rubakhin, S. S.; Sweedler, J. V. *J. Neurosci. Methods* **2008**, *168*, 373.

11. Yang, Y.; Seidlits, S. K.; Adams, M. M.; Lynch, V. M.; Schmidt, C. E.; Anslyn, E. V.; Shear, J. B. *J. Am. Chem. Soc.* **2010**, *132*, 13114.

12. Miles, A. M.; Chen, Y.; Owens, M. W.; Grisham, M. B. *Methods* **1995**, *7,* 40.

13. Nagano, T.; Takizawa, H.; Hiiobe, M. *Tet. Lett.* **1995**, *36*, 8239.

14. Kojima, H.; Nakatsubo, N.; Kikuchi, K.; Kawahara, S.; Kirino, Y.; Nagoshi, H.; Hirata, Y.; Nagano, T. *Anal. Chem.* **1998**, *70*, 2446.

15. Heiduschka, P.; Thanos, S. *NeuroReport* **1998**, *9*, 4051.

16. Kojima, H.; Hirotani, M.; Nakatsubo, N.; Kikuchi, K.; Urano, Y.; Higuchi, T.; Hirata, Y.; Nagano, T. *Anal. Chem.* **2001**, *73*, 1967.

17. Gabe, Y.; Urano, Y.; Kikuchi, K.; Kojima, H.; Nagano, T. *J. Am. Chem. Soc.* **2004**, *126*, 3357.

18. Jourd'heuil, D. *Free Radical Biol. Med.* **2002**, *33*, 676.

19. Roychowdhury, S.; Luthe, A.; Keilhoff, G.; Wolf, G.; Horn, T. F. W. *Glia* **2002**, *38*, 103.

20. Wardman, P. *Free Radical Biol. Med.* **2007**, *43*, 995.

21. Zhang, X.; Kim, W. S.; Hatcher, N.; Potgieter, K.; Moroz, L. L.; Gillette, R.; Sweedler, J. V. *J. Biol. Chem.* **2002**, *277*, 48472.

22. Shiue, T.-W.; Chen, Y.-H.; Wu, C.-M.; Singh, G.; Chen, H.-Y.; Hung, C.-H.; Liaw, W.-F.; Wang, Y.-M. *Inorg. Chem.* **2012**, *51*, 5400.

23. Katayama, Y.; Takahashi, S.; Maeda, M. *Anal. Chim. Acta.* **1998**, *365*, 159.

24. Kim, S.; Deinum, G.; Gardner, M. T.; Marletta, M. A.; Babcock, G. T. *J. Am. Chem. Soc.* **1996**, *118*, 8769.

25. Hilderbrand, S. A.; Lim, M. H.; Lippard, S. J. *J. Am. Chem. Soc*. **2004**, *126*, 4972.

26. Lim, M. H.; Wong, B. A.; Pitcock, W. H.; Mokshagundam, D.; Baik, M. H.; Lippard, S. J. *J. Am. Chem. Soc.* **2006,** *128*, 14364.

27. McQuade, L. E.; Ma, J.; Lowe, G.; Ghatpande, A.; Gelperin, A.; Lippard, S. J. *Proc. Natl. Acad. Sci. U. S. A.* **2010,** *107*, 8525.

28. Pluth, M. D.; McQuade, L. E.; Lippard, S. J. *Org. Lett*. **2010**, *12*, 2318.

29. McQuade, L. E.; Pluth, M. D.; Lippard, S. J. *Inorg. Chem.* **2010**, *49*, 8025.

30. Lundeberg, J. O.; Weitzberg, E.; Gladwin, M.T. *Nature Reviews Drug Discovery* **2008**, 156.

31. Yu, C.; Guo, J.; Gu, H. *Electroanalysis* **2010**, *22*, 1005.

32. Yang, C.; Lu, Q.; Hu, S. *Electroanalysis* **2006**, *18*, 2188.

33. Quan, D.; Shin, W. *Sensors* **2010**, *10*, 6241.

34. Spataru, N.; Rao, T. N.; Tryk, D. A.; Fujishima, A. *J. Electrochem. Soc*. **2001**, *148*, E112.

35. Mohamed, A. A.; Ricci, S.; Burini, A.; Galassi, R.; Santini, C.; Chiarella, G. M.; Melgarejo, D. Y.; Fackler, J. P. Jr. *Inorg. Chem*. **2011**, *50*, 1014.

36. Martínez-Manez, R.; Sancenon, F. *Chem. Rev*. **2003**, *103*, 4419.

37. Schmittel, M.; Lin, H.-W. *Angew. Chem., Int. Ed.* **2007**, *46*, 893.

38. Sawicki, E.; Stanley, T. W.; Pfaff, J.; D'Amico, A. *Talanta* **1963**, *10*, 641.

39. Riley, J. P.; Skirrow, G. *Chemical Oceanography* Academic Press: London, 1965.

40. Dey, R.; Chatterjee, T.; Ranu, B. C. *Tetrahedron Lett.* **2011**, *52*, 461.

41.(a) Stanley, M. A.; Maxwell, J.; Forrestal, M.; Doherty, A. P.; Maccraith, B. D.; Diamond, D.; Vos, J. G. *Anal. Chim. Acta* **1994**, *299*, 81. (b) Kuban, P.; Nguyen, H. T. A.; Macka, M.; Haddad, P. R.; Hauser, P. C. *Electroanalysis* **2007**, *19*, 2059. (c) Pietrzak, M.; Meyerhoff, M. E. *Anal. Chem*. **2009**, *81*, 3637.

42. (a) Daniel, W. L.; Han, M. S.; Lee, J.-S.; Mirkin, C. A. *J. Am. Chem. Soc.* **2009**, *131*, 6362. (b) Adarsh, N.;. Shanmugasundaram, M; Ramaiah, D. *Anal. Chem*. **2013**, *85*, 10008.

Chapter 2

Selective chromogenic and fluorogenic probe for nitric oxide from dark background

Abstract

Sodium 5-aminonaphthalene-1-sulfonate (**ANS**) and sodium 6-amino-4-hydroxynaphthalene-2-sulfonate (**AHS**) undergo very fast reaction with NO in aerobic condition to produce sodium benzo [cd] indazole-5-sulfonate (**AZO-ANS)** and sodium 4, 6-dihydroxynaphthalene-2-sulfonate (**AHS-OH)** respectively. The fluorescence and UV-visible absorbance appear from a dark background due to the formation of new molecules. Excellent selectivity was observed against other reactive oxygen/nitrogen species.

2.1 Introduction

Nitric oxide (NO), produced by nitric oxide synthases in the biological systems, is known as a ubiquitous signalling molecule. NO is involved in diverse physiological and pathological pathways.[1] Also studies have shown that its down-regulation is closely linked with various pathophysiological conditions including the endothelial dysfunction, cancer and neurodegenerative diseases.[2] Although NO is a key biological messenger, the mechanisms by which it performs its diverse biological roles remain elusive. Thus, for better understanding of NO's origins, activities, and biological functions, it is very important to search for methods and tools that can sensitively and selectively probe NO in biological systems. Several techniques such as colorimetry, electron paramagnetic resonance, electrochemistry and chemiluminescence have been developed.[3] Fluorescence techniques is considered ideal for sensing NO because of their sensitivity and high spatiotemporal resolution.[4-6] The most common NO detection techniques involve the use of *o*-diamino aromatics under aerobic conditions.[7-11] They react with the oxidized products, i.e. NO^+ or N_2O_3 to yield the corresponding triazole species which are fluorescent.[7-11] Examples involving fluoresceines, rhodamines, cyanines, BODIPYs, anthraquinones as fluorescent probes for NO sensing have been reported.[7-12] However, their sensitivity towards H_2O_2, peroxynitrite, hydroxyl radical etc. actually complicate their practical use. Thus, the NO-related bio-events would not be detected in real time. Recently, a highly selective fluorescent imaging agent, NO_{550}, for NO has been reported which displays rapid and linear response with a red-shifted turn-on signal.[13]

In the present study sodium 5-aminonaphthalene-1-sulfonate (**ANS**) and sodium 6-amino-4-hydroxynaphthalene-2-sulfonate (**AHS**) have been used as fluorescent sensor for selective detection of NO.

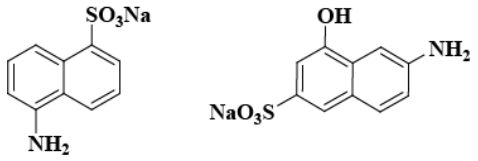

ANS AHS

Figure 2.1: Fluorophores used for the present study.

2.2 Results and discussion

Both the fluorophores were purchased from commercial source. Sodium 5-aminonaphthalene-1-sulfonate (**ANS**) is a brown solid compound. It is highly soluble in methanol and water. It shows an absorption band at 335 nm in the UV-visible spectroscopy in methanol solution (Figure 2.2).

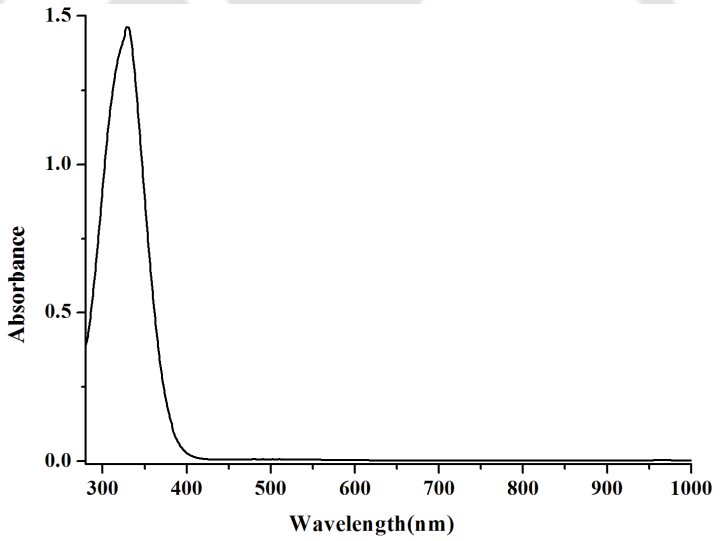

Figure 2.2: UV-visible spectrum of **ANS** in methanol medium.

Sodium 6-amino-4-hydroxynaphthalene-2-sulfonate (**AHS**) is a reddish brown solid compound. It shows an absorption band at 320 nm in the UV-visible spectroscopy in methanol solution (Figure 2.3). In both the fluorophores the reactive site is the primary amino group, which reacts with NO in aerobic condition.

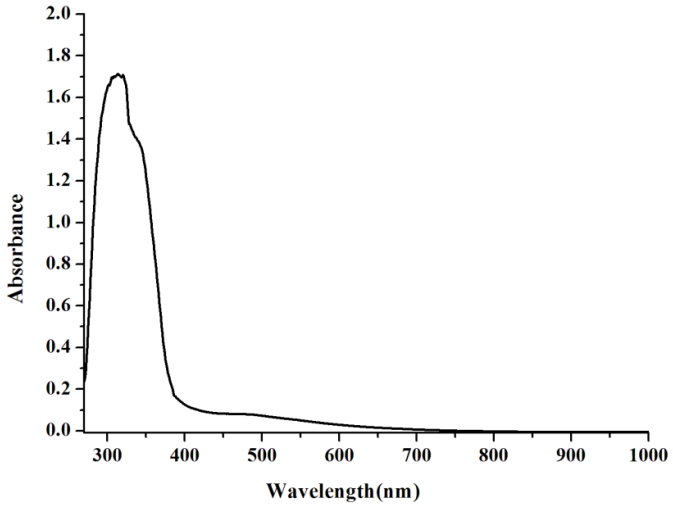

Figure 2.3: UV-visible spectrum of **AHS** in methanol medium.

2.3 Nitric oxide reactivity

After addition of NO gas into the methanol solution of **ANS**, a colour change from light-yellow to deep-red was immediately observed. In UV-visible spectroscopy; upon addition of NO in methanol solution of **ANS** under aerobic condition, a new band around 480 nm slowly developed (Figure 2.4). The red shifting of the absorption wavelength is due to the formation of a new molecule as shown in scheme 2.1.

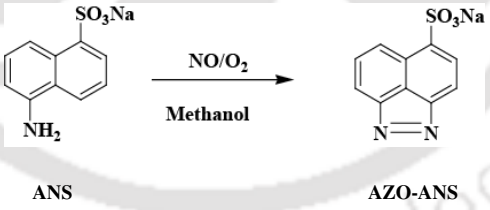

Scheme 2.1

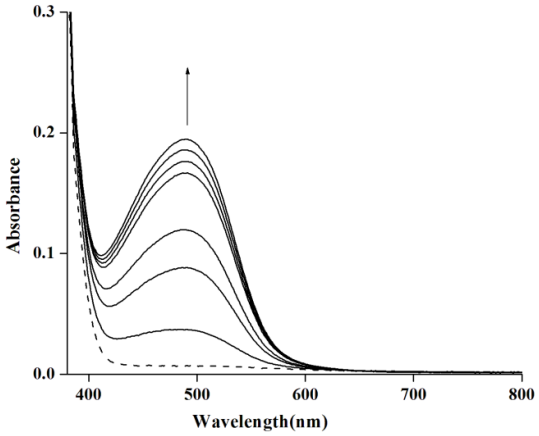

Figure 2.4: UV-visible spectra of **ANS** (dashed line) and after addition of NO (solid lines) in aerobic condition in methanol medium.

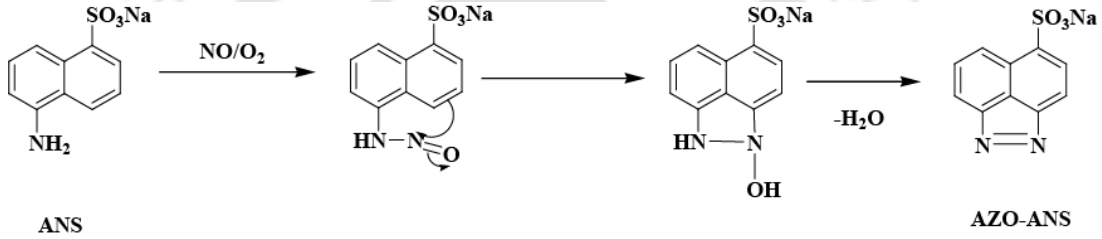

Scheme 2.2

The primary amino group of **ANS** in an aerobic condition is believed to react with NO to produce the corresponding N-nitrosamine intermediate. The nitrogen atom of the nitrosamine group is electrophilic in nature. In successive steps, the electrophilic aromatic substitution on the electron deficient nitrosamine occurs resulting a hydroxyl hydrazine derivative and finally, elimination of water leads to the formation of sodium benzo [cd] indazole-5-sulfonate (**AZO-ANS**) (Scheme 2.2). The formation of **AZO-ANS** was unambiguously established by ^{1}H-NMR, ^{13}C-NMR, ESI-mass and FT-IR spectroscopy and elemental analyses (Experimental section). Similar reaction was found to take place in aqueous medium also.

On the other hand 6-amino-4-hydroxynaphthalene-2-sulfonate (**AHS**) shows an absorption band at 320 nm in the UV-visible spectroscopy in methanol solution. After addition of NO to the methanolic solution of **AHS**, immediately the color changed from light-red to dark-red. In UV-visible spectroscopy upon addition of NO with **AHS** in an aerobic condition, a new band

around 450 nm developed in methanol medium. This band was presumably due to the formation of N-nitrosamine intermediate. The band at 450 nm disappeared and a new band around 530 nm slowly developed (Figure 2.5). The red shifting of the absorption wavelength was due to the formation of **AHS-OH** as shown in scheme 2.3.

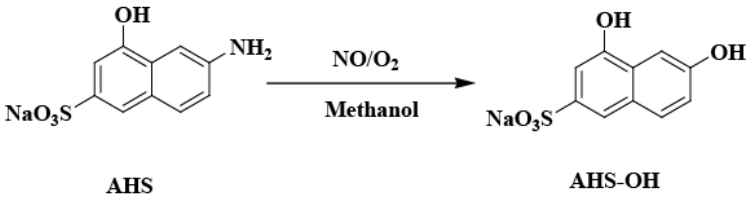

AHS **AHS-OH**

Scheme 2.3

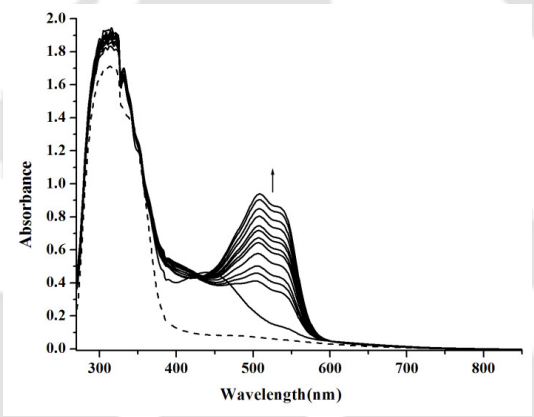

Figure 2.5: UV-visible spectra of **AHS** (dashed line) and after addition of NO in aerobic condition (solid lines) in methanol medium.

The proposed reaction mechanism of **AHS** with NO is shown in scheme 2.4. First, the amino group of **AHS** is nitrosylated by NO in aerobic condition to produce the N-nitrosamine intermediate.[7] The diazonium compound formed then results in 4, 6-dihydroxynaphthalene-2-sulfonate (**AHS-OH**).

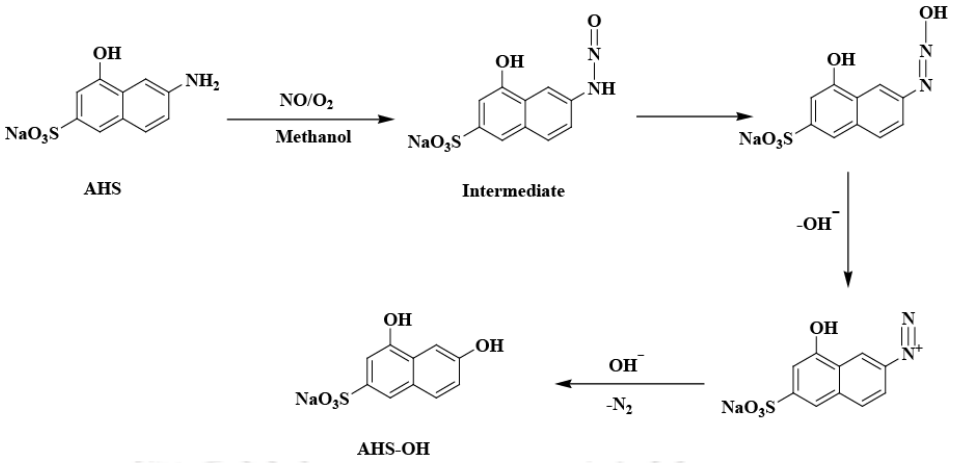

Scheme 2.4

The formation of hydroxyl product **AHS-OH** was confirmed by FT-IR, ^{1}H-NMR, ^{13}C-NMR, ESI-mass and elemental analyses.

2.4 Fluorescence study

ANS absorbs at 335 nm. Upon excitation at 335 nm, it shows significant fluorescence emission centred at 475 nm in methanol at room temperature. The quantum yield was found to be 0.237 in methanol with respect to quinine sulphate. The fluorescence emission band of **ANS** centred at 475 nm was found to disappear upon addition of NO (Figure 2.6).

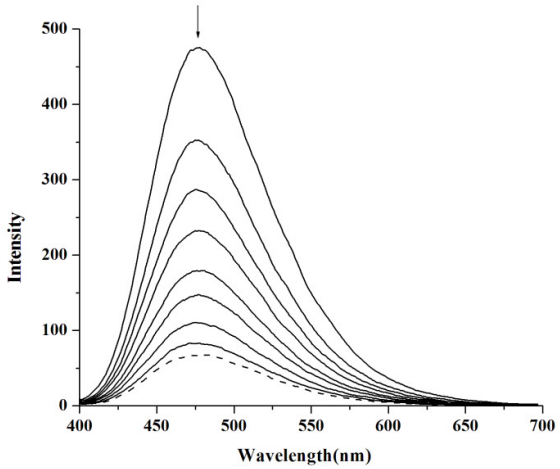

Figure 2.6: Fluorescence spectra of **ANS** (solid line) (λ_{ex}, 335 nm) and after addition of NO (dashed line) in methanol medium.

But when it was excited at 480 nm, a significant fluorescence enhancement of 8 fold at 580 nm was observed from a dark background (Figure 2.7). This was attributed to **AZO-ANS**. The spectra were identical to the purified **AZO-ANS**. To study the selectivity of the probe with the other competitive reactive oxygen and nitrogen species, the fluorescence study has been done with ~ 100 fold excess of H_2O_2, KO_2, NO_2^-, NO_3^- however, no detectable fluorescence was observed in any case suggesting a high selectivity towards NO. It should be noted that diazotization occurs in acidic media to form diazonium salts from nitrosamines. In contrast, the reaction between **ANS** and NO occurs rapidly under neutral (pH, 7.4) or even basic (pH, 10) aqueous conditions. It has been found to display significant fluorescence intensity at 1nM NO concentration.

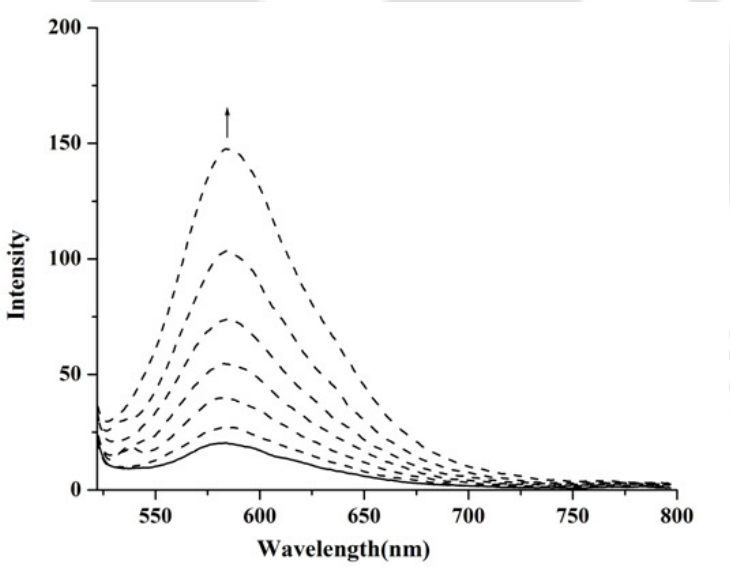

Figure 2.7: Fluorescence enhancement (λ_{ex}, 480 nm) of **ANS** before (solid line) and after addition of NO (dashed lines) in aerobic condition in methanol medium.

6-amino-4-hydroxynaphthalene-2-sulfonate (**AHS)** absorbs at 320 nm. Upon excitation at 320 nm, it shows significant fluorescence emission centred at 410 nm in methanol or water at room temperature. The quantum yield was found to be 0.207 and 0.254 respectively in methanol and water with respect to quinine sulphate. The fluorescence emission band of **AHS**

centred at 410 nm was found to disappear immediately upon addition of NO (Figure 2.8). But slowly the fluorescence starts appearing from a dark back ground at 350 nm (Figure 2.9). The new emission was due to the formation of **AHS-OH**, which was confirmed from the fluorescence spectra of the isolated compound. The selectivity of the NO probe was checked by doing the experiment in the presence of other anions (CH_3COO^-, NO_2^-, NO_3^-, Cl^-, ClO_4^- and H_2O_2) and it was found that there was no enhancement of fluorescence after addition of these anions. This confirmed the selectivity of **AHS** towards NO.

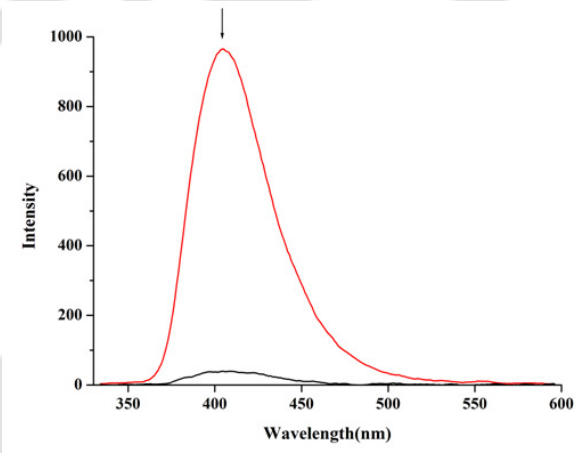

Figure 2.8: Fluorescence spectra of **AHS** (λ_{ex}, 320 nm) (red line) and after addition of NO (black line) in methanol medium.

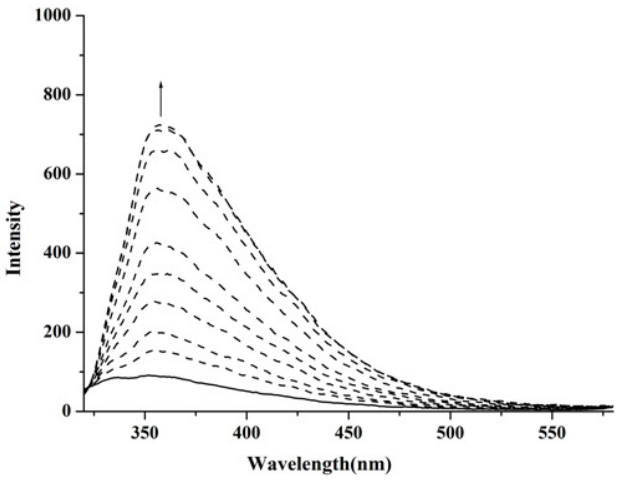

Figure 2.9: Fluorescence enhancement (λ_{ex}, 320 nm) of **AHS** before (solid line) and after addition of NO (dashed lines) in aerobic condition in methanol medium.

The fluorescence intensity of the **AHS** solution under optimized condition was found to be nearly proportional to NO concentration. It has been found to display significant fluorescence intensity at 1nM NO concentration.

2.5 Conclusion

Sodium 5-aminonaphthalene-1-sulfonate (**ANS**) and Sodium 6-amino-4-hydroxynaphthalene-2-sulfonate (**AHS**) undergo very fast reaction with NO in aerobic condition to produce sodium benzo [cd] indazole-5-sulfonate (**AZO-ANS)** and sodium 4,6-dihydroxynaphthalene-2-sulfonate (**AHS-OH)** respectively. The fluorescence and UV-visible absorbance appear from dark background due to the formation of new molecules. Excellent selectivity was observed against other reactive oxygen/nitrogen species.

2.6 Experimental Section

2.6.1 General Methods

All reagents and solvents were purchased from commercial sources and were of reagent grade. Deoxygenation, wherever necessary, of the solvents and solutions were done by repeated vacuum/purge cycles or bubbling with nitrogen for 30 minutes. NO gas was purified by passing through KOH and P_2O_5 column. UV-visible spectra were recorded on a Perkin Elmer Lamda 25 UV-visible spectrophotometer. FT-IR spectra were taken on a Perkin Elmer spectrophotometer with samples prepared as KBr pellets. The fluorescence spectra were recorded in solution in VARIAN Cary Eclipse Fluorescence Spectrophotometer at room temperature. Quinine sulfate in acidic medium was used as the reference compound for the determination of fluorescence quantum yield. ^{1}H- NMR spectra were obtained with a 400 MHz Varian FT spectrometer. Chemical shifts (ppm) were referenced either with an internal standard (Me_4Si) for organic compounds or to the residual solvent peaks.

2.6.2 Isolation of AZO-ANS

Sodium 5-aminonaphthalene-1-sulfonate (**ANS**) (1.225 g, 5 mmol) was dissolved in 20 ml of distilled and degassed methanol. To this solution, NO gas was bubbled through a needle for 5 minutes. The light yellow color of the solution turned deep red. Then the excess of NO gas was removed and the solution mixture was dried under reduce pressure. The combined organic extracts was washed with brine (80 ml), dried over anhydrous sodium sulphate; filtered and concentrated under reduced pressure. The crude product was purified by column chromatography on neutral alumina to afford of sodium benzo [cd] indazole-5-sulfonate (**AZO-ANS)**. Yield: 0.83 g (~ 65%). Elemental analyses for $C_{10}H_5N_2O_3SNa$: Calcd.(%): C, 46.88; H, 1.97; N, 10.93; found(%): C, 46.82; H, 1.90; N, 10.98. FT-IR (in KBr pellet): 2923, 1640, 1608, 1563, 1412, 1368, 1187, 1041, 785, 661, 628 cm^{-1}. ^{1}H-NMR (400 MHz, D_2O) δ_{ppm}: 8.66 (d, 1H), 8.48 (d, 1H), 7.93 (m, 2H), 7.81 (d, 1H), 7.63 (d, 3H), 7.21 (m, 2H). ^{13}C-NMR: (100 MHz, D_2O) δ_{ppm}: 141.9, 137.3, 128.2, 127.5, 125.6, 125.0, 124.0, 122.8, 115.9, 111.2. ESI-mass (m+1) Calcd. 234.22; found, 234.11.

2.6.3 Isolation of AHS-OH

Sodium 6-amino-4-hydroxynaphthalene-2-sulfonate (**AHS**) (1.31 g, 5 mmol) was dissolved in 20 ml of distilled and degassed methanol. To this solution, NO gas was bubbled through a needle for 1 minute. The light red color of the solution turned dark red. Then the excess of NO gas was removed and the solution mixture was dried under reduce pressure. The solid compound obtained was washed with diethyl ether to get the pure compound 4,6-dihydroxynaphthalene-2-sulfonate (**AHS-OH)**. Yield: 1.08 g (~ 80%). Elemental analyses for $C_{10}H_7O_5SNa$: Calcd.(%): C, 45.80; H, 2.69; found (%): C, 45.76; H, 2.74. FT-IR (in KBr pellet): 2086, 1609, 1571, 1217, 1060, 749, 648 cm^{-1}. ^{1}H-NMR (400 MHz, D_2O) δ_{ppm}: 8.29 (t, 1H), 7.47 (m, 1H), 7.34 (t, 1H), 7.19 (m, 1H), 6.99 (m, 1H). ^{13}C-NMR: (100 MHz, D_2O)

δ_{ppm}: 149.9, 144.3, 135.4, 129.3, 127.0, 126.0, 119.3, 117.2, 103.8, 103.3. ESI-mass ($m+Na^+$): Calcd. 262.21; found, 262.47.

2.7 References

1. (a) Palmer, R. M. J.; Ferrige, A. G.; Moncada, S. *Nature* **1987,** *327,* 524. (b) *Nitric Oxide: Biology and Pathobiology*, 1st ed.; Ignarro, L. J., Ed. Academic Press: San Diego, CA, 2000. (c) Nitric Oxide; Mayer, B., Ed. Springer: Berlin, 2000.
2. (a) Sutbeyaz, M. Y. *Surg. Today* **2003**, *33*, 651. (b) Cobbs, C. S.; Brenman, J. E.; Aldape, K. D.; Bredt, D. S.; Israel, M. A. *Cancer Res*. **1995**, *55*, 727. (c) Biro, G. P. *Curr. Drug Discovery Technol*. **2012**, *9*, 194. (d) Giedt, R. J.; Yang, C. J.; Zweier, J. L.; Matzavinos, A.; Alevriadou, B. R. *Free Radicals Biol. Med*. **2012**, *52*, 348.
3. (a) Lalezari, P.; Lekhraj, R.; Casper, D. *Anal. Biochem*. **2011**, *416*, 92. (b) Hogg, *N. Free Radicals Biol. Med*. **2010**, *49*, 122. (c) Rodriguez- Rodriguez, R.; Simonsen, U. Curr. *Anal. Chem*. **2012**, *8*, 485. (d) Mandon, J.; Hogman, M.; Merkus, J. F. M.; van Amsterdam, J.; Harren, F. J. M.; Cristescu, S. M. *J. Biomed. Opt*. **2012**, *17*, 017003.
4. (a) Nagano, T.; Yoshimura, T. *Chem. Rev*. **2002**, *102*, 1235. (b) Hilderbrand, S. A.; Lim, M. H.; Lippard, S. J. *Topics in Fluorescence Spectroscopy*, Geddes, C. D.; Lakowicz, J. R. Spinger: Berlin, 2005; pp 163.
5. Sasaki, E.; Kojima, H.; Nishimatsu, H.; Urano, Y.; Kikuchi, K.; Hirata, Y.; Nagano, T. *J. Am. Chem. Soc.* **2005**, *127*, 3684.
6. Lim, M. H.; Lippard, S. J. *Acc. Chem. Res.* **2007**, *40,* 41.
7. Kojima, H.; Nakatsubo, N.; Kikuchi, K.; Kawahara, S.; Kirino, Y.; Nagoshi, H.; Hirata, Y.; Nagano, T. *Anal. Chem.* **1998**, *70,* 2446.
8. Heiduschka, P.; Thanos, S. *Neuro. Report* **1998**, *9,* 4051.

9. Meineke, P.; Rauen, U.; de Groot, H.; Korth, H.-G.; Sustmann, R. *Chem. Eur. J.* **1999**, *5*, 1738.

10. Kojima, H.; Hirotani, M.; Nakatsubo, N.; Kikuchi, K.; Urano, Y.; Higuchi, T.; Hirata, Y.; Nagano, T. *Anal. Chem.* **2001**, *73,* 1967.

11. Gabe, Y.; Urano, Y.; Kikuchi, K.; Kojima, H.; Nagano, T. *J. Am. Chem. Soc.* **2004**, *126,* 3357.

12. (a) Lim, M. H.; Xu, D.; Lippard, S. J. *Nat. Chem. Biol.* **2006**, *2*, 375. (b) Lim, M. H.; Wong, B. A.; Pitcock Jr., W. H.; Mokshagundam, D.; Baik, M. H.; Lippard, S. J. *J. Am. Chem. Soc.* **2006**, *128*, 14363. (c) Zheng, H.; Shang, G. Q.; Yang, S. Y.; Gao, X.; Xu, J. G. *Org. Lett.* **2008**, *10*, 2357.

13. Yang, Y.; Seidlits, S. K.; Adams, M. M.; Lynch, V. M.; Schmidt, C. E.; Anslyn, E. V.; Shear, J. B. *J. Am. Chem. Soc.* **2010**, *132*, 13114.

Chapter 3

Fluorescence based nitric oxide detection of a copper(II) complex of naphthol derivative

Abstract

Copper(II) complex, **3.1** with 4-amino-3-hydroxy-1-naphthalene sulphonic acid (**AHNS**) was synthesized and characterized. Upon addition of NO, the Cu(II) center of the complex **3.1** in methanol medium was found to undergo reduction through unstable [Cu^{II}-NO] intermediate. The formation of the intermediate was evidenced by UV-visible and FT-IR spectroscopy. The reduction of the Cu(II) center was accompanied with simultaneous C-nitrosation of the aromatic ring of the ligand. The C-nitroso product was responsible for fluorescence enhancement for the complex **3.1** after its reaction with NO. Hence complex **3.1** can be used as a fluorescence based NO sensor.

3.1 Introduction

Nitric oxide (NO) is produced by inducible and constitutive nitric oxide synthases (iNOS and cNOs), resulting in a wide range of concentration in biological systems.[1-3] Depnding on its concentration and location, NO can have diverse biological functions. At low concentrations, NO regulates vasodilation in the circulatory system and long term potentiation in the brain. In contrast, micromolar concentration of NO can trigger the formation of reactive nitrogen species (RNS), leading to carginogenesis and neurodegenerative disorders but also providing a defense against pathogens. These essentially inspired a wide range of research to identify the precise roles of NO in biology. To study the NO induced reactions in cellular systems, most challenging aim is to detect the location of its formation. Thus, a selective probe to detect the formation and migration of NO with spatiotemporal resolution is highly desirable. In this aspect, the fluorescence-based detection technique is found to satisfy almost all the requirements.[4,5] A number of metal complex-based fluorescence sensors for NO are reported recently based on fluorophore displacement strategy.[6-11]

In aqueous medium, since the replacement of the fluorophore ligand from the metal can also be achieved by water, the turn-on fluorescence may also be possible in absence of NO. Hence, the reduction of metal center by NO has been found to be a more effective strategy. The fluorescence intensity of a ligand comprising a fluorophore is expected to be quenched on its complexation with paramagnetic Cu(II) center and the reduction of Cu(II) center to diamagnetic Cu(I) by NO will restore the quenched fluorescence intensity of the fluorescent ligand.[12-18]

In continuation to our study of the reduction of Cu(II) complexes by NO and ligand nitrosation, we report here the NO reactivity of Cu(II) complex of a naphthol derivative and utilizing this complex as NO sensor.

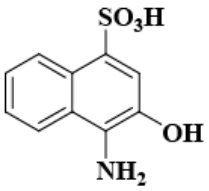

Figure 3.1: Ligand (**AHNS**) used for the present study.

3.2 Results and discussion

The ligand, 4-amino-3-hydroxy-1-naphthalene sulphonic acid (**AHNS**) was purchased from commercial source. Cu(II) complex, **3.1**, was synthesized by refluxing a mixture of copper(II) perchlorate hexahydrate and two equivalent of the ligand, **AHNS** in methanol (Scheme 3.1).

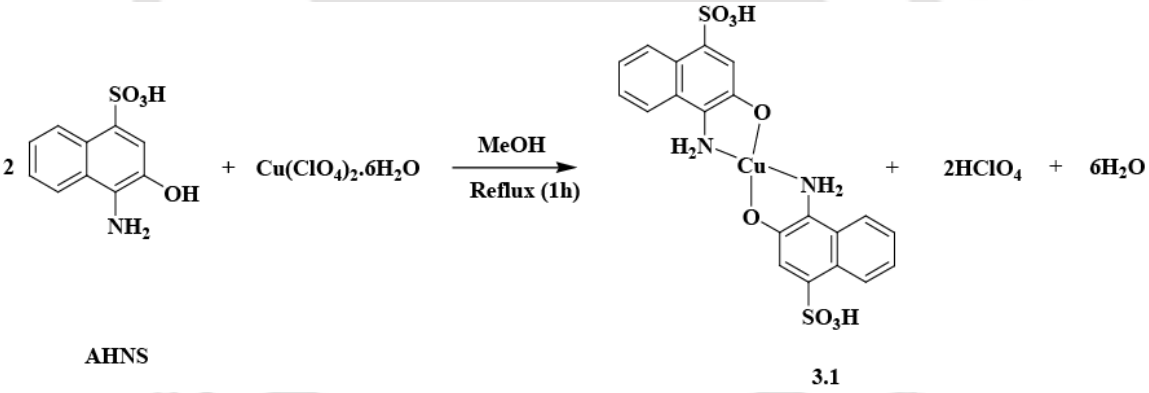

Scheme 3.1

The complex was characterized by various spectroscopic analyses as well as by elemental analysis (Experimental section). Complex **3.1** in methanol shows an absorption at 480 nm (ε, 1016 M^{-1} cm^{-1}) in the UV-visible spectroscopy with strong intra-ligand transitions in the UV region (Figure 3.2). This is attributed to the phenolate → Cu^{II} charge transfer transition. Phenolate → Cu^{II} charge transfer transition is reported to appear in this range in other examples.[19] Solution conductivity measurement in methanol indicates the neutral nature of

the complex. The absence of perchlorate vibration in the FT-IR spectrum of complex **3.1** is also in accord with the phenolate binding of the ligand to copper center (Appendix II).

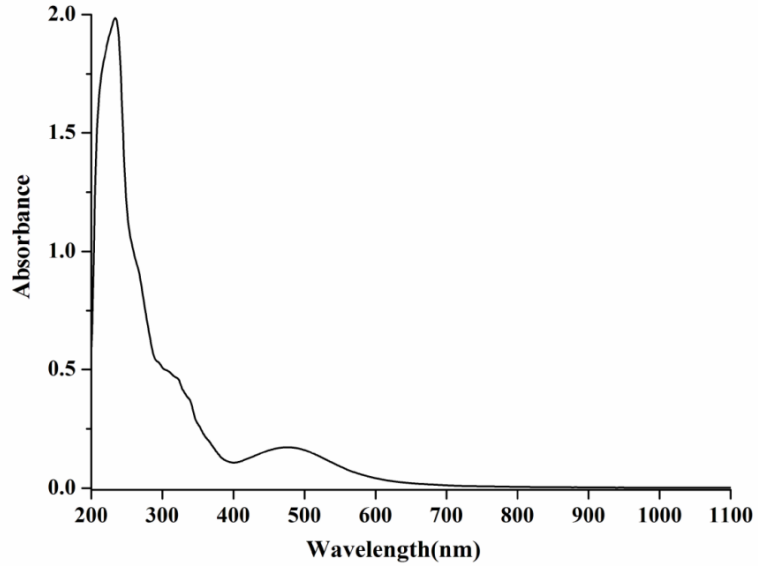

Figure 3.2: UV-visible spectrum of complex **3.1** in methanol.

The X-band EPR spectrum of the complex was recorded in methanol at 77 K and was found to be anisotropic with $g_{\parallel}$, 2.382, $g_{\perp}$, 2.101 and $A_{\parallel} = 123 \times 10^{-4}$ cm^{-1}. The spectrum is axial in nature having $g_{\parallel} > g_{\perp} > 2.0023$, indicating $d_{x^2-y^2}$ ground state which is characteristic of square planar geometry (Figure 3.3).[20]

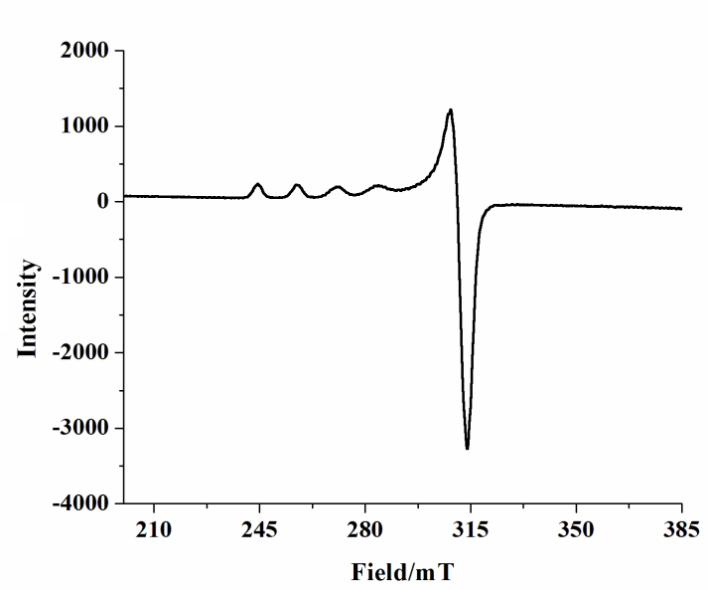

Figure 3.3: X-band EPR spectrum of complex **3.1** in methanol at 77 K.

Cyclic voltammetry studies of complex **3.1** were carried out in methanol. A single quasi-reversible couple at −0.17 V *versus* Ag/Ag^+ was observed and this has been attributed to the Cu^{II}/Cu^{I} couple (Appendix II). The Cu^{II}/Cu^{I} couple was observed to appear varyingly in the range from −0.84 to −0.66 V against SCE in the cases of Cu(II) complexes of alkyl substituted N,N′-ethylenediamine ligands and analogous reported compounds.[21] The difference in potential is attributed to the presence of an electron rich ligand framework in the present case. On the positive side of Ag/Ag^+, in the potential range of up to 1.8 V, no characteristic couple was observed.

3.3 Nitric oxide reactivity

Addition of nitric oxide (NO) gas to a degassed methanol solution of complex **3.1** resulted in the shift of the band at 480 nm to 440 nm with the concomitant formation of other band at 617 nm (Figure 3.4). The intensity of the band at 617 nm was found to decrease with time indicating the presence of an unstable intermediate (Figure 3.5).

Presumably, the intermediate is the corresponding [Cu^{II}-NO] species which decomposes to result in Cu(I) with simultaneous nitrosation of a substrate (e.g. solvent or ligand). In other reported examples, the [Cu^{II}-NO] species absorbs in the range of 610 - 640 nm in acetonitrile solvent.[22,23]

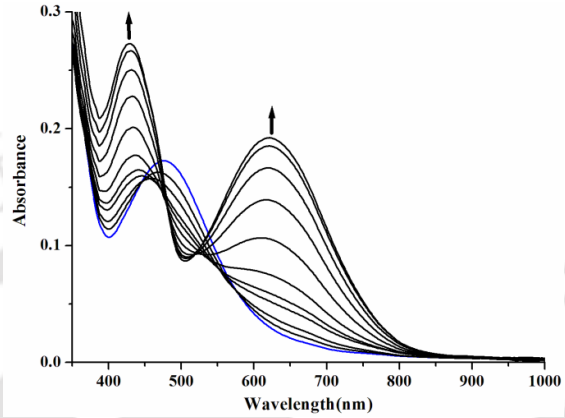

Figure 3.4: UV-visible spectra of complex **3.1** before (blue line) and after (black lines) purging NO in methanol.

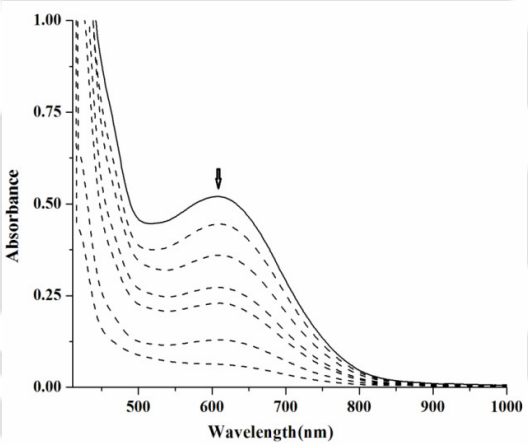

Figure 3.5: UV-visible spectra of intermediate [Cu^{II}-NO] species (solid line) and it's decay (dashed lines) in methanol at room temperature**.**

Thermal instability and moisture sensitivity precluded the isolation and further characterization of the [Cu^{II}-NO] intermediate. Though, a number of examples of [Cu^{II}-NO] intermediate have been reported recently in the reaction of Cu(II) complexes with NO, the examples of stable [Cu^{II}-NO] are still very limited. In case of $[Cu(bemim)_2]^{2+}$ {bemim = *bis*-(2-ethyl-4-methylimidazole-5-yl)methane}, in acetonitrile solution, addition of NO resulted

in the corresponding [Cu^{II}-NO] complex which has been isolated as solid.[24] The only structurally characterized [Cu^{II}-NO] complex was prepared by the reaction of corresponding Cu(I) complex with $NOBF_4$.[25]

The formation of the [Cu^{II}-NO] intermediate was further supported from the solution FT-IR spectroscopic studies. In FT-IR spectroscopy, upon addition of NO to the methanol solution of complex **3.1**, a new strong frequency at 1650 cm^{-1} appeared which is attributed to the coordinated NO stretching in the corresponding [Cu^{II}-NO] species (Figure 3.6). The intensity of the band was found to decay with time (Appendix II) and finally disappeared indicating the unstable nature of the intermediate complex.

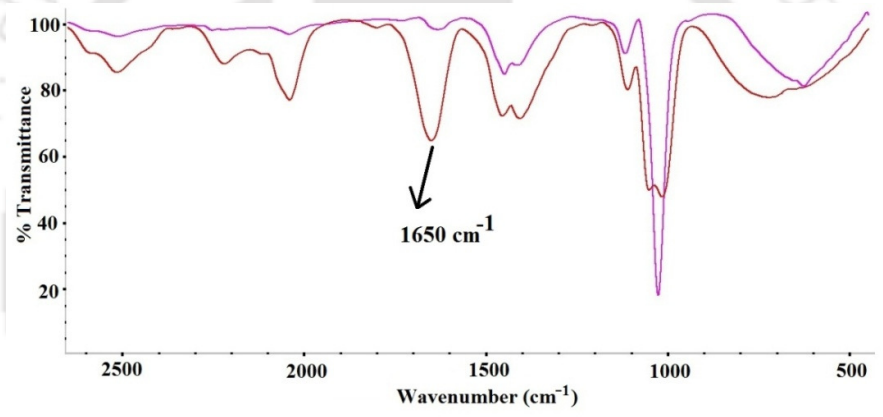

Figure 3.6: Solution FT-IR spectra of complex **3.1** before (magenta) and immediately after (red) purging NO gas in methanol at room temperature.

In case of the isolated copper(II)-nitrosyl from the reaction of $[Cu(bemim)_2]^{2+}$ and NO, it was observed at 1662 cm^{-1}.[24] For air-stable solid copper-nitrosyl of copper(II)-dithiocarbamate, the ν_{NO} appears at 1682 cm^{-1}.[26]

Hayton et al reported the appearance of ν_{NO} band at 1933 cm^{-1} for structurally characterized copper(II)-nitrosyl.[25] The stretching frequency of the nitrosyl group in metal nitrosyls are known to vary depending upon various factors like (i) charge on the metal ion, (ii) coordination geometry around the central metal, (iii) nature of the ancillary ligands present

and (iv) mode of binding of the NO to the metal. In case of Hayton's compound, the ancillary ligands were methyl nitrite and the complex was distorted octahedral with bent NO at an equatorial position. In the present case, the FT-IR of the nitrosyl complex was recorded in methanol solution. The copper(II) ion is coordinated to the chelating ligand, **AHNS** through electron rich phenolate moiety. These might have caused such a large variation of the nitrosyl stretching frequency. The intermediate species, as expected was EPR silent (Appendix II).

The decay of the 617 nm band in UV-visible spectroscopy is attributed to the reduction of the Cu(II) center with concomitant formation of NO^+. The reduction was further supported by the EPR silent nature of the colorless reaction mixture.

Removal of copper ion from the reaction mixture followed by isolation and characterization of the modified ligand suggests the formation of 4-amino-3-hydroxy-1-nitrosonaphthalene (**AHNN**) (Experimental section) (Scheme 3.2).

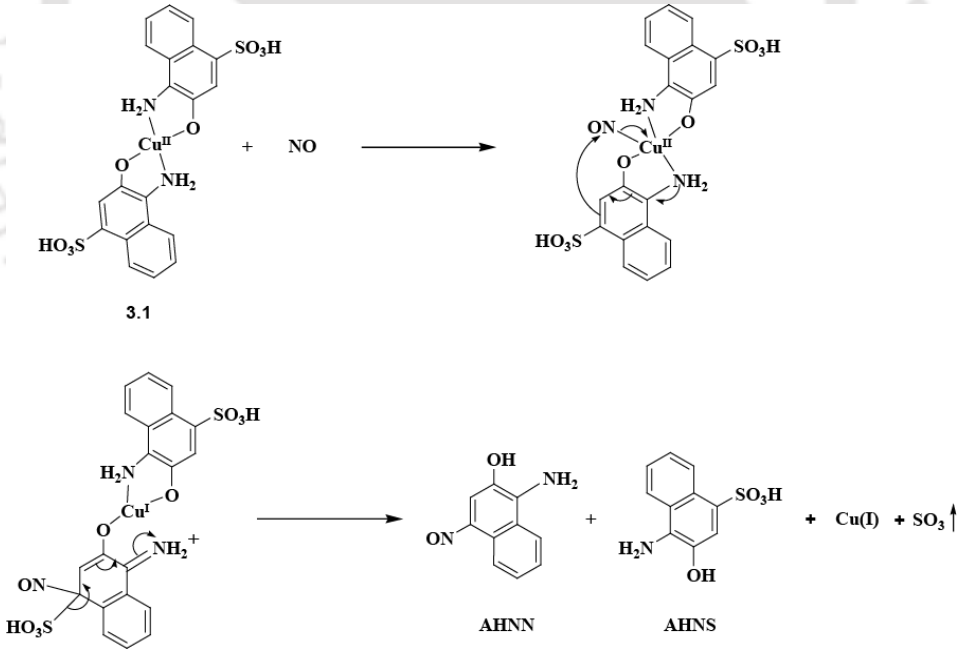

Scheme 3.2 Probable mechanism of the reaction.

Nitrosation of arenes was achieved mostly by using nitrosonium salt such as nitrosonium tetrafluoroborate in acetonitrile under inert atmosphere.[27,28] Degassed trifluoroacetic acid

under NO atmosphere has also been used for successful nitrosation of some arenes like toluene, 1,2-dimethyl benzene and 1,3-dimethyl benzene etc.[27,28] In these cases also the reaction was reported to proceed through the formation of nitrosonium ion. In case of phenols and naphthols nitrous acid, sodium nitrite/trifluoroacetic acid, nitrosonium tetrafluoroborate, nitrosyl sulphuric acid, sulphuric acid under NO atmosphere etc. are common and successful agent for nitrosation reactions.[29] On the other hand, aromatic amines undergo direct nitrosation by nitrous acid or sodium nitrite and HCl mixture.[29] For aromatic secondary amines, nitrosation initially occurs at nitrogen resulting in N-nitrosoamine which then undergoes Fischer-Hepp rearrangement in acidic medium to yield *para*-nitrosoamine product.[30,31] In majority of the cases, the nitrosation occurs through nitrosonium ion. In case of primary aromatic amines, the presence of NO^+ may lead to the diazotization rather than nitrosation.[23] C-nitroso arenes are also reported to form through nitrosative decarboxylation in presence of NO^+.[32] $[1,3,5\text{-}Me_3C_6H_3NO]PF_6$ is also reported to induce arene nitrosation.[24,25] On the other hand, C-nitrosation at the active methylene position of β-diketiminate ligand framework by NO is also known though not explored much.[33]

In the present study, though there is no direct evidence of formation of NO^+, it is now established that the reduction of Cu(II) by NO leads to the formation of NO^+. The NO^+ formed during the reduction of Cu(II) by NO presumably attacks the naphthalene ring at sulphonic acid position to yield the modified ligand through an intramolecular pathway. To check this, the same reaction was carried out in presence of *p*-toluene sulphonic acid. The formation of *p*-nitroso toluene was not observed. This suggests the involvement of an intramolecular mechanism in the present case (Scheme 3.2). The presence of SO_3^- stretching frequency in the FT-IR spectrum of the intermediate complex indicates the release of sulphonate group after the decomposition of the copper(II)-nitrosyl complex. The liberated SO_3 was trapped by passing through an 80% isopropanol/water mixture. Quantification has

been done by titrating SO_3 trapped in 80% isopropanol/water solution using $BaCl_2$ in presence of thorin indicator (Experimental section). This confirms the release of ~70% SO_3 from the reaction. The desulphonation of aromatic rings are known with H^+, Br^+ or NO_2^+.[34] In all the cases, it takes place through the initial attack by the electrophile at the C-center attached with the $–SO_3H$ group. However, desulphonation of aromatic ring by NO^+ is not known. On the other hand, nitrosative decarboxylation of arenes are well known in literature. In this case also, initially NO^+ attacks the C-center attached to the $–CO_2H$ group prior to decarboxylation.[32]

The role of NO^+ in the reaction was further confirmed by the addition of $NOClO_4$ in the free ligand (Experimental section). This results in the formation of **AHNN.**

It should be noted that [Cu^{II}-NO] complexes are known to afford methyl nitrite upon reaction with methanol.[35] In the present reaction case, we have observed the formation of methyl nitrite in a negligible (~5%) quantity. This is also in accord with the intramolecular/concerted mechanism of the reaction.

NO itself, under degassed condition was not found to react with the free ligand, **AHNS**. However, under aerobic condition, it reacts with the ligand and results in the formation of sodium naphtho[1,2-d][1,2,3]oxadiazole-5-sulfonate (**NODS)** (Scheme 3.3). This reaction perhaps takes place through a cascade of reactions that starts with the air oxidation of NO to NO_2. It somewhat similar to that observed in cases of the reaction of NO with *o*-diamines.[30]

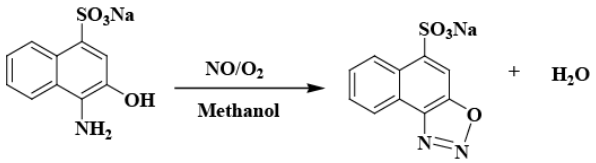

AHNS **NODS**

Scheme 3.3

Though, it resembles to the synthesis of azo compounds *via* diazaotization or coupling reactions, a significant difference was observed. Diazotization are known to take place in acidic medium; however, here the reaction occurs readily in neutral (pH, ~ 7.2) and even in basic condition (pH, ~9). Analogous example was reported in case of NO_{550} where electrophilic aromatic substitution on the electron deficient nitroso-amine was observed yielding a hydroxyl hydrazine derivative; which on subsequent water elimination results in the formation of AZO_{550} (Appendix II). [36]

3.4 Fluorescence study

Since the free ligand is not highly soluble in methanol, for fluorescence study the mono sodium salt of the ligand (**NaAHNS**) was used. It shows absorption band with λ_{max} at 350 nm (ε/lit $mol^{-1}cm^{-1}$, 1020) in methanol. Upon excitation at 350 nm, significant fluorescence emission was observed centered at 435 nm in methanol or water at room temperature. The quantum yield was found to be 0.207 in methanol with respect to quinine sulfate.

The fluorescence emission band of **NaAHNS** centered at 435 nm was found to disappear upon addition of equivalent amount of Cu(II) ion (Figure 3.7). Addition of NO gas to this solution restores the emission. This is because of the formation of **AHNN**, which is evidenced from the shift of UV-visible absorption band from 480 nm (in case of complex **3.1**) to 440 nm (after purging NO to the solution of complex **3.1**).

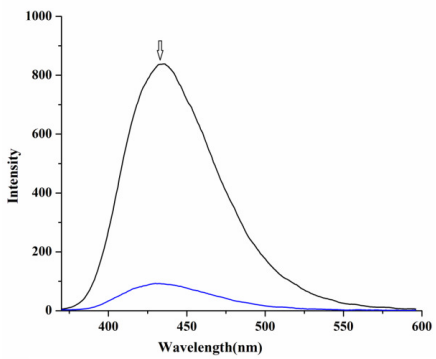

Figure 3.7: Fluorescence responses upon excitation at 350 nm for 20 μM solution of **NaAHNS** (black line) and after addition of 10 μM of $Cu(ClO_4)_2.6H_2O$ (blue line) in methanol.

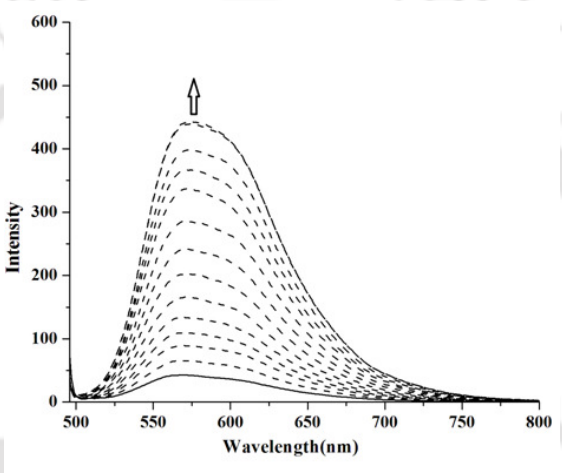

Figure 3.8: Fluorescence enhancement upon excitation at 440 nm of 20 μM solution of complex **3.1** (solid line) and after addition of 1 equivalent of NO (dashed lines) in methanol with time.

The change in excitation wavelength from 350 nm to 440 nm results in a strong emission centered at 580 nm from the dark background. This is attributed to the emission of **AHNN** and has been confirmed with free **AHNN**, also. Similar result was observed upon addition of equivalent amount of $NOClO_4$ as a source of NO^+ in methanol solution of **NaAHNS** which in turn confirms the involvement of NO^+ .

3.5 Conclusion

Copper(II) complex, **3.1** with 4-amino-3-hydroxy-1-naphthalene sulphonic acid (**AHNS**) was synthesized and characterized. Upon addition of NO, the Cu(II) center of the complex **3.1** in

methanol was found to undergo reduction through unstable [Cu^{II}-NO] intermediate. The reduction of the Cu(II) center was accompanied with simultaneous C-nitrosation of the aromatic ring of the ligand. The C-nitroso product was responsible for fluorescence enhancement for the complex **3.1**. Hence complex **3.1** can be used as a fluorescence-based NO sensor.

3.6 Experimental Section

3.6.1 General Methods

All reagents and solvents were purchased from commercial sources and were of reagent grade. Deoxygenation, wherever necessary, of the solvents and solutions were done by repeated vacuum/purge cycles or bubbling with argon for 30 minutes. NO gas was purified by passing through KOH and P_2O_5 column. UV-visible spectra were recorded on a Perkin Elmer Lamda 25 UV-visible spectrophotometer. FT-IR spectra were taken on a Perkin Elmer spectrophotometer with samples prepared as KBr pellets. The fluorescence spectra were recorded in solution in VARIAN Cary Eclipse Fluorescence Spectrophotometer at room temperature. Quinine sulphate in acidic medium was used as the reference compound for the determination of fluorescence quantum yield. ^{1}H- NMR spectra were obtained with a 400 MHz Varian FT spectrometer. Chemical shifts (ppm) were referenced either with an internal standard (Me_4Si) for organic compounds or to the residual solvent peaks. The X-band Electron Paramagnetic Resonance (EPR) spectra were recorded on a JES-FA200 ESR spectrometer, at room temperature and 77 K with microwave power, 0.998 mW; microwave frequency, 9.14 GHz and modulation amplitude, 2. Elemental analyses were obtained from a Perkin Elmer Series II Analyzer. The magnetic moment of complexes was measured on a Cambridge Magnetic Balance. The electrical conductivity of the complex in solution was measured using a Sytronic 305 conductivity bridge.

For the electrochemical studies, a Pt working electrode, Pt wire auxiliary electrode and a Ag/Ag^+ reference electrode were used in a three-electrode configuration. All electrochemical measurements were performed at 298 K under a nitrogen atmosphere in acetonitrile containing tetra-butyl ammonium perchlorate (TBAP) as a supporting electrolyte. The scan rate used was 50 mV s^{-1}. The half-wave potential E^0_{298} was set equal to 0.5 (E_{pa} + E_{pc}), where E_{pa} and E_{pc} are the anodic and cathodic cyclic voltammetric peak potentials, respectively. All the electrochemical data are uncorrected for a junction potential.

3.6.2 Synthesis of complex 3.1

Copper(II) perchlorate hexahydrate (0.370 g, 1 mmol) was dissolved in 10 ml distilled methanol. To this solution, 0.478 g (2 mmol) of the ligand **AHNS**, was added slowly with constant stirring. The color of the solution turned into reddish brown from light blue. The reaction mixture was stirred and refluxed for 1 h. The volume of the solution was then reduced to ~2 ml. To this, 5 ml of diethyl ether was added to make a layer on it and kept it overnight on freezer. This resulted into the precipitation of complex **3.1** as deep brown solid. Yield: 0.680 g (~ 80%). Elemental analyses for $C_{21}H_{20}N_2O_9S_2Cu$: Calcd (%): C, 44.09; H, 3.52; N, 4.90. Found (%): C, 44.13; H, 3.51; N, 4.99. UV-visible (methanol): λ_{max}, 480 nm (ε, 1016 M^{-1} cm^{-1}). X-band EPR: $g_{\parallel}$, 2.382, $g_{\perp}$, 2.101 and $A_{\parallel}$ = 123 × 10^{-4} cm^{-1}. FT-IR (in KBr pellet): 1621, 1541, 1183, 1049, 766, 656 cm^{-1}. μ_{eff}, 1.53 BM.

3.6.3 Isolation of AHNN

Complex **3.1** (0.538 g, 1 mmol) was dissolved in 20 ml of dry methanol. The solution was degassed by bubbling Ar for 30 minutes. To this solution $NO_{(g)}$ was purged for ~ 1-2 minute and the mixture was then kept at room temperature for 4 h while the color of the solution turned yellowish. The excess NO was removed then by applying several cycles of vacuum and Ar purge. The reaction mixture was then opened to air and stirred for 2 h to ensure

complete oxidation of the Cu(I) to Cu(II). The volume of the solution was then reduced to 5 ml and 25 ml of water was added. To this 5 ml saturated aqueous solution of Na_2S was added and stirred for ½ h while black precipitate of CuS appeared. The precipitate was filtered off. The organic part was extracted from the solution using $CHCl_3$ (30 ml × 3 portions). After removal of the solvent under reduced pressure, the crude organic mass was subjected to column chromatography on neutral alumina to get the unreacted ligand, **AHNS** and modified ligand **AHNN** as yellowish oil. Yield of **AHNN**: 150 mg (~ 40%). Elemental analyses for **AHNN**, $C_{10}H_8N_2O_2$: Calcd (%): C, 63.82; H, 4.28; N, 14.89; found (%): C, 63.85; H, 4.27; N, 14.80. FT-IR (in KBr pellet): 2924, 1685, 1607, 1243, 1043, 722 cm^{-1}. ^{1}H-NMR (400 MHz, $CDCl_3$) δ_{ppm}: 8.12 (m, 2H), 7.67 (m, 2H), 6.16 (s, 1H). ^{13}C-NMR: (100 MHz, $CDCl_3$) δ_{ppm}: 185.0, 180.3, 160.6, 134.5, 133.5, 132.2, 131.2, 126.9, 126.4, 110.1. ESI-mass ($m+Na^+$): Calcd. 211.06; found, 211.02.

Yield of unreacted **AHNS**, ~40%.

3.6.4 Isolation of AHNN from the reaction of AHNS with $NOClO_4$

Sodium 4-amino-3-hydroxynaphthalene-1-sulfonate (**NaAHNS**) (0.65 g, 2.5 mmol) was dissolved in 20 ml dried methanol under Ar atmosphere in a 50 ml round bottom flask fitted with a stirring bar. To this solid $NOClO_4$ (~3 mmol) was added under Ar flow. The reaction mixture was stirred for 1h at room temperature. The solvent was then dried under reduced pressure. To the solid mass thus obtained, 30 ml of distilled water was added. The organic part was extracted with chloroform (25 ml × 3 portions). Removal of solvent followed by chromatographic purification afforded pure **AHNN.** Yield: 155 mg (~ 82%).

3.6.5 Isolation of NODS

Sodium 4-amino-3-hydroxynaphthalene-1-sulfonate (**NaAHNS**) (1.31 g, 5 mmol) was dissolved in 20 ml distilled methanol. To this solution, NO gas was bubbled through a needle

for 1-2 minute and then oxygen gas was bubbled for 1 minute. The dark red color of the solution turned pink. Then the excess of gases were removed by vacuum and Ar purging and the solution mixture was dried under reduce pressure. The solid compound obtained was washed with diethyl ether to get the pure compound **NODS**. Yield: 1.08 g (~80%). Elemental analyses for $C_{10}H_5N_2O_4SNa$: Calcd(%): C, 44.12; H, 1.85; N, 10.29; found (%): C, 44.17; H, 1.86; N, 10.22. FT-IR (in KBr pellet): 2086, 1609, 1571, 1217, 1060, 749, 648 cm^{-1}. ^{1}H-NMR (400 MHz, D_2O) δ_{ppm}: 8.25 (t, 1H), 7.47 (m, 1H), 7.30 (t, 1H), 7.19 (m, 1H), 6.99 (m, 1H). ^{13}C-NMR: (100 MHz, DMSO-d_6) δ_{ppm}: 134.9, 132.1, 131.4, 130.9, 128.0, 127.4, 126.5, 126.3, 118.1. ESI-mass ($m+2K^+$): Calcd. 327.15; found, 327.26.

3.6.6 Estimation of SO_3 released during reaction

Complex **3.1** (500 mg) was dissolved in 20 ml dry methanol in a 50 ml Schlenk flask connected with another flask containing 20 ml of degassed isopropanol-water mixture (4:1) by a rubber tubing. The stopper of both the flask kept closed and NO gas was purged through the solution of complex **3.1** for 30 sec. The excess of NO gas was removed by applying several cycles of vacuum and Ar purge. The reaction was allowed to stir at room temperature. The stoppers of both the flask were released and Ar gas was allowed to bubble though the reaction mixture by a long needle. This ensures the flushing out of all SO_3 produced from the reaction vessel through the isopropanol solution. It was continued for 2 h. Then 5 drops of 10% thorin solution was added to it and titrated against 0.005 N $BaCl_2$ till the pink end point. Observed yield of SO_3 is ~70%.

3.7 References

1. Murad, F. *Angew. Chem. Int. Ed*. **1999**, *38*, 1856.
2. Moncada, S.; Palmer, R. M. J.; Higgs, E. A. *Pharmacol. Rev*. **1991**, *43*, 109.
3. Conner, E. M.; Grisham, M. B. *Methods Enzymol* **1995**, *7*, 3.
4. Hilderbrand, S. A.; Lim, M. H.; Lippard, S. J. *Topics in Fluorescence Spectroscopy*, C. D. Geddes and J. R. Lakowicz, Springer, Berlin, 2005; p. 163.
5. Sasaki, E.; Kojima, H.; Nishimatsu, H.; Urano, Y.; Kikuchi, K.; Hirata, Y.; Nagano, T. *J. Am. Chem. Soc.* **2005**, *127*, 3684.
6. Franz, K. J.; Singh, N.; Lippard, S. J. *Angew. Chem Int. Ed.* **2000**, *39*, 2120.
7. Franz, K. J.; Singh, N.; Spingler, B.; Lippard, S. J. *Inorg. Chem.* **2000,** *39*, 4081.
8. Hilderbrand, S. A.; Lim, M. H.; Lippard, S. J. *J. Am. Chem. Soc.* **2004**, *126*, 4972.
9. Lim, M. H.; Lippard, S. J. *Inorg. Chem.* **2004**, *43*, 6366.
10. Lim, M. H.; Kuang, C.; Lippard, S. J. *ChemBioChem*. **2006**, *7*, 1571.
11. Hilderbrand, S. A.; Lippard, S. J. *Inorg. Chem.* **2004**, *43*, 5294.
12. Lim, M. H.; Lippard, S. J. *Inorg. Chem.* **2006**, *45*, 8980.
13. Lim, M. H.; Lippard, S. J. *J. Am. Chem. Soc.* **2005**, *127*, 12170.
14. Smith, R. C.; Tennyson, A. G.; Lim, M. H.; Lippard, S. J. *Org. Lett.* **2005**, *7*, 3573.
15. Dı´az, A.; Ortiz, M.; Sa´nchez, I.; Cao, R.; Mederos, A.; Sanchiz, J.; Brito, F. *J. Inorg. Biochem.* **2003**, *95,* 283.
16. Tran, D.; Skelton, B. W.; White, A. H.; Laverman, L. E.; Ford, P. C. *Inorg. Chem.* **1998**, *37,* 2505.
17. Tsuge, K.; DeRosa, F.; Lim, M. D.; Ford, P. C. *J. Am. Chem. Soc.* **2004**, *126*, 6564.
18. Lim, M. H.; Xu, D.; Lippard, S. J. *Nat. Chem. Biol.* **2006**, *2,* 375.
19. (a) Kumar, V.; Kalita, A.; Mondal, B. *Dalton Trans*., **2013**, *42*, 16264. (b) Jazdzewski, B. A.; Tolman, W. B. *Coord. Chem. Rev*., **2000**, *200*, 633.

20. (a) Mendola, D. L.; Magri, A.; Vagliasindi, L. I.; Hansson, O.; Bonomo, R. P.; Rizzarelli, E. *Dalton Trans*. **2010**, *39*, 10678. (b) Hathaway, B. J. *Coord. Chem. Rev*. **1970**, *5*, 143.

21. (a) Ghachtouli, S. E.; Cadiou, C.; Déchamps-Olivier, I.; Chuburu, F.; Aplincourt, M.; Turcry, V.; Baccon, M. L.; Handel, H. *Eur. J. Inorg. Chem.* **2005**, 2658. (b) Sarma, M.; Mondal, B. *Dalton Trans*. **2012**, *41*, 2927.

22. (a) Sarma, M.; Kalita, A.; Kumar, P.; Singh, A.; Mondal, B. *J. Am. Chem. Soc.* **2010**, *132*, 7846. (b) Sarma, M.; Mondal, B. *Inorg. Chem*. **2011**, *50*, 3206.

23. (a) Kalita, A.; Kumar, P.; Deka, R. C.; Mondal, B. *Inorg. Chem.* **2011**, *50*, 11868. (b) Sarma, M.; Kumar, V.; Kalita, A.; Deka, R. C.; Mondal, B. *Dalton Trans*. **2012**, *41*, 9543. (c) Kumar, P.; Kalita, A.; Mondal, B. *Dalton Trans.* **2013**, *42*, 5731.

24. Kalita, A.; Kumar, P.; Deka, R. C.; Mondal, B. *Chem. Commun.* **2012**, *48*, 1251.

25. Wright, A. M.; Wu, G.; Hayton, T. W. *J. Am. Chem. Soc.* **2010**, *132*, 14336.

26. Diaz, A.; Ortiz, M.; Sanchez, I.; Cao, R.; Mederos, A.; Sanchiz, J.; Brito, F. *J. Inorg. Biochem.* **2003**, *95*, 283.

27. Bosch, E.; Kochi, J. K. *J. Org. Chem.* **1994**, *59*, 5573.

28. Atherton, J. H.; Moodie, R. B.; Noble, D. R. *J. Chem. Soc., Perkin Trans.* **1999**, *2,* 699.

29. Adams, R.; Coleman, G. H. *Organic Synthesis*; Wiley & Sons: New York, 1941; Collective Volume 1, p 214.

30. Jin, D.; Mendenhall, G. D. *Tetrahedron Lett.* **1996**, *37*, 4881.

31. Radner, F.; Wall, A.; Loncar, M. *Acta Chem. Scand.* **1990**, *44*,152.

32. Ibne-Rasa, K. M. *J. Am. Chem. Soc*. **1962**, *84*, 4962.

33. Melzer, M. M.; Mossin, S.; Cardenas, A. J. P.; Williams, K. D.; Zhang, S.; Meyer, K.; Warren, T. H. *Inorg. Chem*. **2012**, *51*, 8658.

34. (a) Cannell, I. C. *J. Am. Chem. Soc.* **1957***, 79*, 2927. (b) Lisitsyn; V. N.; Stankevich, G. S. *Zhurnal Organicheskoi Khimii*. **1977**, *13*, 1286.

35. Tran, D.; Ford, P. C. *Inorg. Chem.* **1996**, *35*, 2411.

36. Yang, Y.; Seidlits, S. K.; Adams, M. M.; Lynch, V. M.; Schmidt, C. E.; Anslyn, E. V.; Shear, J. B. *J. Am. Chem. Soc.* **2010**, *132*, 13114.

Chapter 4

Copper(II) complex as a selective turn on fluorosensor for nitric oxide and its intracellular application

Abstract

A highly water soluble copper(II) complex, **4.1** of a fluorophore ligand 4-(2-hydroxybenzylamino)-5-hydroxynaphthalene-2,7-disulfonic acid (**HBNS)** was synthesized and characterized. The nitric oxide (NO) induced fluorescence enhancement of complex **4.1** occurred by reduction of Cu(II) to Cu(I) with subsequent dissociation of the N-nitrosated fluorophore ligand from copper ion. The selective turn on fluorogenic nature of the complex **4.1** was used to study the endogenously produced NO in living cells.

4.1 Introduction

Nitric oxide (NO) is produced in biological systems by nitric oxide synthases (NOS).[1-3] It has been identified as an important signalling agent in the immune response, cardiovascular, and nervous system.[4-6] In order to understand the precise roles of NO in biological systems, different strategies have been developed to sense it .[7-11] Amongst the strategies used to detect NO directly or indirectly, the fluorescent probes are found to offer some distinct advantages over the others. Water solubility, cell-membrane permeability, visible excitation and emission wavelengths are amongst the basic requirements necessary to design a biologically useful fluorescent NO probe.[12,13] In addition, these sensors must have the ability for direct, specific, and rapid detection of NO. For imaging in biological systems, the most preferred sensors are those that enhance the fluorescence upon reaction with NO. The general strategy for NO sensing is to coordinate a fluorophore ligand to a metal ion to quench the fluorescence, which is restored by the interaction of NO with the metal center.[13,14]

This chapter describes a highly water soluble Cu(II) complex of a fluorophore ligand,4-(2-hydroxybenzylamino)-5-hydroxynaphthalene-2,7-disulfonic acid (**HBNS**) which detects NO in methanol and aqueous media. This complex exhibits turn-on fluorescence emission *via* NO induced nitrosation of the fluorophore. This probe has been utilized for the detection of NO in living cells.

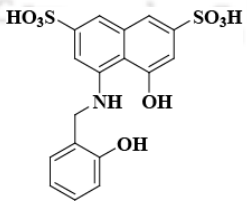

Figure 4.1: Ligand used for the present study.

4.2 Results and discussion

The ligand, **HBNS** was prepared by reduction of azomethine–H monosodium salt hydrate with sodium borohydride in methanol medium (Experimental section). Microanalyses, FT-IR, ^{1}H and ^{13}C-NMR and ESI-mass spectral analyses confirmed the formation of the ligand unambiguously (Experimental section). Cu(II) complex, **4.1**, was synthesized by reacting copper(II) perchlorate hexahydrate with equivalent amount of ligand **HBNS** in methanol medium (Scheme 4.1).

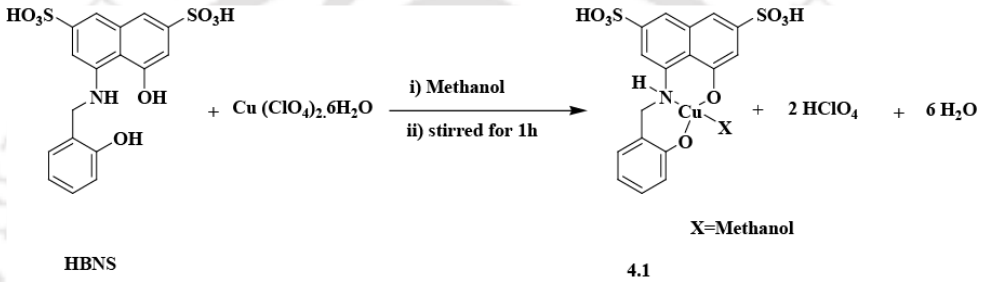

Scheme 4.1

Complex **4.1** was characterized by various spectroscopic analyses as well as by elemental analyses (Experimental section). Even after several attempts we could not grow the X-ray quality single crystals. Complex **4.1** in methanol shows absorption at 460 nm (ε, 2500 M^{-1} cm^{-1}) in UV-visible spectroscopy (Figure 4.2). The band is assigned to the phenolate-Cu(II) charge transfer transition. This transition is reported to appear in this range in other examples.[15] The bands at 762 nm and 850 nm is due to the *d-d* transition of the Cu(II) ion.

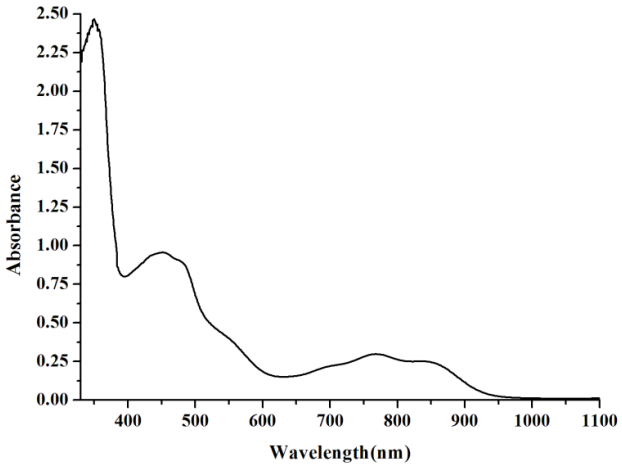

Figure 4.2: UV-visible spectrum of complex **4.1** in methanol.

Solution conductivity in methanol shows the neutral nature of the complex **4.1**. The absence of perchlorate vibration in the FT-IR spectrum supports the phenolate binding of the ligand to copper center. The X-band EPR spectrum of the complex **4.1** was recorded in methanol at 77 K and the calculated values are, $g_{\parallel}$, 2.402, $g_{\perp}$, 2.100 and $A_{\parallel}$, 122.089×10^{-4} cm^{-1} (Figure 4.3). The values suggest a square planar geometry around the Cu(II) center with $d_{x^2-y^2}$ ground state.[16]

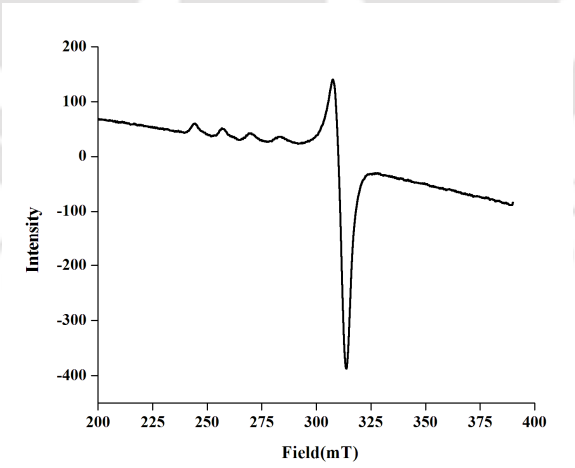

Figure 4.3: X-band EPR spectrum of complex **4.1** in methanol at 77 K.

4.3 Nitric oxide reactivity

Addition of NO gas in the degassed methanol solution of complex **4.1** resulted in the reduction of Cu(II) center to Cu(I). The reduction was monitored by UV-visible spectroscopy. The *d-d* band of complex **4.1** disappeared in presence of NO suggesting the formation of Cu(I) (Figure 4.4). In X-band EPR spectroscopy, the characteristic signals of Cu(II) disappeared upon addition of NO in the methanol solution of complex **4.1** and the reaction mixture became EPR silent (Figure 4.5). This is attributed to reduction of paramagnetic Cu(II) to diamagnetic Cu(I). Further, in ^{1}H-NMR spectroscopy, the broad signals from complex **4.1** became sharp and well resolved after addition of NO. This also supports the reduction of Cu(II) (Appendix III). Earlier, it was noticed that the reduction of Cu(II) center by NO leads to the nitrosation of the secondary amine of the ligand framework. In the present case, isolation and characterization of the ligand after the reaction of the complex with NO, reveals N-nitrosation. The stretching band at ~1450 cm^{-1} in FT-IR

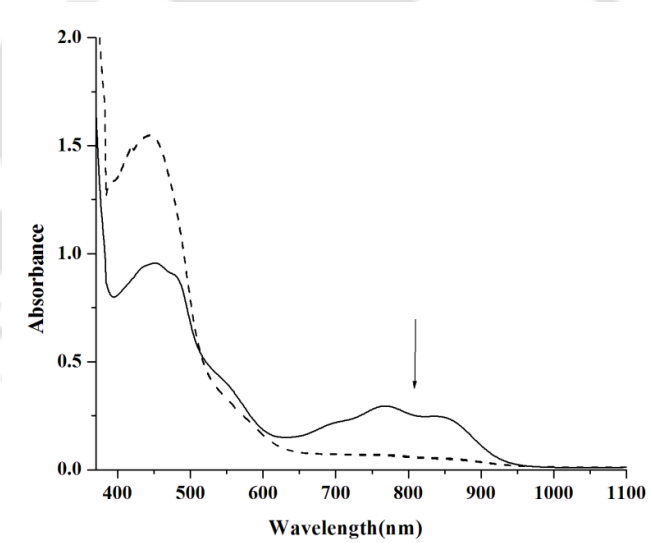

Figure 4.4: UV-visible spectra of complex **4.1** before (solid line) and after addition of NO (dashed line) in methanol.

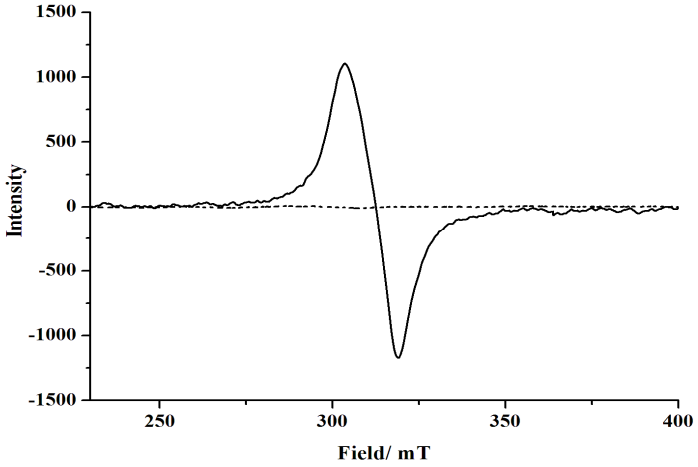

Figure 4.5: X-band EPR spectra of complex **4.1** in methanol before (solid line) and after addition of NO (dotted line) at 298 K.

spectroscopy indicates the presence of N-NO in the modified ligand (Appendix III). Other characterization including mass, ^{1}H-NMR and ^{13}C-NMR spectroscopy, suggest N-nitrosation unambiguously (Experimental section). The reaction of complex **4.1** with NO was also studied in aqueous medium buffered at pH, 7.2. NO induced reduction of the Cu(II) center was observed in this case also. However, N-nitrosation of the ligand was not observed owing to the faster reaction of NO^{+} with water. This was confirmed by the presence of NO_2^{-} stretching frequency in the FT-IR spectrum of the crude reaction mixture. On the other hand, by Greiss test with the crude reaction mixture, the presence of NO_2^{-} was authenticated.[17] NO_2^{-} formation in the reduction of Cu(II) by NO in water was reported earlier in cases of Cu(II) complexes of tren, mimpea and pepma [tren = tris(2-aminoethyl)amine; mimpea = 1-methyl-1H-imidazol-2-ylmethyl)-(2-pyridin-2-yl-ethyl)amine; pepma = (2-pyridin-2-yl-ethyl)-pyridin-2 ylmethylamine][18].

4.4 Fluorescence study

Ligand **HBNS** shows significant fluorescence emission upon excitation at 320 nm in methanol solution at room temperature. The quantum yield was found to be 0.21 with respect

to quinine sulfate in methanol. The fluorescence emission of **HBNS** centered at 410 nm was found to disappear upon the addition of equivalent amount of Cu(II) ion in methanol medium. In this case fluorescence displayed a significant (>90%) quenching of the ligand fluorescence (Figure 4.6).

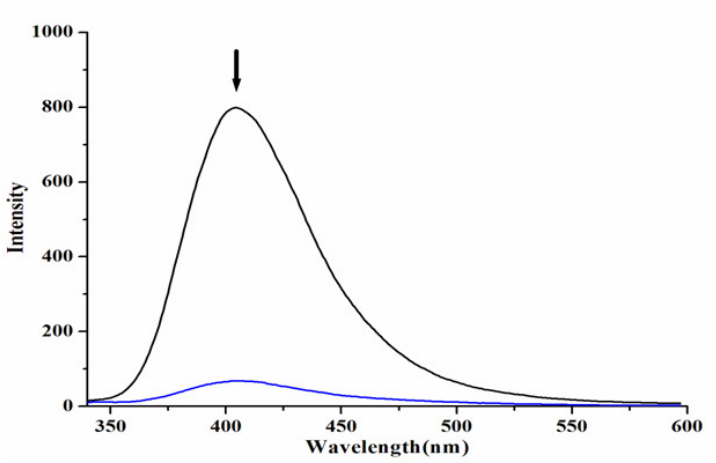

Figure 4.6: Fluorescence responses (λ_{ex}, 320 nm) of 20 μM solution of free ligand **HBNS** (black line) and after addition of 20 μM of $Cu(ClO_4)_2.6H_2O$ (blue line) in methanol medium.

Addition of NO gas to this solution was found to restore the emission intensity significantly at 350 nm and 375 nm (Figure 4.7). The blue shifting of the emission wave length was probably due to the modification of the ligand framework after reaction of the complex **4.1** with NO gas. The restored intensity in the complex **4.1** starts appearing within 10 seconds of NO addition and becomes (9±1) fold increment of fluorescence intensity in 10 minutes.

For earlier reported complexes such as $[Cu(Ds\text{-}en)_2]$ and $[Cu(Ds\text{-}AMP)_2]$, the quenching of the ligand fluorescence intensity upon addition of Cu(II) were 31(±2) and 23(±0.5)-fold relative to free ligands, Ds-Hen and Ds-HAMP (40 μM), respectively.[19] Addition of 100 equivalent of NO to the methanol or buffered aqueous solution of the complexes $[Cu(Ds\text{-}en)_2]$ and $[Cu(Ds\text{-}AMP)_2]$, restored the emission intensity significantly with 6.1 (±0.2) and 8.8 (±0.1) fold, enhancements respectively.[19] In the present case the restored emission intensity was found to be 9 (±1) fold in methanol.

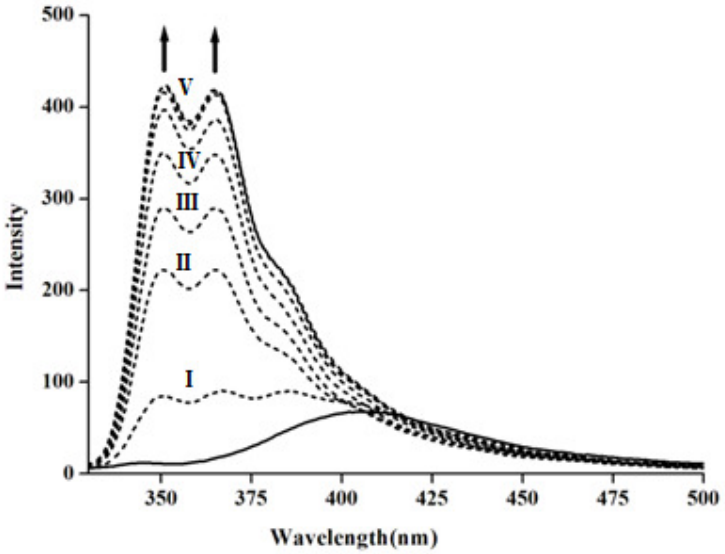

Figure 4.7: Fluorescence responses (λ_{ex}, 320 nm) of deoxygenated methanol solution of complex **4.1** (20 μM) before (solid line) and after addition of equivalent amount of NO (dashed lines) at 2, 4, 6, 8, and 10 minutes at 298 K (lines I– V, respectively).

Addition of NO gas in degassed buffered aqueous solution of complex **4.1** was found to restore the emission intensity (Figure 4.8). The enhancement of the restored emission was less (3.3±0.3) fold in aqueous medium buffered at pH 7.2, compared to that in methanol. It should be noted that no ligand modification occurs in aqueous medium. In the present study the complex **4.1** was found to display fluorescence enhancement for as low as 1nM NO.

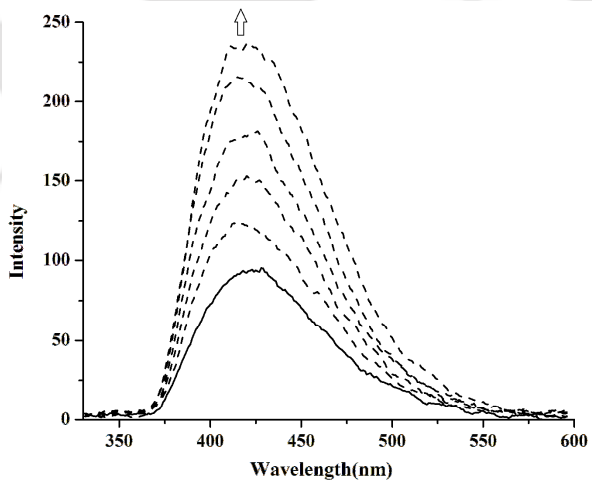

Figure 4.8: Fluorescence responses (λ_{ex}, 320 nm) of complex **4.1** (20 μM) before (solid line) and after addition of equivalent amount of NO (dashed lines) in aqueous medium.

The enhancement of fluorescence in methanol was attributed to the formation of Cu(I) species after reduction of Cu(II) by NO and the formation of N-nitrosamine, **HBNS-NO**, as shown in scheme 4.2. The quantum yield of **HBNS-NO** was higher than **HBNS**. To confirm the mechanism, equivalent amount of **HBNS** was added with $[Cu(CH_3CN)_4]ClO_4$ in methanol medium under argon atmosphere. The mixture of **HBNS** and $[Cu(CH_3CN)_4]ClO_4$ has the same fluorescence intensity as **HBNS** and there was no blue shifting of the emission wavelength. This proves that **Cu(I)HBNS** is not the species responsible for fluorescence enhancement in the reaction of NO with complex **4.1** in methanol medium.

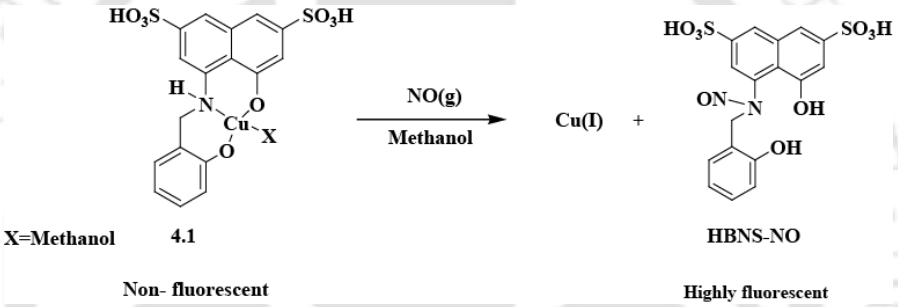

Scheme 4.2

The selectivity of the NO probe was checked with other anions like CH_3COO^-, NO_2^-, NO_3^-, Cl^-, ClO_4^- and H_2O_2 and it was found that there was no enhancement of fluorescence after addition of these anions (Figure 4.9).

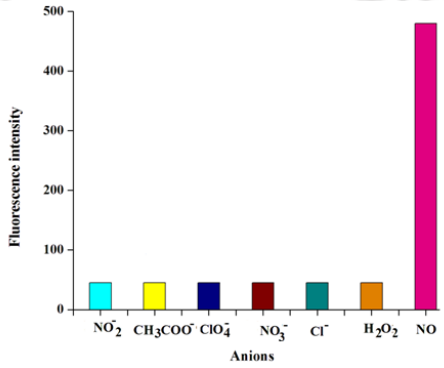

Figure 4.9: Fluorescence responses after addition of different anions to the solution of complex **4.1** in methanol.

4.5 Fluorescence cell imaging

The ability of complex **4.1** to detect NO directly, rapidly and specifically encouraged us to study it inside living cells. For this purpose SK-N-SH human neuroblastoma cell line was used. Because in this cell line cNOS can be activated by estrogen to produce NO. [20] The NO production is induced by 17-β estradiol in cells of neuronal origin. 17-β estradiol activated SK-N-SH cells were incubated with 10 μM complex **4.1**. On excitation at 320 nm, the activated cells without complex **4.1** did not show any fluorescence (Figure 4.10, A bottom); whereas the complex **4.1** incubated cells, after washing with cold phosphate-buffered saline (PBS) for three times, displayed significant fluorescence (Figures 4.10, B and 4.10, C). Images were taken with a fluorescent microscope (Axio, HBU 50/ AC; Zeiss, Gottingen, Germany) after removing the DMEM media and washing the cells with PBS. Longer incubation time (>15 minutes) did not lead to further enhancement of the fluorescence intensity indicating that the probe reached the diffusive equilibrium in the cell. Incubation of 10 μM complex with quiescent SK-N-SH cells (with no 17-β estradiol) for 12 h served as a negative control. To test the cytotoxicity of complex **4.1** we conducted an MTT assay on SK-N-SH cells, which showed 92.53% cell viability. This result indicates that the probe is non toxic to SK-N-SH cells under the condition of NO imaging.

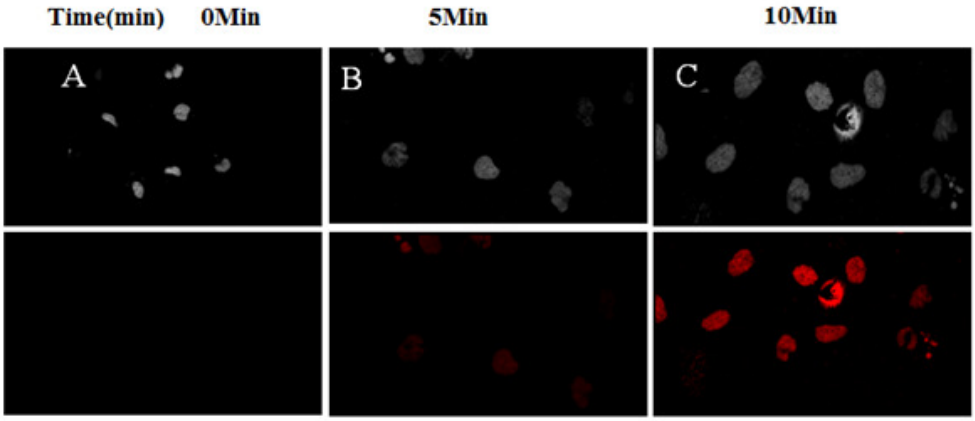

Figure 4.10: NO detection produced by cNOS. NO detection in SK-N-SH cells by complex **4.1**. Left to right, 10-min incubation of complex **4.1** (10 μM) and 0, 5, 10 min after co-treatment of complex **4.1** (10 μM) and 17*β*-estradiol (100 nM). Images were taken with a fluorescent microscope (Axio, HBU 50/ AC; Zeiss, Gottingen, Germany).Top, phase contrast images; bottom, fluorescence images.

4.6 Conclusion

A highly water soluble Cu(II) complex, **4.1** of a fluorophore ligand 4-(2-hydroxybenzylamino)-5-hydroxynaphthalene-2,7-disulfonic acid (**HBNS)** was synthesized. The NO-triggered fluorescence enhancement of the complex **4.1** occurred by reduction of Cu(II) to Cu(I) with subsequent dissociation of the N-nitrosated fluorophore ligand from copper. The selective turn on fluorogenic nature of the complex was used to sense endogenously produced NO in living cells.

4.7 Experimental Section

4.7.1 General Methods

All reagents and solvents of reagent grade were purchased from commercial sources and used as received except specified. Methanol was dried by heating over iodine activated magnesium with a magnesium loading of 5 gm/lit. Then the dried methanol was kept over 20% m/v 3Å molecular sieves for 4-5 days before using. Acetonitrile was dried over calcium hydride. Deoxygenation of the solvent and solutions was effected either by repeated vacum/purge cycles or bubbling with argon for 30 minutes or using freeze-pump-thaw cycles. UV-visible spectra were recorded on a Perkin Elmer Lambda 25 UV visible spectrophotometer. FT-IR spectra of the solid samples were taken on a Perkin Elmer spectrophotometer with samples prepared as KBr pellets. Solution electrical conductivity was measured using a Systronic 305 conductivity bridge. ^{1}H-NMR spectra were recorded in a 400 MHz Varian FT spectrometer. Chemical shifts (ppm) were referenced either with an internal standard (Me_4Si) or to the residual solvent peaks. The fluorescence spectra were recorded in solution in VARIAN Cary Eclipse Fluorescence Spectrophotometer at room temperature. Quinine sulphate in acidic medium was used as the reference compound for the determination of fluorescence quantum yield. The X-band Electron Paramagnetic Resonance (EPR) spectra were recorded on a JES-FA200 ESR spectrometer, at room temperature and 77 K with microwave power, 0.998 mW; microwave frequency, 9.14 GHz and modulation amplitude, 2. Elemental analyses were obtained from a Perkin Elmer Series II Analyzer. The magnetic moment of complexes was measured on a Cambridge Magnetic Balance.

4.7.2 Synthesis of HBNS

Azomethine-H monosodium salt hydrate (0.445g) was taken in methanol medium. 2.5 equivalent of $NaBH_4$ was added slowly and the reaction mixture was stirred for 2 h at room temperature. The color of the solution changed from dark yellow to light red. The volume

was reduced by using rotavapor. The solution was acidified by using dilute HCl and dried under reduced pressure. The brown solid thus obtained was subjected to chromatographic purification using silica gel column to yield the pure ligand **HBNS** as brown dark solid. Yield: 0.340 g (~ 80%). Elemental analyses for $C_{17}H_{15}NO_8S_2$: Calcd (%): C, 47.99; H, 3.55; N, 3.29. Found (%): C, 47.95; H, 3.56; N, 3.25. FT-IR (in KBr pellet): 1601, 1483, 1374, 1227, 1039, 755, 677 and 627cm^{-1}. ^{1}H-NMR: (400 MHz, D_2O): δ_{ppm}: 8.23 (1H, d), 7.81 (1H, s), 7.21 (1H, s), 7.04 (1H, t), 6.82 (1H, d), 6.60 (3H, m), 4.47 (2H, s). ^{13}C-NMR: (100 MHz, D_2O) $\delta_{ppm:}$ 155.2, 152.8, 151.9, 142.4, 134.5, 132.2, 131.7, 130.5, 128.3, 127.9, 120.2, 118.9, 118.7, 115.8, 115.2, 108.7, and 52.8. ESI-mass (m+1) Calcd. 426.02; found, 425.99.

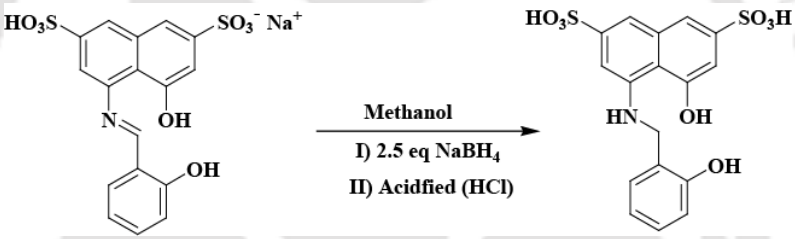

Scheme 4.3

4.7.3 Synthesis of complex 4.1

0.370 g (1 mmol) of $Cu(ClO_4)_2.6H_2O$ was dissolved in 10 ml distilled methanol. To this solution, 0.425 g (1 mmol) of the ligand **HBNS** was added slowly with constant stirring. The color of the solution turned into reddish brown from light blue. The stirring was continued for 1h at room temperature. The volume of the solution then reduced to ~2 ml. To this, 5 ml of diethyl ether was added to make a layer on it and kept it overnight on freezer. This resulted into deep brown color solid of complex **4.1**. Yield: 0.680 g (~ 85%). Elemental analyses for $C_{18}H_{17}NO_9S_2Cu$: Calcd (%): C, 41.66; H, 3.30; N, 2.70. Found (%): C, 41.50; H, 3.32; N, 2.81. UV-visible (Methanol): λ_{max}, 460 nm (ε, 2500 M^{-1}cm^{-1}). X-band EPR data: $g_{\parallel}$, 2.402, $g_{\perp}$,

2.100 and $A_{\parallel}$, 122.089×10^{-4} cm^{-1}. FT-IR (KBr pellet): 2962, 1633, 1504, 1088, 879, 663 and 625 cm^{-1}. μ_{obs} is 1.62 BM.

4.7.4 Isolation of modified ligand HBNS-NO

0.520 g (1 mmol) of the complex **4.1** was dissolved in 20 ml of degassed methanol. To this excess NO gas was purged and the solution was kept for 30 minutes. Then the solvent was removed under reduced pressure using rotavapor. 5 ml of water was added to the dried mass followed by the addition of 5 ml of saturated Na_2S solution. The black precipitate of CuS was filtered out. The crude organic part was then acidified by using dilute HCl. The product, obtained after removal of solvent, was then purified by column chromatography using silica gel column and chloroform/ethyl acetate solvent mixture to get the pure modified ligand. Yield: 0.295g (~ 65%). Elemental analyses for $C_{17}H_{14}N_2O_9S_2$: Calcd (%): C, 44.93; H, 3.11; N, 6.16. Found (%): C, 44.82; H, 3.12; N, 6.25. FT-IR (in KBr pellet): 1640, 1628, 1523, 1450, 1384, 1227, 1050 and 732cm^{-1}. ^{1}H-NMR**:** (400 MHz, D_2O): δ_{ppm}: 7.99 (1H, s), 7.55 (1H, s), 7.00 (1H, m), 6.80 (1H, m), 6.57 (1H, d), 6.36 (1H, d), 4.21 (2H, s). ^{13}C-NMR: (100 MHz, D_2O) δ_{ppm}: 155.2, 151.8, 142.4, 140.5, 134.6, 132.2, 131.7, 130.5, 128.4, 120.2, 118.9, 118.8, 115.8, 115.2, 108.8, and 52.9. ESI-mass ($m+Na^+$) Calcd. 477.42; found, 477.43.

4.7.5 Cell cultures and imaging methods

SK-N-SH cells were purchased from the National centre for cell science, Pune India. Cells were cultured in DMEM supplemented with 10% fetal bovine serum (FBS, HyClone), 1% penicillin-streptomycin, 1% sodium pyruvate, and 1% MEM nonessential amino acids (Sigma) and maintained at 37 °C with 10% CO_2 in a humidified incubator. For imaging studies, cells grown to confluence were passed and plated into poly-D-lysine coated plates (Mat Tek) containing 2 ml of DMEM. After incubation at 37° C with 10% CO_2 for at least 4 h, the media was removed, the cells were washed with 2 ml of PBS buffer and 2 ml of fresh

DMEM along with the complex **4.1** and cNOS stimulants. For imaging, cells were incubated for 12-14 h.

4.7.6 Cell cytotoxicity studies

The cytotoxicity of Complex **4.1** was investigated by incubating various concentrations of Complex with SK-N-SH cells. After 24 h, cell viability was examined by the MTT dye. The cells were plated at a density of 5×10^4 per well in a 96-well culture plate, and cultured for 72 hours at 37 °C. The cells were subsequently exposed to complex **4.1** using a concentration range of (0.01–100 μM). The plates were incubated for 48 hours, and cell proliferation was measured by adding 20 μL of MTT dye (5 mg/mL in phosphate-buffered saline) per well. The plates were incubated for a further 4 hours at 37 °C in a humidified chamber containing 5% CO_2. The intracellular Formazan crystals formed were dissolved in 150 μL dimethyl sulfoxide, and absorbance at 570 nm was read using a SpectraMax M2 plate reader (Molecular Devices, San Jose, CA). Results were expressed as absorbance relative to the plain gold particles used as the control. The results demonstrated that complex **4.1** displayed low cytotoxicity to SK-N-SH cells.

4.8 References

1. Murad, F. *Angew. Chem. Int. Ed.* **1999**, *38*, 1856.

2. Moncada, S.; Palme, R. M. J.; Higgs, E. A. *Pharmacol. Rev*. **1991**, *43,* 109.

3. Conner, E. M.; Grisham, M. B. *Methods Enzymol* **1995**, *7,* 3.

4. Ignarro, L. J. *Nitric Oxide Biology and Pathobiology,* 1st ed.; Academic Press: San-Diego, 2000.

5. Garthwaite, J. E. *J. Neurosci.* **2008**, *27,* 2783.

6. Pluth, M. D.; Tomat, E.; Lippard, S. J. *Annu. Rev. Biochem*. **2011**, *80,* 333.

7. Ye, X.; Rubakhin, S. S.; Sweedler, J. V. *Analyst* **2008,** *133,* 423.

8. Hetrick, E. M.; Schoenfisch, M. H. *Annu. Rev. Anal. Chem*. **2009**, *2*, 409.

9. McQuade, L. E.; Lippard, S. J. *Curr. Opin. Chem. Biol.* **2010**, *14*, 43.

10. Nagano, T. J. *Clin. Biochem. Nutr.* **2009**, *45,* 111.

11. Nagano, T.; Yoshimura, T. *Chem. Rev.* **2002**, *102,* 1235.

12. Hilderbrand, S. A.; Lim, M. H.; Lippard, S. J. *Topics in Fluorescence Spectroscopy*; Geddes, C. D.; Lakowicz, J. R. *Springer* 2005, 163-188.

13. (a) Lim, M. H.; Wong, B. A.; Pitcock, W. H.; Mokshagundam, D.; Baik, M.; Lippard, S. J. *J. Am. Chem. Soc*. **2006**, *128,* 14364. (b) Lim, M. H.; Kuang, C.; Lippard, S. J. *Chem. Bio. Chem.* **2006**, *7*, 1571. (c) Lim, M. H.; Xu, D.; Lippard, S. J. *Nat. Chem. Biol.* **2006**, *2,* 375. (d) Lim, M. H.; Lippard, S. J. *Inorg. Chem*. **2006**, *45,* 8980.

14. (a) Tsuge, K.; Rosa, F. De.; Lim, M. D.; Ford, P. C. *J. Am. Chem. Soc*. **2004**, *126,* 6564. (b) Khin, C.; Lim, M. D.; Tsuge, K.; Iretskii, A.; Wu, G.; Ford, P. C. *Inorg. Chem*. **2007**, *46,* 9323.

15. (a) Kumar, V.; Kalita, A.; Mondal, B. *Dalton Trans.* **2013**, *42,* 16264. (b) Jazdzewski, B. A.; Tolman, W. B. *Coord. Chem. Rev*. **2000**, *633*, 200. (c) Rout, K. C.; Mondal, B. *Dalton Trans*. **2015**, *44*, 1829.

16. (a) Mendola, D. L.; Magri, A.; Vagliasindi, L. I.; Hansson, O.; Bonomo, R. P.; Rizzarelli, E. *Dalton Trans*. **2010**, *39,* 10678. (b) Hathaway, B. J. *Coord. Chem. Rev*. **1970**, *5*, 143.

17. Sarma, M.; Kumar, V.; Kalita, A.; Deka, R. C.; Mondal, B. *Dalton Trans.* **2012**, *41*, 9543.

18. (a) Sarma, M.; Singh, A.; Gupta, S. G.; Das, G.; Mondal, B. *Inorg. Chim. Acta* **2010**, *363,* 63. (b) Kumar, P.; Kalita, A.; Mondal, B. *Dalton Trans.* **2011**, *40*, 8656.

19. (a) Lim, M. H.; Lippard, S. J. *J. Am. Chem. Soc.* **2005**, *127,* 12170. (b) Smith, R. C.; Tennyson, A.G.; Lim, M. H.; Lippard, S. J. *Org. Lett.* **2005**, *7,* 3573.

20. Xia, Y.; Krukoff, T.L. *Endocrinology* **2004**, *145,* 4550.

Chapter 5

Copper(II) complex as selective turn-on fluorescent probe for nitrite ion

Abstract

The Cu(II) complex, **5.1** with 3-(pyren-8-yl)-1-(pyridine-2-yl)prop-2-en-1-one (**PYAC**) was synthesized. Addition of aqueous nitrite (NO_2^-) solution to the acetonitrile solution of the complex **5.1** resulted in reduction of Cu(II) center. The NO_2^- ion was found to be oxidized to NO_3^- during the reaction. Labeling studies suggested water as the source of oxygen atom. The reduction of Cu(II) center restored the quenched fluorescence intensity of the ligand in the complex and thus can be utilized as turn-on fluorescent sensor for NO_2^- ion .

5.1 Introduction

The nitrite ion (NO_2^-), an inorganic contaminant, is found in drinking water and is a threat to human health. When present in high concentration in human blood, it can oxidize hemoglobin and myoglobin to methemoglobin and metmyoglobin, respectively.[1] Upon interaction with protein, it leads to the formation of carcinogenic N-nitrosoamines.[2] Thus, a selective probe to detect NO_2^- ion would be important from various angles. Several methods for NO_2^- sensing have been reported including chemical, optical, ion chromatography and electrochemical methods.[3,4] The well known Griess reagent is a chemical and optical method of sensing NO_2^- ion which involves the diazotization of sulphanilamide by nitrous acid under acidic conditions followed by the coupling of the in situ generated diazonium ion with N-(1-naphthyl)ethylenediamine to afford azochromophore.[5] In literature, a number of electrochemical and colorimetric sensors have been reported.[6,7] However, all these processes have some drawbacks and one method which satisfies almost all the requirement is a fluorometric one. Interestingly, the fluorescence based nitric oxide (NO) sensor, 2,3-diaminonaphthalene (DAN) was prepared for NO_2^- ion detection in solution.[8] The sensor molecule, DAN, undergoes diazotization at one amine center in acidic medium in presence of NO_2^- leading to the formation of fluorophore, 2,3-naphthatriazole. The reaction was found to proceed through the formation of corresponding nitrosoamine intermediate.

Chalcones, naturally occurring flavonoids, are bichromophoric molecules separated by a ketovinyl chain and exhibiting a wide range of biological activities.[9] They find various optical applications including fluorescent probes for sensing of metal ions.[10]

This chapter describes the development of highly selective fluorescent sensor for NO_2^- ion based on Cu(II) complex of chalcone ligand with pyrene fluorophore.

5.2 Results and discussion

The ligand,**PYAC** [**PYAC**=3-(pyren-8-yl)-1-(pyridine-2-yl)prop-2-en-1-one], was prepared by stirring a mixture of acetyl pyridine with 1-pyrenecarbaldehyde in presence of sodium hydroxide in ethanol.[11] Precipitated ligand was filtered off, washed with cold ethanol and recrystallized from hot ethanol. It was characterized by various spectroscopic techniques (Experimental section). The single crystal X-ray structure of **PYAC** was determined. The perspective ORTEP view is shown in figure 5.1. Crystallographic data are given in appendix IV. The complex **5.1** was prepared by stirring copper(II) perchlorate hexahydrate with equivalent amount of the ligand in acetonitrile (Scheme 5.1). It was characterized by spectroscopic analyses (Experimental section). Even after several attempts the X-ray quality crystals were not obtained.

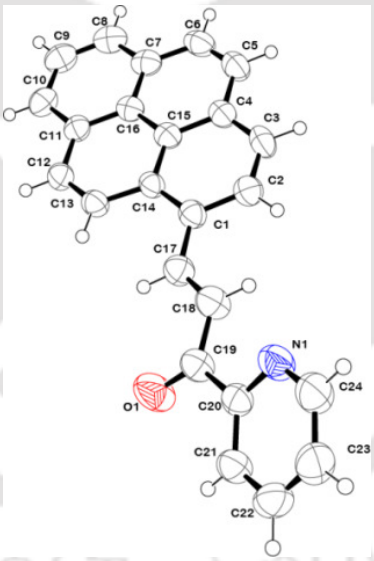

Figure 5.1: ORTEP diagram of ligand **PYAC** (50% thermal ellipsoid plot).

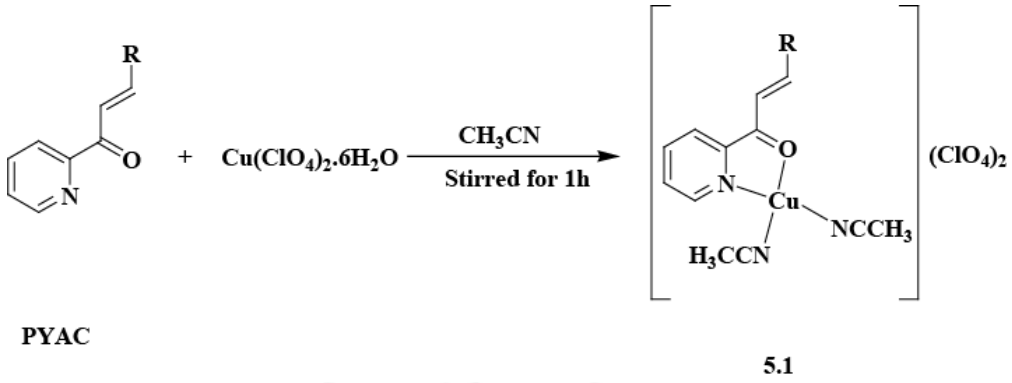

PYAC

5.1

Scheme 5.1 Synthesis of complex **5.1** (R=Pyrene).

Complex **5.1**, in acetonitrile solution displays absorption at 555 nm due to MLCT transition from the filled up *d*-orbital of the metal ion to the low lying π* orbital of the ligand.[12] The absorptions at 425 and 377 nm are attributed to ligand based charge transfer transitions which are clear from the spectrum of the free ligand (Appendix IV). In methanol, the MLCT band appears at 530 nm (Appendix IV). In FT-IR spectrum of complex **5.1**, the stretching frequency for C=O group appears at 1596 cm^{-1} indicating that the C=O group is bonded to the metal ion (Figure 5.2).

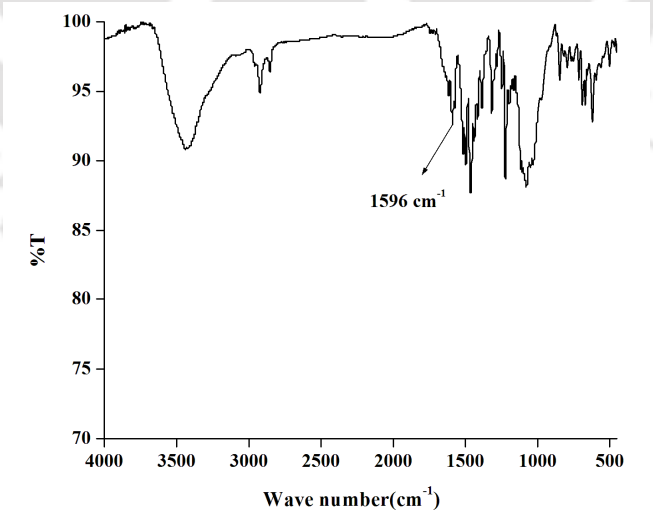

Figure 5.2: FT-IR spectrum of complex **5.1** in KBr pellet.

The theoretical studies on similar framework with Cu(II) showed that the ligand binds

through N_{py} and $O_{C=O}$ in a bidentate fashion.[13] However, Reedijk et al earlier reported that ligand **PYAC** can bind in both *cis* and *trans* form.[14] While bonded through *cis* form to Pt(II) ion, it binds only through N_{py}. On the other hand, *trans* form binds the Pt(II) through N_{py} as well as C=C unit. In X-band EPR spectroscopy, the complex **5.1** displays signals at 77 K which are characteristic of square planar Cu(II). The calculated parameters for complex **5.1** are $g_{\parallel}$, 2.2555, $g_{\perp}$, 2.0842 and A, 124×10^{-4} cm^{-1} (Figure 5.3).[15]

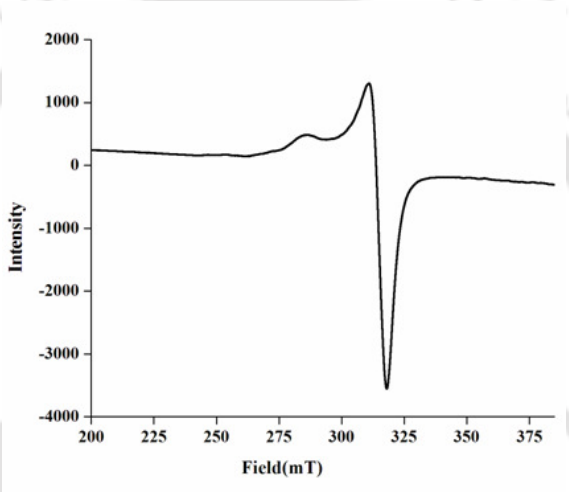

Figure 5.3: X-band EPR spectrum of complex **5.1** in methanol at 77 K.

5.3 Reactivity of nitrite ion

Addition of aqueous NO_2^- solution to the acetonitrile solution of complex **5.1** was found to result in the immediate decrease of the intensity of 555 nm band in UV-visible spectrum (Figure 5.4).

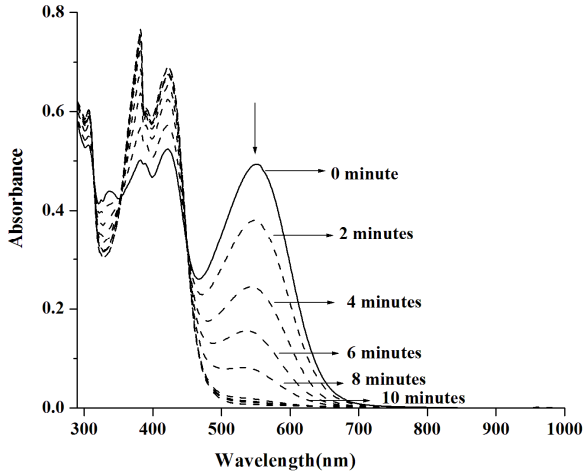

Figure 5.4: UV-visible spectra of complex **5.1** (solid line) and after addition of aqueous $NaNO_2$ (dashed lines) at 0-10 minutes time interval in acetonitrile.

In methanol, the band at 530 nm was found to diminish (Appendix IV). This is attributed to the reduction of Cu(II) center to Cu(I). To confirm this, the UV-visible spectra of **PYAC** was recorded in presence of equivalent amount of Cu(I) (Appendix IV). X-band EPR studies also suggested the reduction. The characteristic signal of Cu(II) was found to disappear upon addition of NO_2^- (Figure 5.5).

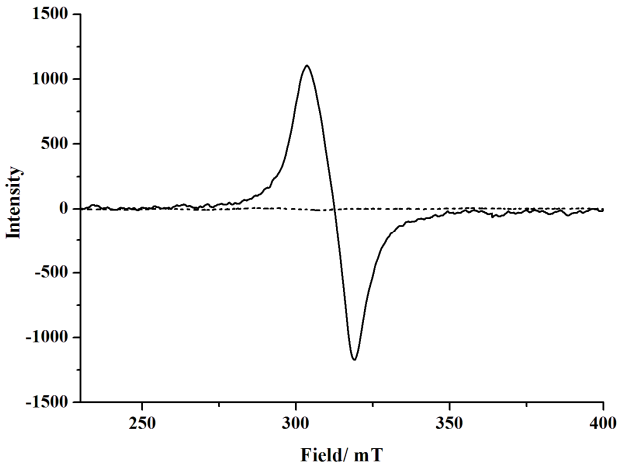

Figure 5.5: X-Band EPR spectra of complex **5.1** before (solid line) and after (dotted line) addition of 0.5eq of $NaNO_2$ in acetonitrile medium at room temperature.

^{1}H-NMR studies also suggested the reduction of Cu(II) center. The broad signals of proton in paramagnetic complex **5.1** in CD_3CN appeared as well-resolved and sharp after addition of NO_2^- solution (Figure 5.6). The shift in peak positions compared to the free ligand was due to the presence of ligand coordinated Cu(I).

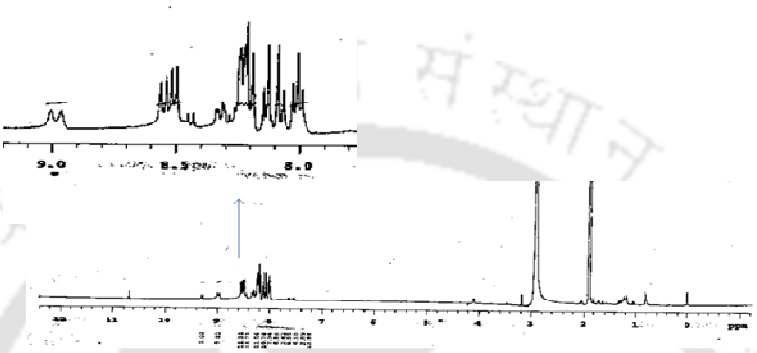

Figure 5.6: ^{1}H-NMR spectrum of complex **5.1** (in CD_3CN) after its reaction with $NaNO_2$ (in D_2O).

In the FT-IR spectrum of complex **5.1**, a new stretching band at ~1384 cm^{-1} appeared after addition of NO_2^- (Figure 5.7). This has been assigned as the NO_3^- stretching frequency.[16]

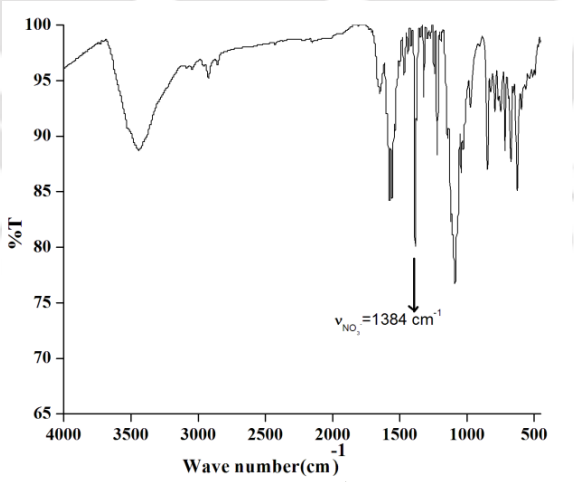

Figure 5.7: FT-IR spectrum of the crude product from the reaction of complex **5.1** with $NaNO_2$ in KBr pellet.

During the reaction, Cu(II) is reduced to Cu(I) and NO_2^- is oxidized to NO_3^-. Analysis of the

reaction mixture revealed the formation of NO_3^- ion as the oxidation product. It should be noted that the reduction of Cu(II) to Cu(I) is one electron transfer process, whereas the oxidation of NO_2^- to NO_3^- involves two electron transfer. Thus, only 0.5 equivalent of nitrite ion is required for the reduction of Cu(II) center (eq. 5.1). This was confirmed by titrating the solution of complex **5.1** with sodium nitrite (Figure 5.8 and 5.9). On the other hand, when the equivalent amount of NO_2^- was added to the solution of complex **5.1**, the appearance of both the NO_3^- and NO_2^- stretching frequencies were observed (Appendix IV).

$$2\,[LCu^{II}(CH_3CN)_2]^{2+} + NO_2^- + H_2O \longrightarrow 2\,[LCu^{I}(CH_3CN)_2]^{+} + NO_3^- + 2H^+ \quad \text{..... eq (5.1)}$$

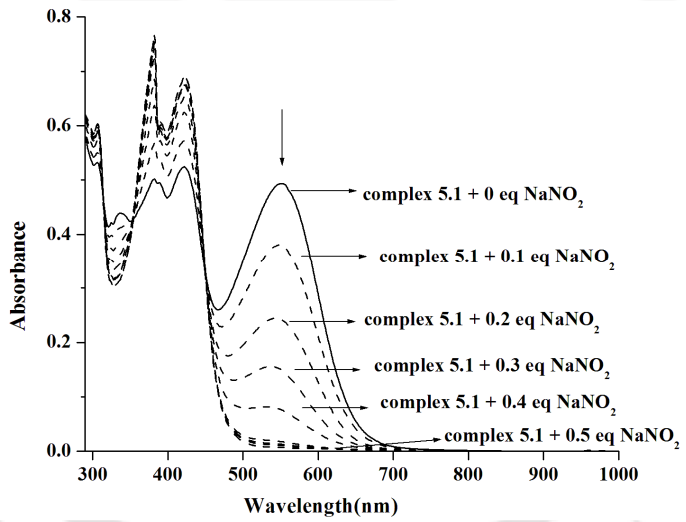

Figure 5.8: UV-visible titration of complex **5.1** with $NaNO_2$ in acetonitrile.

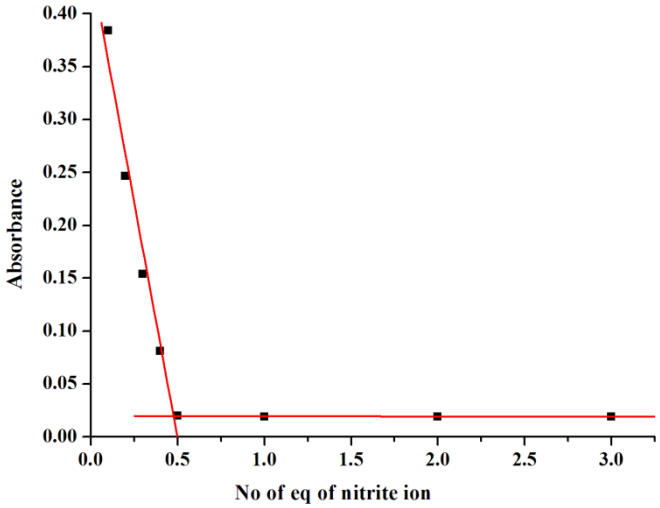

Figure 5.9: UV-visible titration plot for complex **5.1** with $NaNO_2$ in acetonitrile (considering the band at 555 nm).

Labeling experiment with H_2O^{18} afforded the ^{18}O-labelled NO_3^-. In FT-IR spectrum, the nitrate stretching frequency at ~1384 cm^{-1} was found to shift at ~1320 cm^{-1} (Appendix IV). While the reaction was carried out in presence of $^{18}O_2$, incorporation of ^{18}O into the NO_3^- was not observed. This suggests the involvement of water in the reaction. The release of H^+ was qualitatively confirmed from the change of pH of the reaction medium.

The reaction was not found with nitrate, acetate, phosphate, sulphate, carbonate, perchlorate and bicarbonate ions. Addition of NO in the dry and degassed methanol or acetonitrile solution of complex, did not result in the reduction of Cu(II) center.

5.4 Fluorescence study

Several Cu(II) complexes were reported as fluorescent sensors for NO based on the strategy involving the reduction of a metal center by NO.[17,18] A fluorescence intensity of a ligand is expected to be quenched on coordination to the paramagnetic Cu(II) center. NO reduction of a paramagnetic Cu(II) to a diamagnetic Cu(I) will restore the quenched fluorescence of a ligand fluorophore.[17,18] Since, in the present case NO_2^- selectively reduces Cu(II) center to Cu(I), the same strategy of restoring the quenched fluorescence intensity of the ligand in the

complex was adopted. Fluorescence spectroscopic study at 298 K suggested the significant quenching (> 90%) of fluorescence intensity of ligands in presence of equivalent amount of Cu(II) owing to paramagnetic effect in methanol or acetonitrile solution (Figure 5.10).

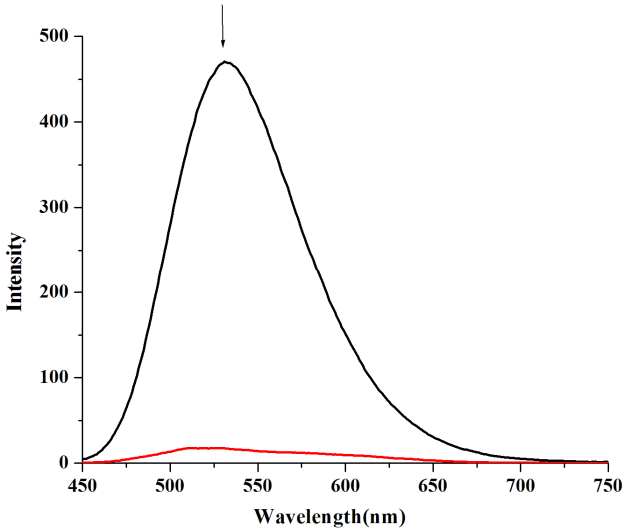

Figure 5.10: Fluorescence responses ($\lambda_{ex,}$ 425 nm) for 20 µM solution of free **PYAC** (black line) and after addition of 20 µM $Cu(ClO_4)_2.6H_2O$ (red line) in acetonitrile.

Addition of 0.5 equivalent of NO_2^- solution to the complex **5.1** was found to restore the quenched intensity instanteneously (Figure 5.11). This was attributed to the reduction of Cu(II) center by NO_2^-. The enhancement was found in methanol solution also (Appendix IV). It should be noted that conjugated enones are known to react with NO_2^- in presence of acid to result in the corresponding β-nitroketones.[19] In the present case, any ligand modification was not observed. It should be noted that presence of NO in a degassed solution of complex **5.1** did not restore the quenched fluorescence intensity of the ligands.

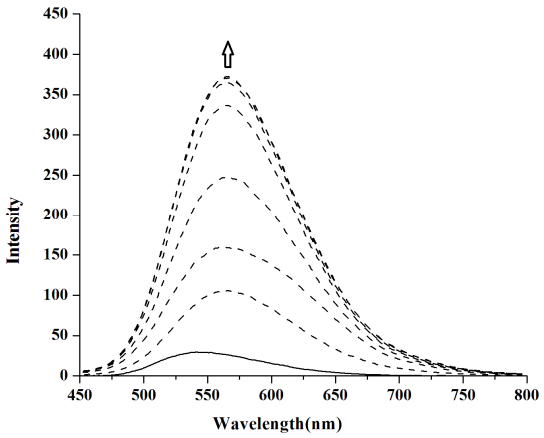

Figure 5.11: Fluorescence enhancement (λ_{ex}, 425 nm) of 20 μM complex **5.1** (solid line) and after addition of $NaNO_2$ (0.5eq) (dashed lines) in acetonitrile.

In the reaction condition, the influence of various other anions like nitrate, acetate, carbonate, sulphate, phosphate, and halides have been studied (Appendix IV). The quenched fluorescence intensity of the ligand in the complex **5.1** was not found to be restored upon addition of these anions in the solution of complex. Further, these anions did not find to interfere the detection of the NO_2^- using the present complex.

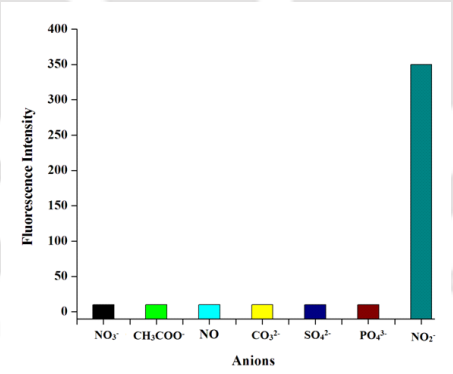

Figure 5.12: Fluorescence responses after addition of different anions to the solution of complex **5.1** in acetonitrile.

5.5 Conclusions

The Cu(II) complex, **5.1** with 3-(pyren-8-yl)-1-(pyridine-2-yl)prop-2-en-1-one (**PYAC**) was prepared. Addition of aqueous NO_2^- solution to the acetonitrile solution of the complex

resulted in reduction of Cu(II) center. The NO_2^- ion was found to be oxidized to NO_3^- during the reaction. Labeling studies suggested water as the source of oxygen atom. The reduction of Cu(II) center restored the quenched fluorescence intensity of the ligand in the complex and thus can be utilized as turn-on fluorescent sensor for NO_2^- ion .

5.6 Experimental Section

5.6.1 General Methods

All reagents and solvents of reagent grade were purchased from commercial sources and used as received except specified. Methanol was dried by heating over iodine activated magnesium with a magnesium loading of 5 gm/lit. Then the dried methanol was kept over 20% m/v 3Å molecular sieves for 4-5 days before using. Acetonitrile was dried over calcium hydride. Deoxygenation of the solvent and solutions was effected either by repeated vacuum/purge cycles or bubbling with argon for 30 minutes or using freeze-pump-thaw cycles. UV-visible spectra were recorded on a Perkin Elmer Lambda 25 UV-visible spectrophotometer. FT-IR spectra of the solid samples were taken on a Perkin Elmer spectrophotometer with samples prepared as KBr pellets. Solution electrical conductivity was measured using a Systronic 305 conductivity bridge. ^{1}H-NMR spectra were recorded in a 400 MHz Varian FT spectrometer. Chemical shifts (ppm) were referenced either with an internal standard (Me_4Si) or to the residual solvent peaks. The X-band Electron Paramagnetic Resonance (EPR) spectra were recorded on a JES-FA200 ESR spectrometer, at room temperature and 77 K with microwave power, 0.998 mW; microwave frequency, 9.14 GHz and modulation amplitude, 2. Elemental analyses were obtained from a Perkin Elmer Series II Analyzer. The magnetic moment of complexes was measured on a Cambridge Magnetic Balance.

Single crystals were grown by slow diffusion followed by slow evaporation technique. The intensity data were collected using a Bruker SMART APEX-II CCD diffractometer, equipped with a fine focus 1.75 kW sealed tube MoKa radiation (l = 0.71073 Å) at 273(3) K, with

increasing w (width of 0.3° per frame) at a scan speed of 3 s/frame. The SMART software was used for data acquisition. Data integration and reduction were undertaken with SAINT and XPREP software.[20] Structures were solved by direct methods using SHELXS-97 and refined with full-matrix least squares on F^2 using SHELXL-97.[21] All non-hydrogen atoms were refined anisotropically. Structural illustrations have been drawn with ORTEP-3 for Windows.[22]

5.6.2 Synthesis of ligand PYAC

Aqueous NaOH (10 ml of a 1.5M solution) was added to a stirred solution of 2-acetyl pyridine (1.20 g, 10 mmol) and 1-pyrenecarbaldehyde (2.30 g, 10 mmol) in ethanol (20 ml). After stirring for 4 h at room temperature, the resultant precipitate was isolated by filtration and re-crystallized from ethanol to give **PYAC** as yellow needles. Yield: 3.00 g (~ 90%). Elemental analyses for $C_{24}H_{15}NO$: Calcd (%): C, 86.46; H, 4.54; N, 4.20. Found (%): C, 86.55; H, 4.55; N, 4.29. FT-IR (in KBr pellet): 1661, 1589, 1576, 1432, 1321, 1217, 1029, 846 and 713 cm^{-1}. ^{1}H-NMR: (400 MHz, $CDCl_3$): δ_{ppm}: 9.10 (1H, d), 8.78 (1H, s), 8.56 (3H, m), 8.18 (5H, m), 8.02 (2H, m), 7.90 (1H, s), 8.69 (1H, d), 7.51 (1H, s). ^{13}C-NMR: (100 MHz, $CDCl_3$) δ_{ppm}: 189.4, 154.6, 149.4, 149.1, 141.3, 137.2, 137.1, 133.2, 131.4, 130.8, 130.7, 129, 128.8, 128.8, 127.5, 127, 126.4, 126.2, 126.1, 125.2, 125.1, 124.8, 124 and 123.2.

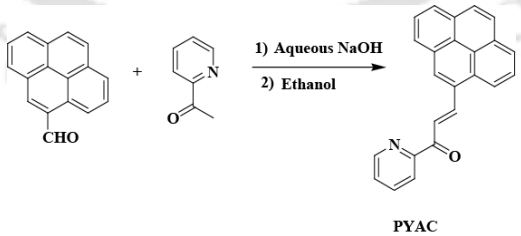

PYAC

Scheme 5.2: Synthesis of PYAC

5.6.3 Synthesis of complex 5.1

Copper(II) perchlorate hexahydrate (0.370 g, 1 mmol) was dissolved in 10 ml distilled acetonitrile. To this solution, **PYAC** (0.333 g, 1 mmol) was added slowly with constant stirring. The color of the solution turned into dark violet from light blue. The stirring was continued for 1h at room temperature. The volume of the solution then reduced to ~2 ml. To this, 5 ml of benzene was added to make a layer on it and kept it overnight on freezer. This resulted into deep color solid of complex **5.1**. Yield: 0.542 g (~ 80%). Elemental analyses for $C_{28}H_{21}N_3O_9Cl_2Cu$: Calcd (%): C, 49.61; H, 3.12; N, 6.20. Found (%): C, 49.55; H, 3.22; N, 6.18. UV-visible (acetonitrile): λ_{max}, 555 nm (ε, 16,093 $M^{-1}cm^{-1}$). X-band EPR data: $g_{\parallel}$, 2.2555, $g_{\perp}$, 2.0842 and A, 124 × 10^{-4} cm^{-1}. FT-IR (in KBr pellet): 2922, 1590, 1515, 1496, 1316, 1224, 1119, 1077, 1029 and 620 cm^{-1}. The complex **5.1** behaves as 1:2 electrolyte in acetonitrile solution [Λ_M ($S\,cm^{-1}$), 270]. μ_{obs} is 1.62 BM.

5.7 References

1. (a) Daniel, W. L.; Han, M. S.; Lee, J.-S.; Mirkin, C. A. *J. Am. Chem. Soc.* **2009**, *131*, 6362. (b) Chen, Z.; Zhang, Z.; Qu, C.; Pana, D.; Chen, L. *Analyst* **2012**, *137*, 5197. (c) Xiao, N.; Yu, C. *Anal. Chem.* **2010**, *82*, 3659.
2. Ye, D.; Luo, L.; Ding, Y.; Chen, Q.; Liu, X. *Analyst* **2011**, *136*, 4563.
3. (a) Xue, Z.; Wu, Z.; Han, S. *Anal. Methods* **2012**, *4*, 2021. (b) Kim, H. J.; Kim, Y. K. *Anal. Chem.* **1989**, *61*, 1485. (c) Shankar, B. H.; Ramaiah, D. *J. Phys. Chem. B.* **2011**, *115*, 13292.
4. (a) Lin, Z.; Xue, W.; Chen, H.; Lin, J. M. *Anal. Chem.* **2011**, *83*, 8245. (b) Li, J.; Li, Q.; Lu, C.; Zhao, L. *Analyst* **2011**, *136*, 2379. (c) Wang, N.; Cao, X.; Cai, X.; Xu, Y.; Guo, L. *Analyst* **2010**, *135*, 2106. (d) Ko, W.; Chen, W.; Cheng, C.; Lin, K. *Sens. Actuators, B* **2009**, *137*, 437.

5. Fox, J. B. *J. Anal. Biochem*. **1979**, *51*, 1493.

6. (a) Stanley, M. A.; Maxwell, J.; Forrestal, M.; Doherty, A. P.; Maccraith, B. D.; Diamond, D.; Vos, J. G. *Anal. Chim. Acta* **1994**, *299*, 81. (b) Kuban, P.; Nguyen, H. T. A.; Macka, M.; Haddad, P. R.; Hauser, P. C. *Electroanalysis* **2007**, *19*, 2059. (c) Pietrzak, M.; Meyerhoff, M. E. *Anal. Chem*. **2009**, *81*, 3637.

7. (a) Daniel, W. L.; Han, M. S.; Lee, J.-S.; Mirkin, C. A. *J. Am. Chem. Soc.* **2009**, *131*, 6362. (b) Adarsh, N.; Shanmugasundaram, M; Ramaiah, D. *Anal. Chem*. **2013**, *85*, 10008.

8. (a) Damiani, P.; Burini, G. *Talanta* **1986**, *33*, 649. (b) Miles, A. M.; Chen, Y.; Owens, M. W.; Grisham, M. B. *Methods* **1995**, *7,* 40.

9. (a) Lin, Y. M.; Zhou, Y.; Flavin, M. T.; Nie, W.; Chen, F. C. *Bioorg. Med. Chem*. **2002**, *8*, 2795. (b) Pinto, D. A. G. C.; Silva, A. M. S.; Cavaleiro, J. A. S.; Elguero, J. *Eur. J. Org. Chem.* **2003**, 747. (c) *The Chemistry of Chalcones and Related Compounds,* Dhar, D. N. Wiley, New York, 1981.

10. (a) Rurack, K.; Bricks, J. L.; Reck, G.; Radeglia, R.; Resch-Genger, U. *J. Phys. Chem. A.* **2000**, *104*, 3087. (b) Marcotte, N.; Fery-Forgues, S.; Lavabre, D.; Marguet, S.; Pivovarenko, V. G. *J. Phys. Chem. A.* **1999**, *103*, 3163.

11. (a) Constable, E. C.; Smith, D. R. *Tetrahedron* **1996**, *52*, 935. (b) Constable, E. C.; Zhang, G.; Housecroft, C. E.; Zampese, J. A. *Dalton Trans*. **2011**, *40*, 12146.

12. Figgis, N. *Introduction to Ligand Fields,* Wiley, New York, 1967.

13. Gaber, M.; El-Daly, S. A.; El-Sayed, Y. S. Y. *J. Mol. Struct*. **2009**, *922*, 51.

14. Marque´s-Gallego, P.; Dulk, H. D.; Brouwer, J.; Kooijman, H.; Spek, A. L.; Roubeau, O.; Teat, S. J.; Reedijk, J. *Inorg. Chem*. **2008**, *47*, 11171.

15. Kalita, A.; Kumar, P.; Deka, R. C.; Mondal, B. *Inorg. Chem*. **2011**, *50*, 11168.

16. Kalita, A.; Kumar, P.; Mondal, B. *Chem. Commun*. **2012**, *48*, 4636.

17. (a) Lim, M. H.; Wong, B. A.; Pitcock Jr., W. H.; Mokshagundam, D.; Baik, M.; Lippard, S. J. *J. Am. Chem. Soc*. **2006**, *128*, 14364. (b) Lim, M. H.; Kuang, C.; Lippard, S. J. *Chem. Bio. Chem.* **2006**, *7*, 1571. (c) Lim, M. H.; Lippard, S. J. *J. Am. Chem. Soc.* **2005**, *127*, 12170. (d) Lim, M. H.; Xu, D.; Lippard, S. J. *Nat. Chem. Biol.* **2006**, *2*, 375. (e) Lim, M. H.; Lippard, S. J. *Inorg. Chem*. **2006**, *45*, 8980.

18. (a) Tsuge, K.; DeRosa, F.; Lim, M. D.; Ford, P. C.; *J. Am. Chem. Soc*. **2004**, *126*, 6564. (b) Khin, C.; Lim, M. D.; Tsuge, K.; Iretskii, A.; Wu, G.; Ford, P. C.; *Inorg. Chem*. **2007**, *46*, 9323.

19. Gabrielli, S.; Palmieri, A.; Perosa, A.; Selva, M.; Ballini, R. *Green Chem*. **2011***, 13*, 2026.

20. *SMART, SAINT and XPREP*; Siemens Analytical X-ray Instruments Inc.: Madison, WI, 1995.

21. Sheldrick, G. M. *SHELXS-97*; University of Gottingen: Gottingen, Germany, 1997.

22. Farrugia, L. J. *J. Appl. Crystallogr.* **1997**, *30*, 565.

Appendix I

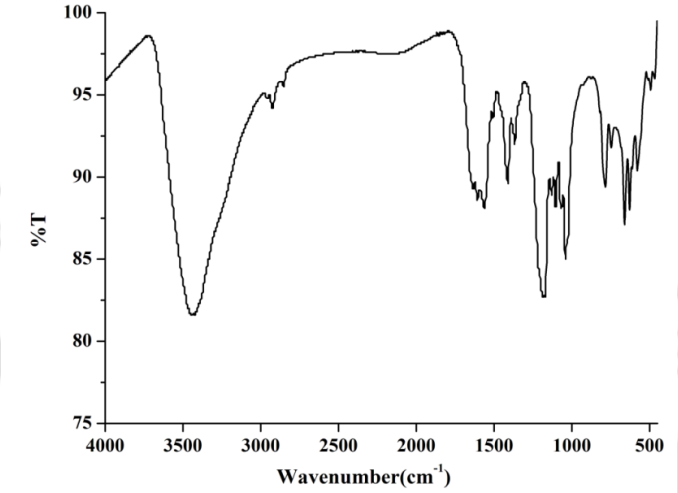

Figure A1.1: FT-IR spectrum of **AZO-ANS** in KBr pellet.

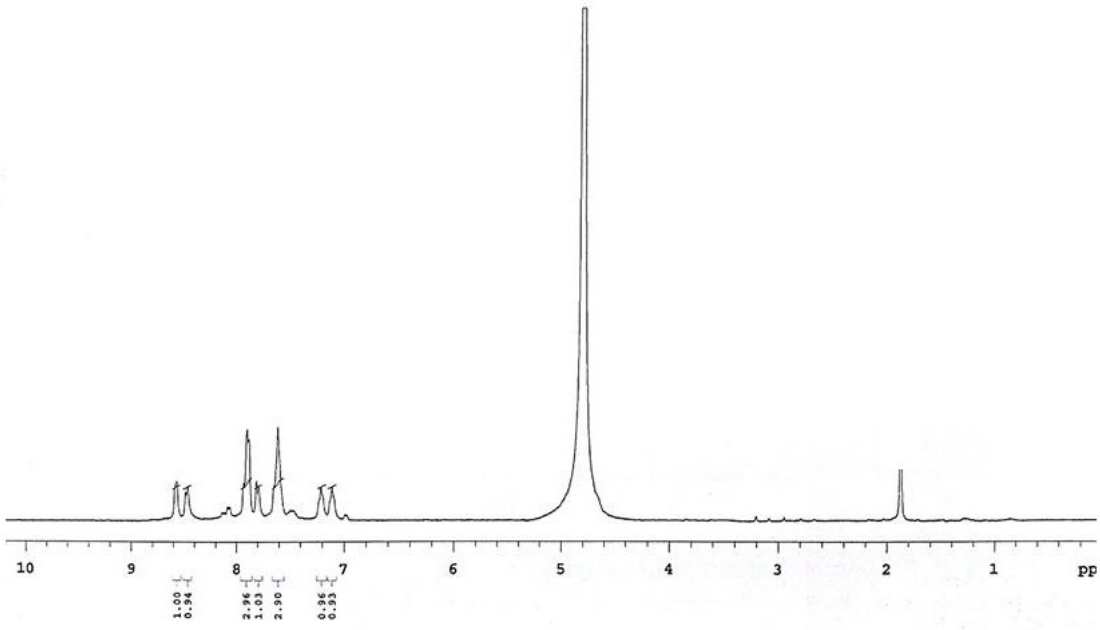

Figure A1.2: ^{1}H-NMR spectrum of **AZO-ANS** in D_2O.

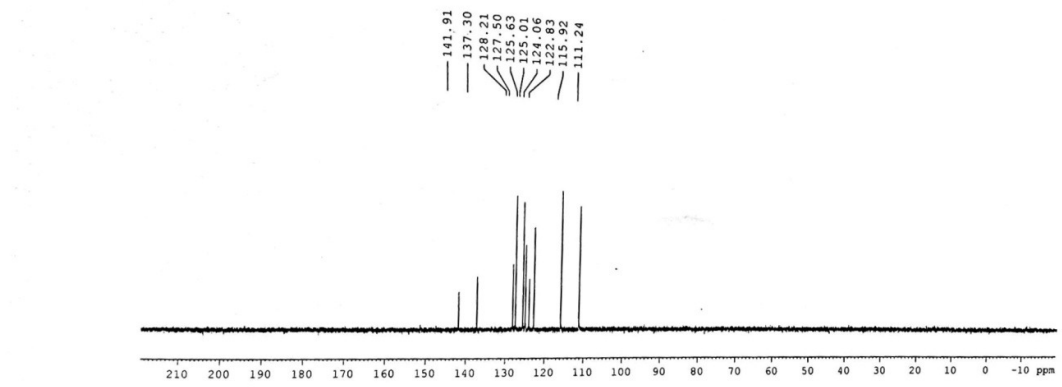

Figure A1.3: ^{13}C-NMR spectrum of **AZO-ANS** in D_2O.

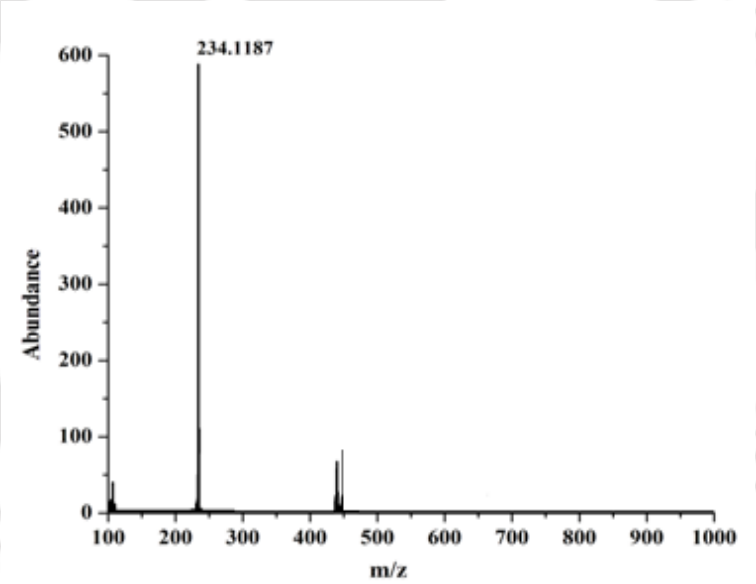

Figure A1.4: ESI-mass spectrum of **AZO-ANS** in methanol**.**

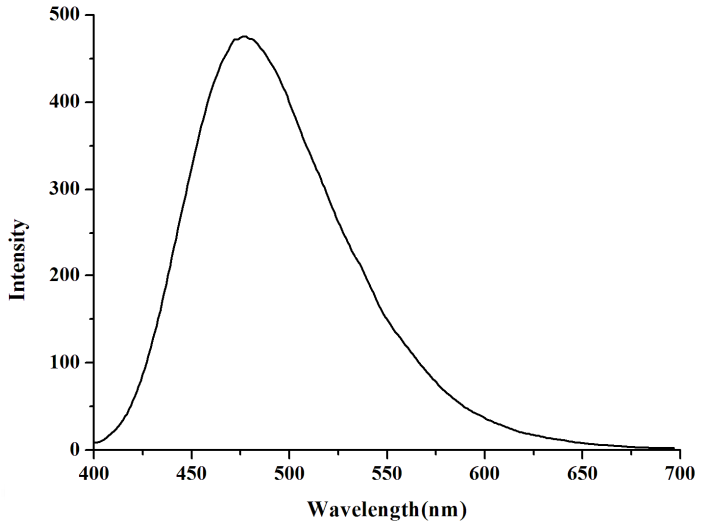

Figure A1.5: Fluorescence spectrum (λ_{ex}, 335 nm) of **ANS** in methanol medium.

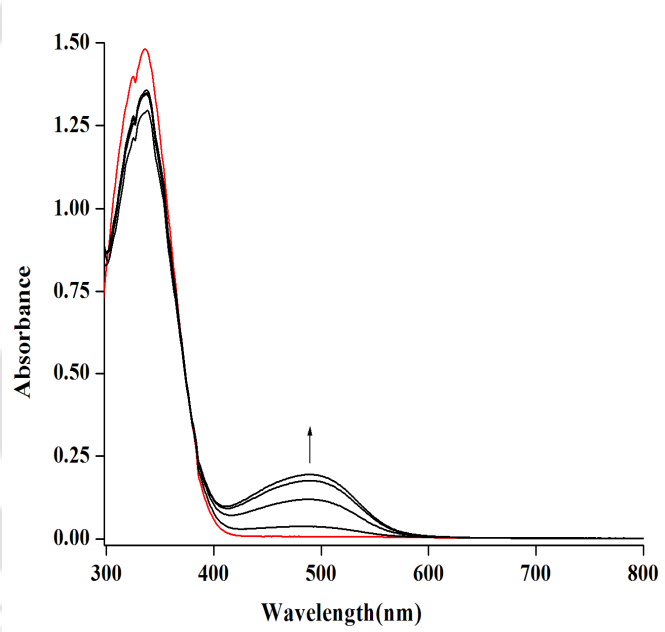

Figure A1.6: UV-visible spectra of **ANS** (red line) and after addition of NO (black lines) in aerobic condition in methanol medium.

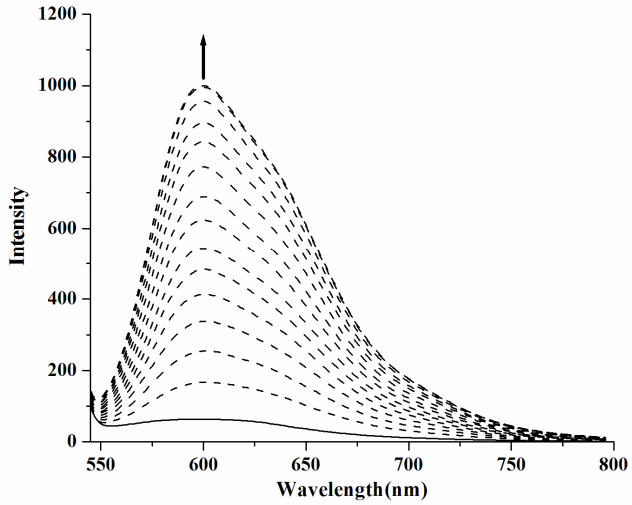

Figure A1.7: Fluorescence enhancement (λ_{ex}, 480 nm) of **ANS** before (solid line) and after addition of NO (dashed lines) in aerobic condition in aqueous medium.

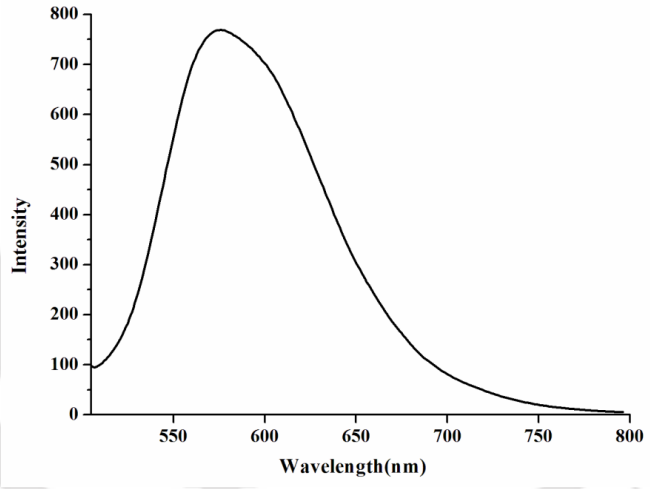

Figure A1.8: Fluorescence emission spectrum (λ_{ex}, 480 nm) of isolated **AZO-ANS** (20 µM) in methanol at 298 K.

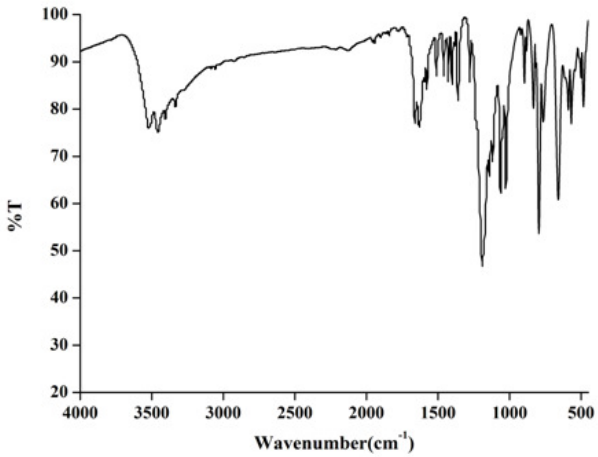

Figure A1.9: FT-IR spectrum of **AHS-OH** in KBr pellet.

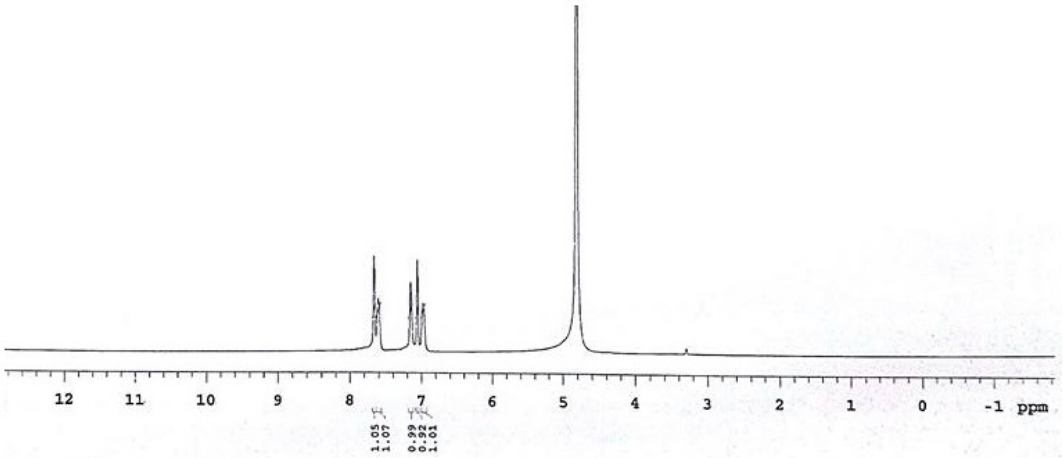

Figure A1.10: ^{1}H-NMR spectrum of **AHS-OH** in D_2O.

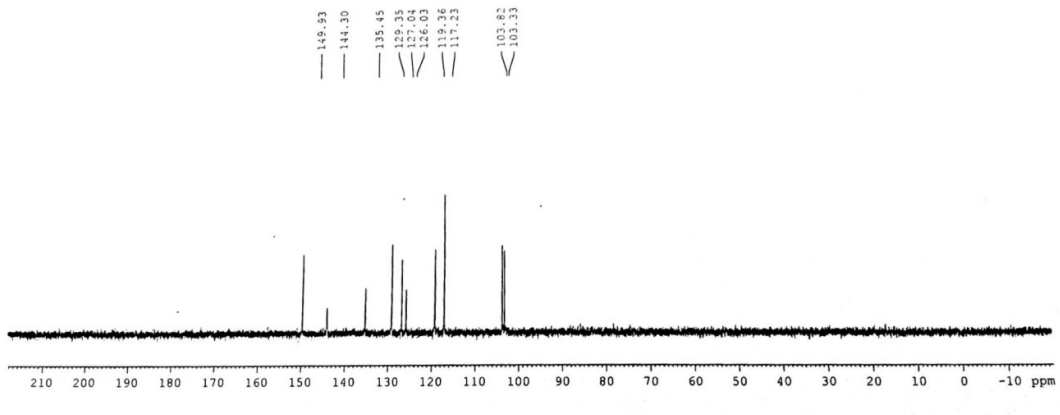

Figure A1.11: ^{13}C-NMR spectrum of **AHS-OH** in D_2O.

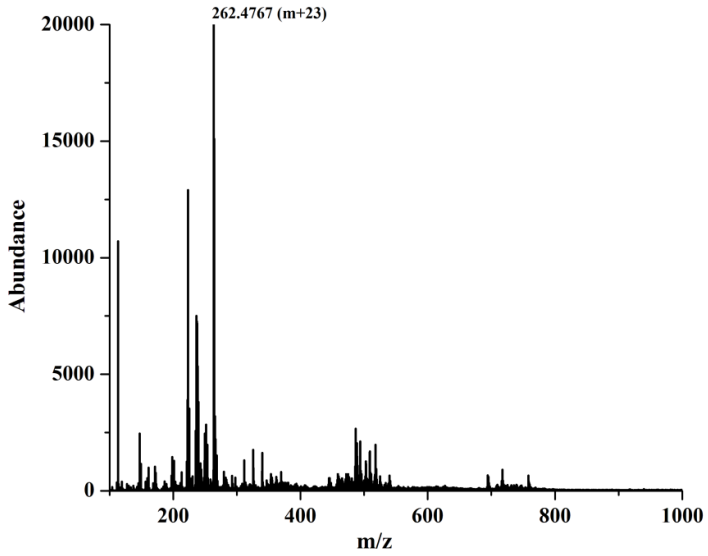

Figure A1.12: ESI-mass spectrum of **AHS-OH** in methanol**.**

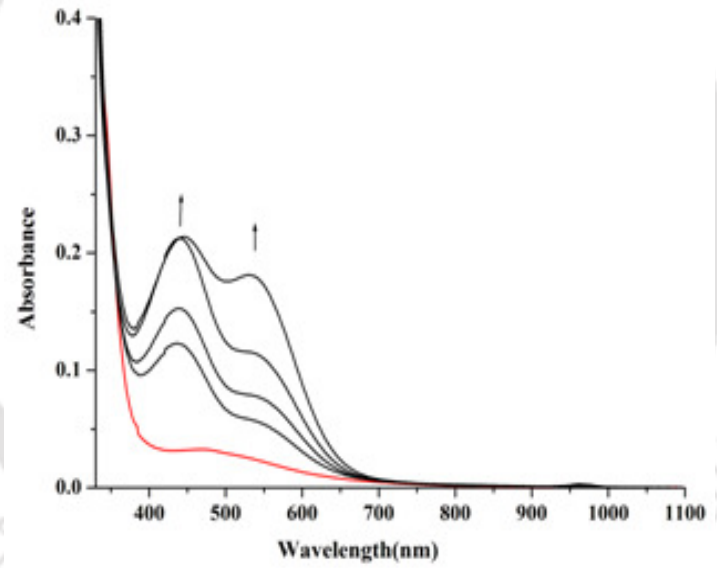

Figure A1.13: UV-visible spectra of **AHS** (red line) and after addition of NO (black lines) in aerobic condition in aqueous medium.

Appendix II

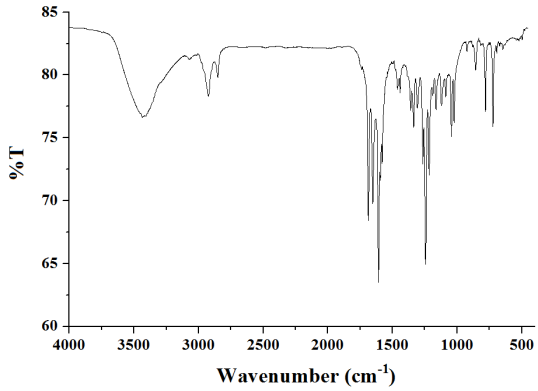

Figure A2.1: FT-IR spectrum of **AHNN** in KBr pellet.

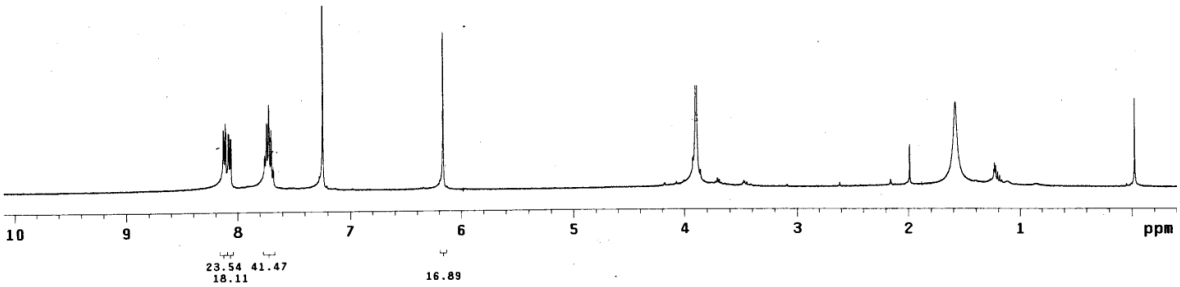

Figure A2.2: ^{1}H- NMR spectrum of **AHNN** in $CDCl_3$.

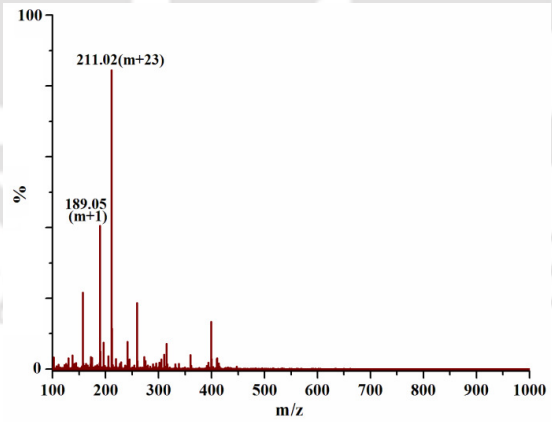

Figure A2.3: ESI-mass spectrum of **AHNN** in methanol.

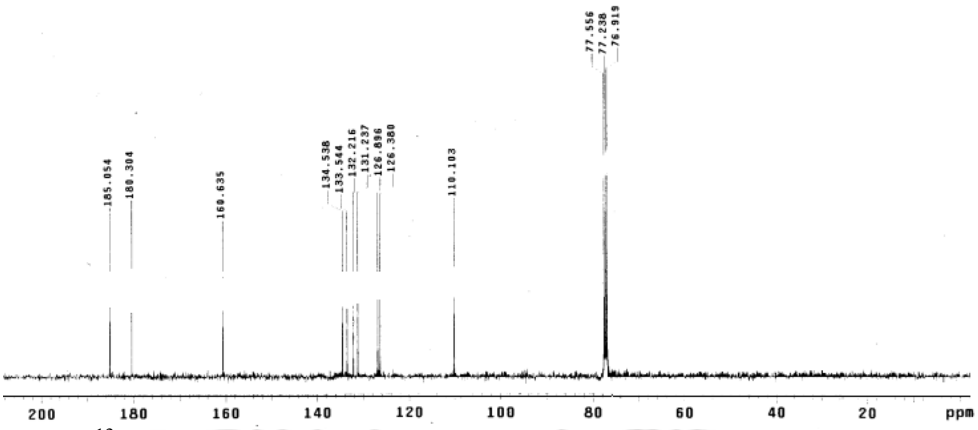

Figure A2.4: ^{13}C- NMR spectrum of **AHNN** in $CDCl_3$.

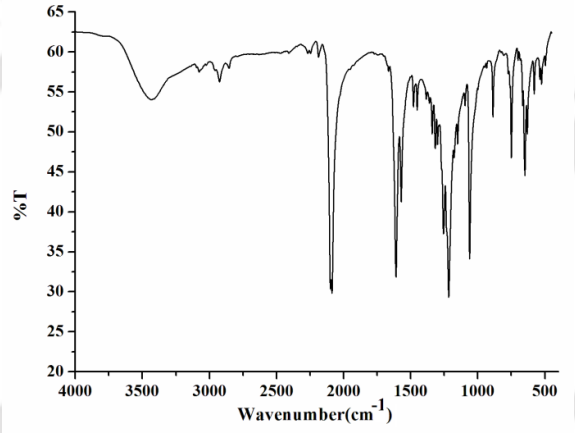

Figure A2.5: FT-IR spectrum of **NODS** in KBr pellet.

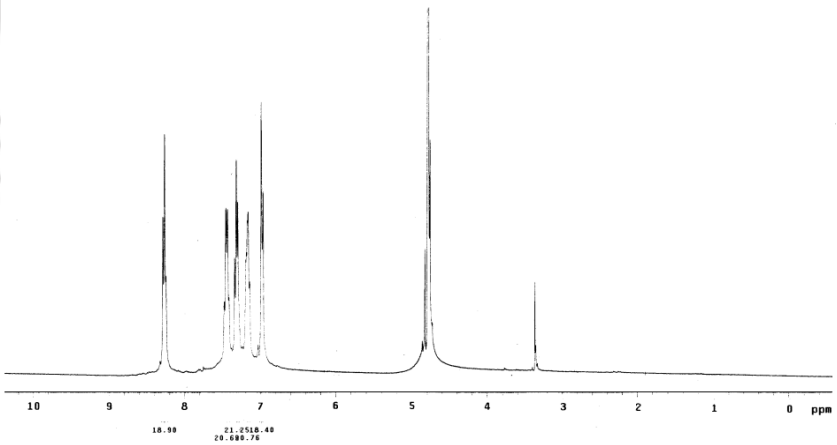

Figure A2.6: ^{1}H-NMR spectrum of **NODS** in D_2O.

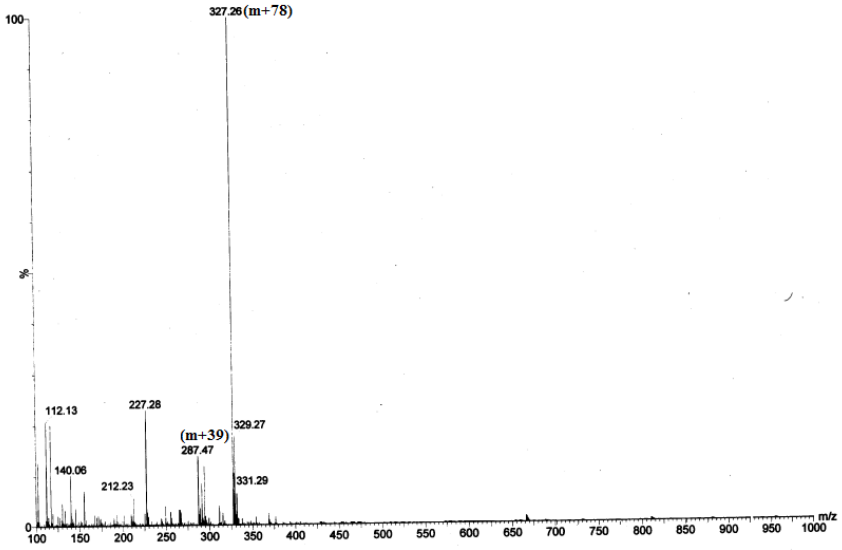

Figure A2.7: ESI-mass spectrum of **NODS** in methanol.

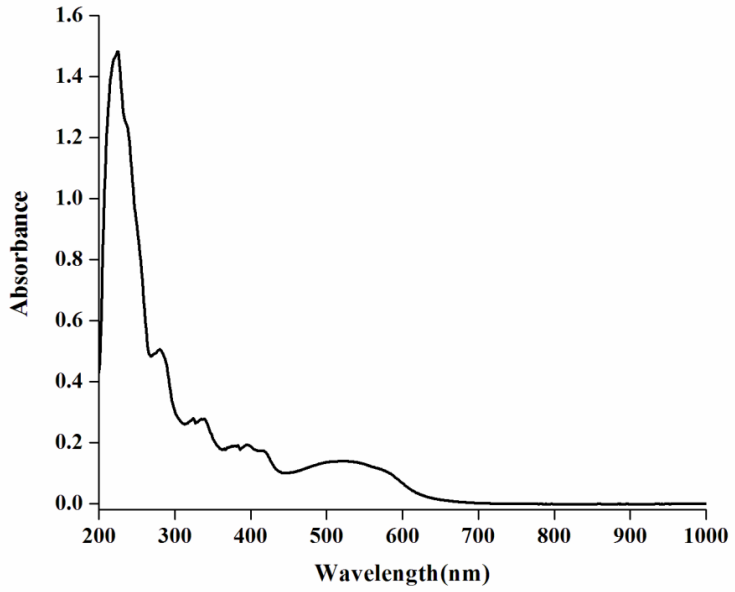

Figure A2.8: UV-visible spectrum of **NODS** in methanol.

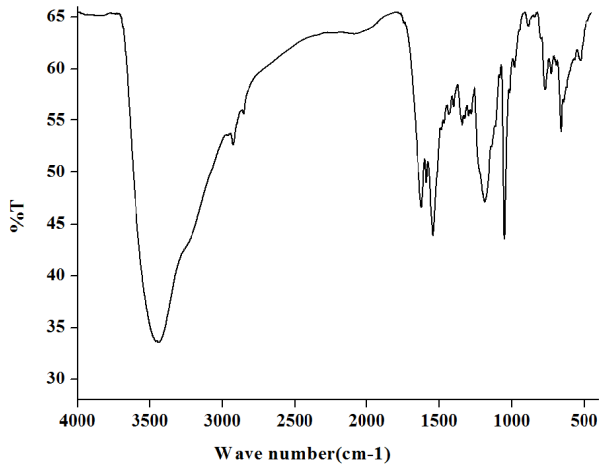

Figure A2.9: FT-IR spectrum of complex **3.1** in KBr pallet.

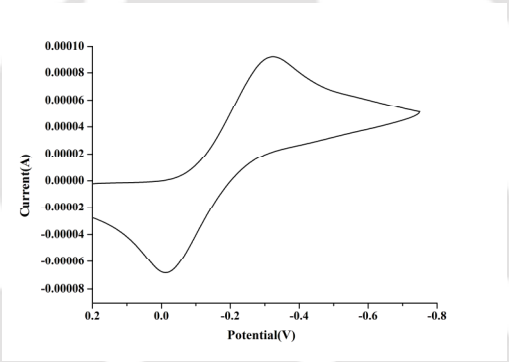

Figure A2.10: Cyclic voltammogram of the complex **3.1** in methanol with glassy carbon working electrode, Ag/Ag^{+} reference electrode, tetrabutyl ammonium perchlorate (TBAP) supporting electrolyte, scan rate; 05 v/s.

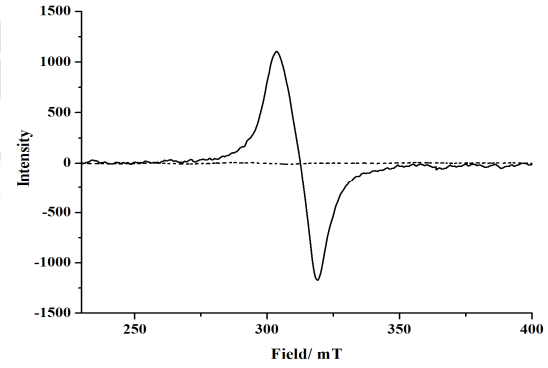

Figure A2.11: X-band EPR spectra of complex **3.1** before (solid line) and after purging NO (dotted line) in methanol.

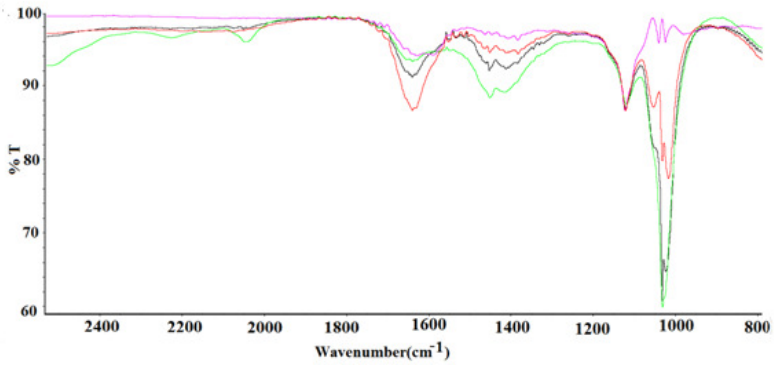

Figure A2.12: Solution FT-IR of [Cu^{II}-NO] complex. The band ~1650 cm^{-1} decays gradually with time indicating the unstable nature of the intermediate.

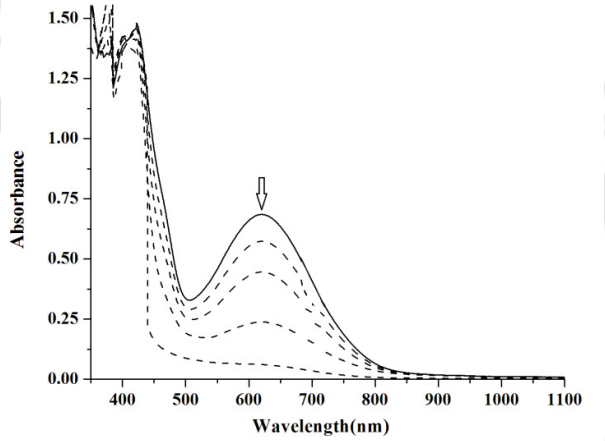

Figure A2.13: UV-visible spectra of intermediate [Cu^{II}-NO] intermediate (solid line) and it's decay (dashed lines) in methanol.

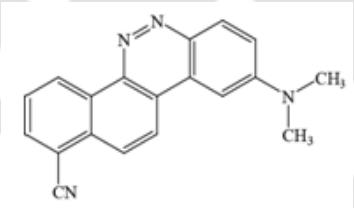

Figure A2.14: Structure of AZO_{550}.

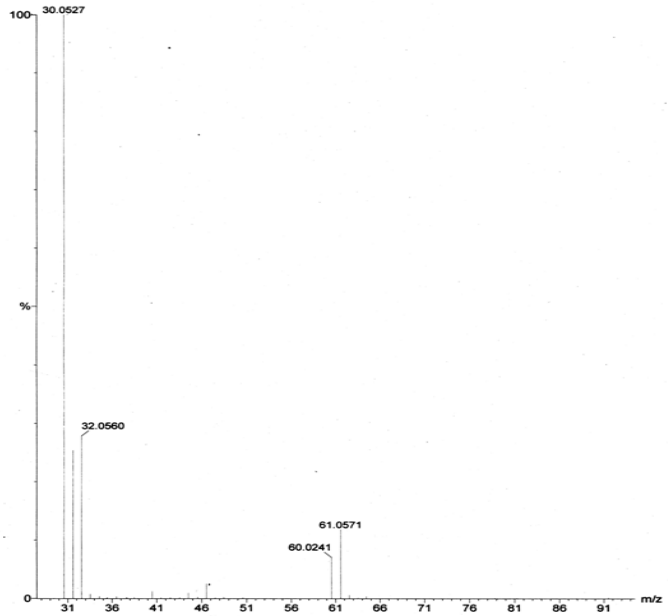

Figure A2.15: GC-mass spectrum of $MeNO_2$.

Appendix III

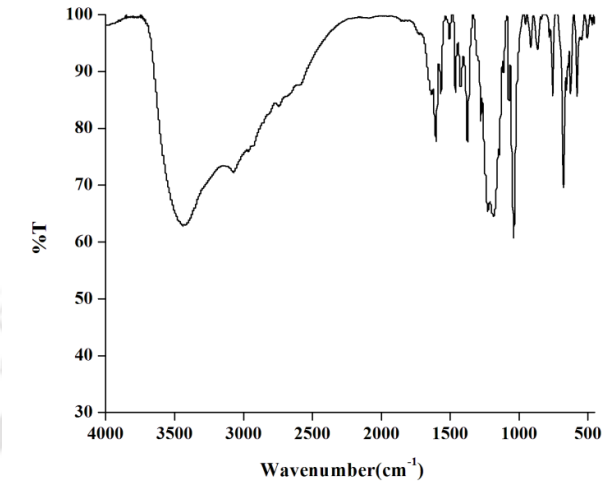

Figure A3.1: FT-IR spectrum of **HBNS** in KBr pellet.

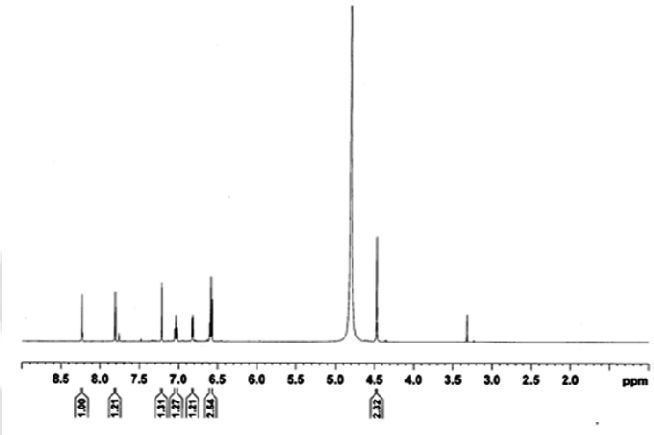

Figure A3.2: ^{1}H-NMR spectrum of **HBNS** in D_2O.

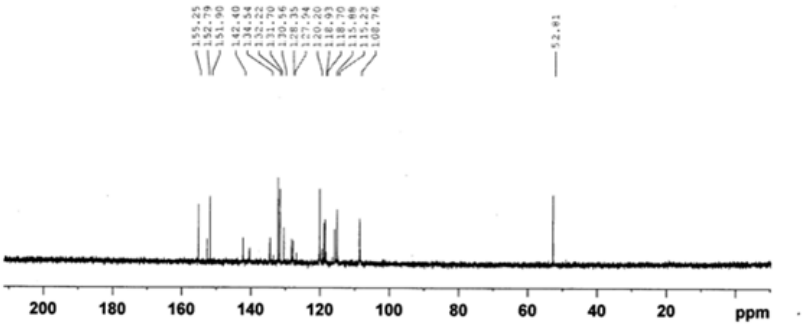

Figure A3.3: ^{13}C-NMR spectrum of **HBNS** in D_2O.

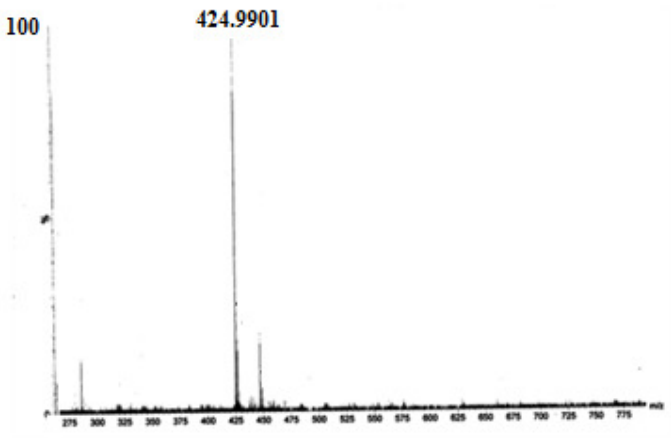

Figure A3.4: ESI-mass spectrum of **HBNS** in methanol.

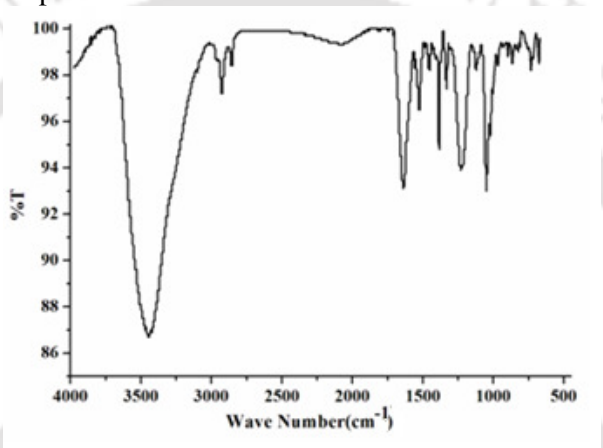

Figure A3.5: FT-IR spectrum of **HBNS-NO** in KBr pellet.

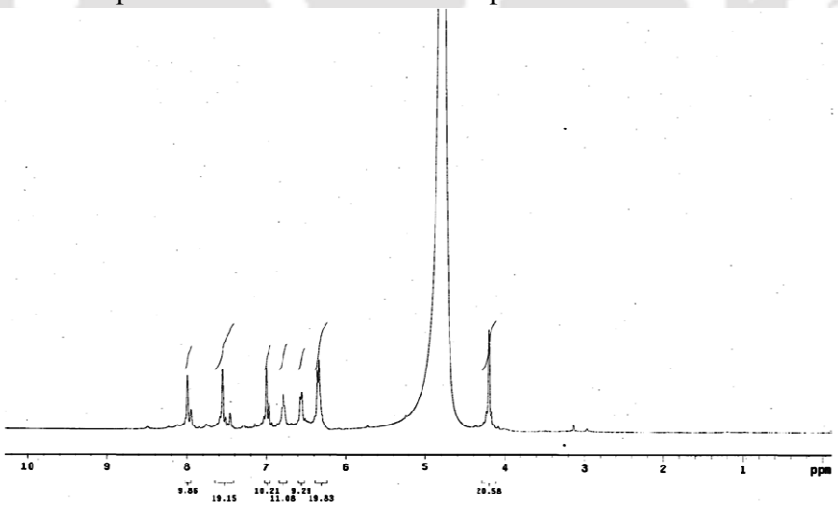

Figure A3.6: ^{1}H-NMR spectrum of **HBNS-NO** in D_2O.

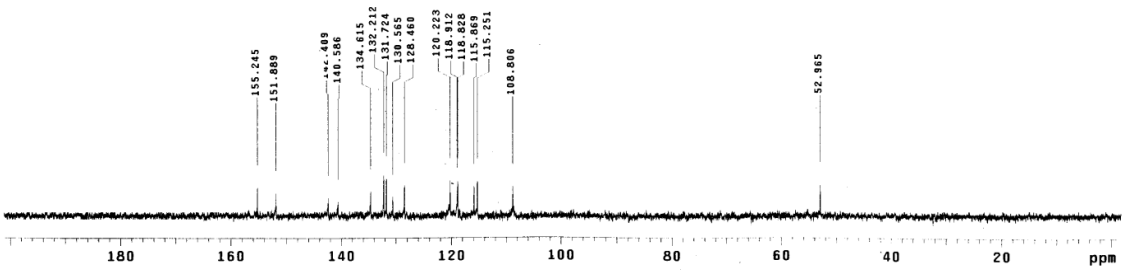

Figure A3.7: ^{13}C-NMR spectrum of **HBNS-NO** in D_2O.

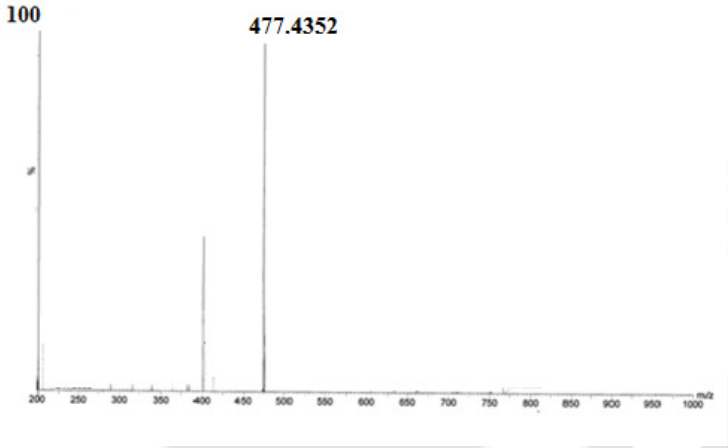

Figure A3.8: ESI-mass spectrum of **HBNS-NO** in methanol**.**

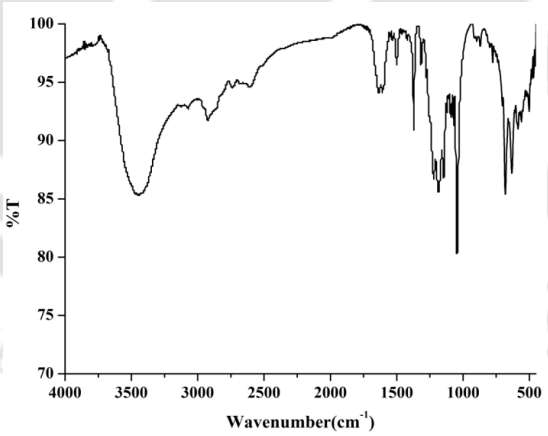

Figure A3.9: FT-IR spectrum of the complex **4.1** in KBr pellet.

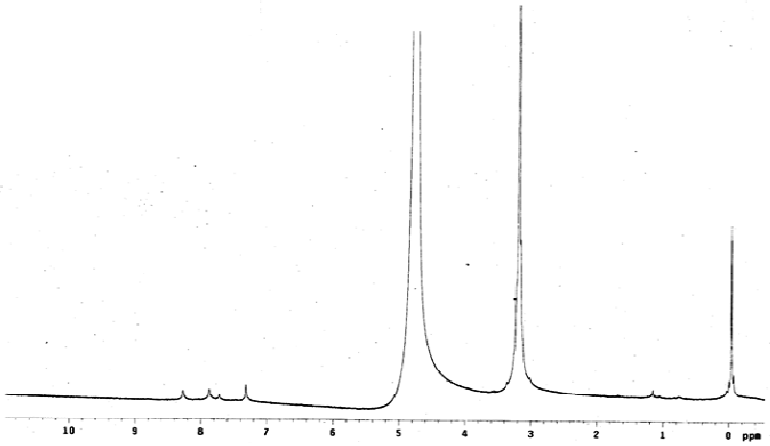

Figure A3.10: ^{1}H-NMR spectrum of Complex **4.1** in CD_3OD.

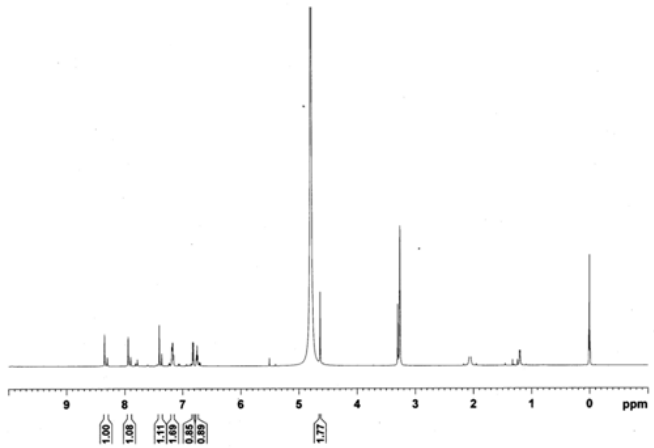

Figure A3.11: ^{1}H-NMR spectrum of Complex **4.1** after addition of NO in CD_3OD.

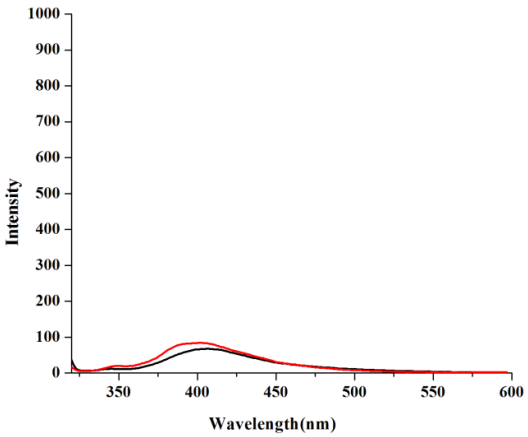

Figure A3.12: Fluorescence responses (λ_{ex}, 320 nm) of methanol solution of complex **4.1**(20 μM) before (red line) and after (black line) adding 5 equivalent of H_2O_2.

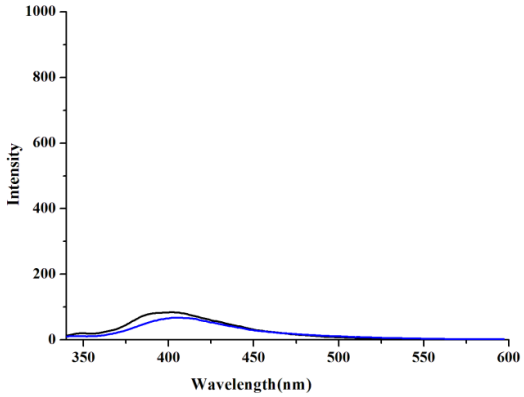

Figure A3.13: Fluorescence responses (λ_{ex}, 320 nm) of methanol solution of complex **4.1**(20 μM) before (black line) and after (blue line) adding 5 equivalent of $NaNO_2$.

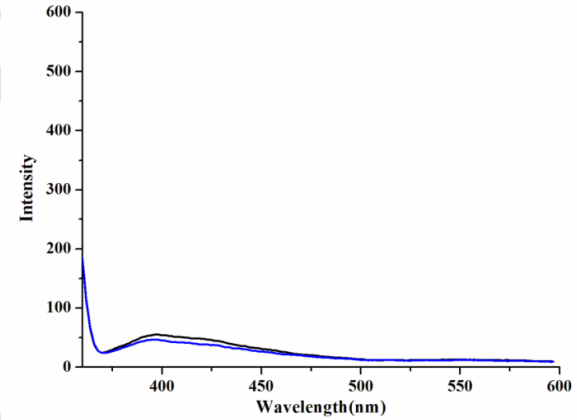

Figure A3.14: Fluorescence responses (λ_{ex}, 320 nm) of methanol solution of complex **4.1**(20 μM) before (black line) and after (blue line) adding 5 equivalent of $NaNO_3$.

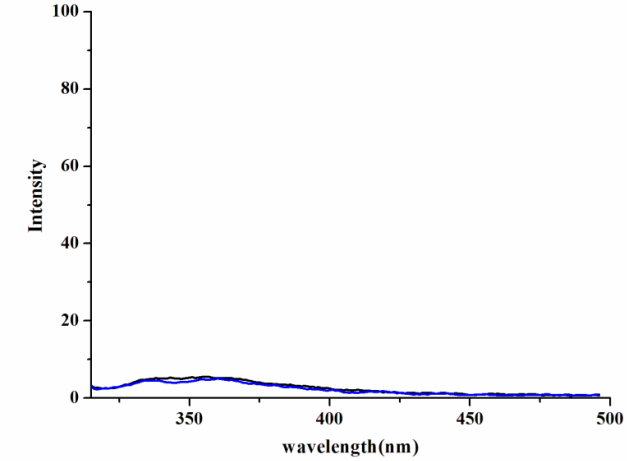

Figure A3.15: Fluorescence responses (λ_{ex}, 320 nm) of methanol solution of complex **4.1**(20 μM) before (black line) and after (blue line) adding 5 equivalent of NaOAc.

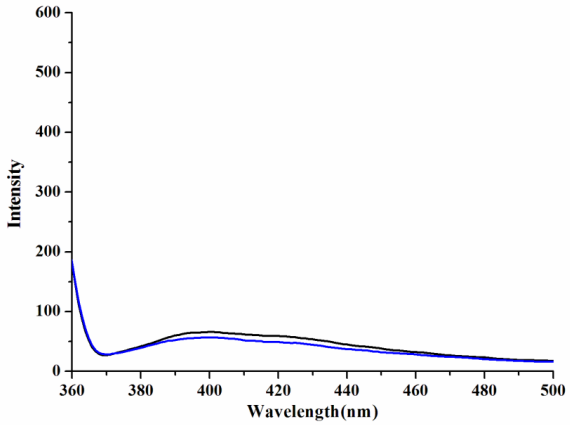

Figure A3.16: Fluorescence responses (λ_{ex}, 320 nm) of methanol solution of complex **4.1** (20 μM) before (black line) and after (blue line) adding 5 equivalent of NaCl.

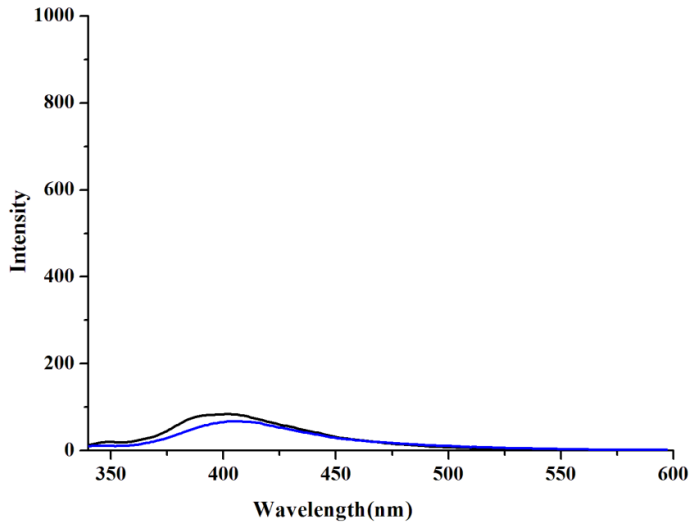

Figure A3.17: Fluorescence responses (λ_{ex}, 320 nm) of methanol solution of complex **4.1** (20μM) before (black line) and after (blue line) adding 5 equivalent of $NaClO_4$.

Appendix IV

Table S1: Crystallographic data of **PYAC**.

	PYAC
Formulae	$C_{24}H_{15}NO$
Mol. wt.	333.37
Crystal system	Orthorhombic
Space group	P 2_1 2_1 2_1
Temperature /K	293(2)
Wavelength /Å	0.71073
a /Å	23.5140(17)
b /Å	16.1378(17)
c /Å	4.3631(3)
α/°	90.00
β/°	90.00
γ/°	90.00
V/ Å^3	1655.64
Z	4
Density/Mgm^{-3}	1.337
Abs. Coeff. /mm^{-1}	0.082
Abs. correction	Multi-scan
F(000)	696
Total no. of reflections	2898
Reflections, $I > 2\sigma(I)$	1864
Max. 2θ/°	28.73
Ranges (h, k, l)	-18≤ h ≤ 27 -19≤ k ≤ 19 -4≤ l ≤ 5
Complete to 2θ (%)	0.9608
Refinement method	Full-matrix least-squares on F^2
Goof (F^2)	1.096
R indices [$I > 2\sigma(I)$]	0.0619
R indices (all data)	0. 0995

Table S2: Selected bond lengths (Å) and bond angles (°) of **PYAC**.

	Bond length (Å)		Bond angles (°)
C1-C17	1.448(5)	C(14)-C(1)-C(2)	118.2(3)
C17-C18	1.341(6)	C(1)-C(17)-C(18)	127.1(4)
C18-C19	1.459(6)	O(1)- C(19)- C(18)	122.5(4)
C19-O1	1.233(5)	C(22)-C(21)-C(20)	118.3(4)
C20-N1	1.341(6)	C(20)-N(1)-C(24)	117.3(4)
N1-C24	1.333(6)	C(24)-C(23)-C(22)	119.8(4)

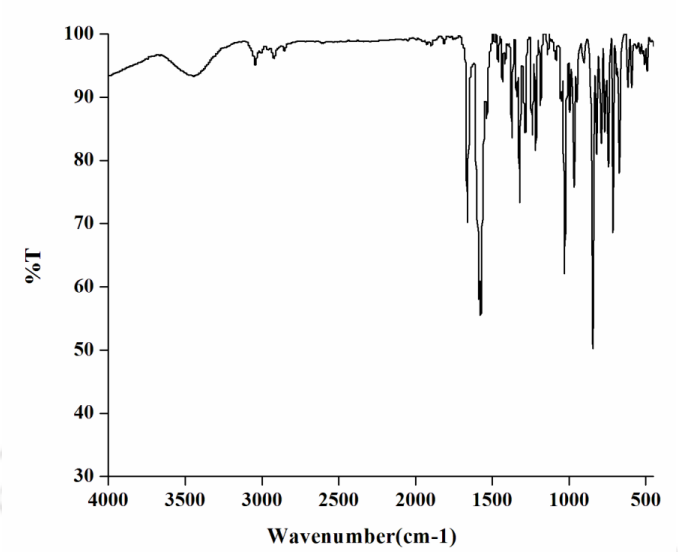

Figure A4.1: FT-IR spectrum of **PYAC** in KBr pellet.

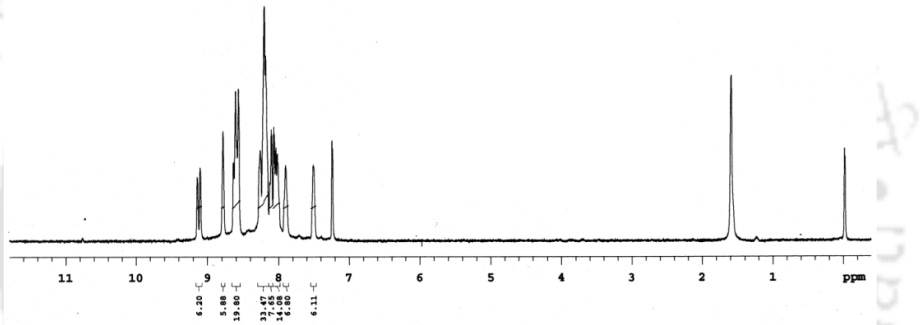

Figure A4.2: ^{1}H- NMR spectrum of **PYAC** in $CDCl_3$.

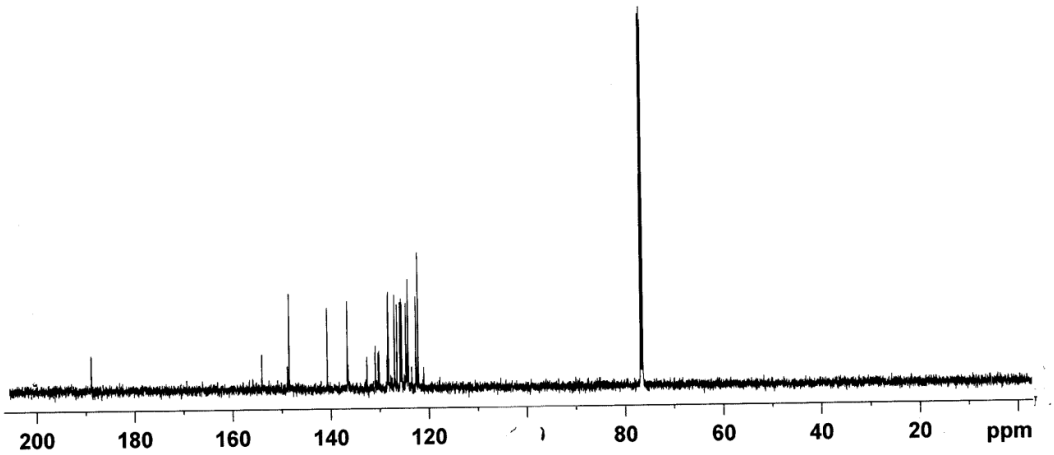

Figure A4.3: ^{13}C-NMR spectrum of **PYAC** in $CDCl_3$.

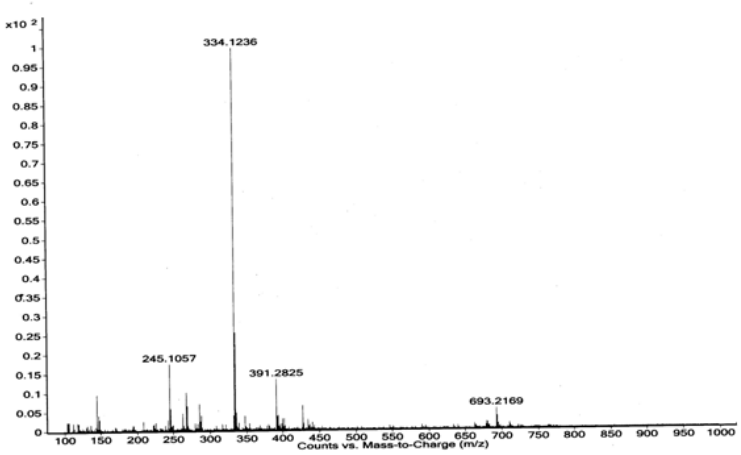

Figure A4.4: ESI-mass spectrum of **PYAC** in methanol**.**

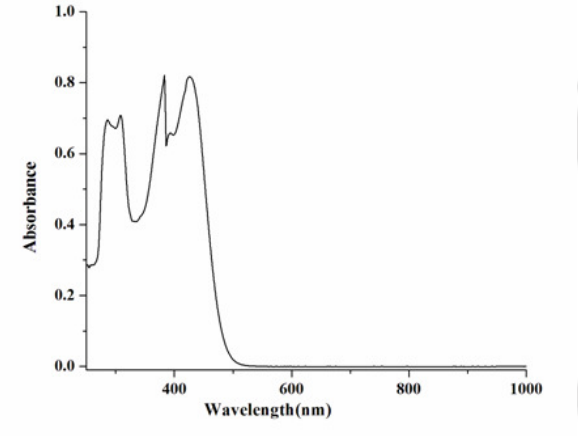

Figure A4.5: UV-visible spectrum of **PYAC** in acetonitrile.

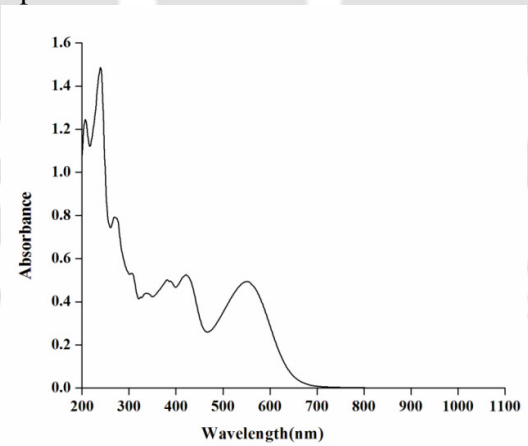

Figure A4.6: UV-visible spectrum of complex **5.1** in acetonitrile.

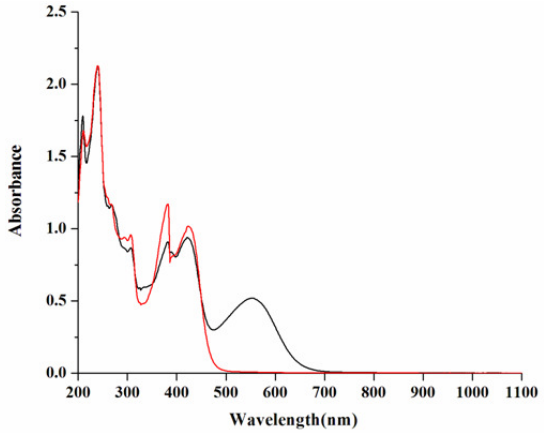

Figure A4.7: UV-visible spectra of complex **5.1**(black line) and after addition of 0.5 equivalent of $NaNO_2$ (red line) in acetonitrile.

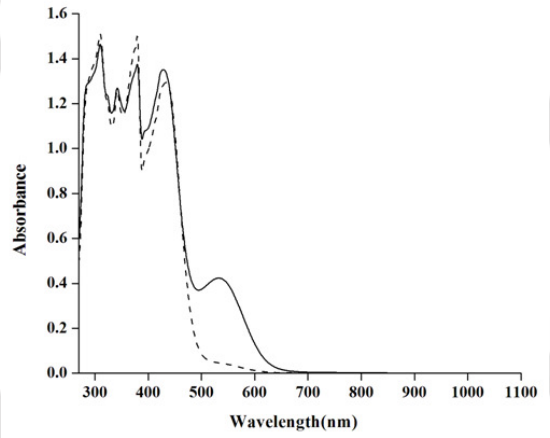

Figure A4.8: UV-visible spectra of complex **5.1** (solid line) and after addition of 0.5 equivalent of $NaNO_2$ (dashed line) in methanol/water.

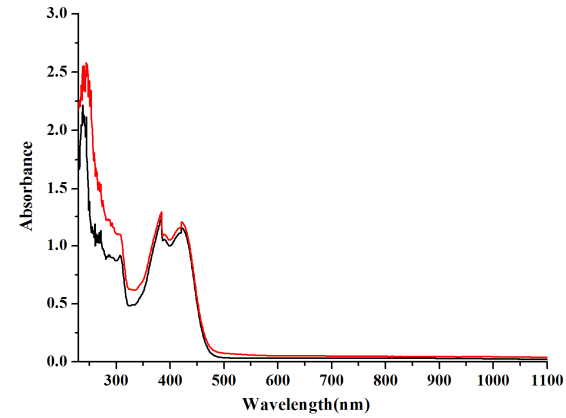

Figure A4.9: UV-visible spectra of **PYAC** (black line) and after addition of 1equivalent of $[Cu(CH_3CN)_4]ClO_4$ (red line) in acetonitrile.

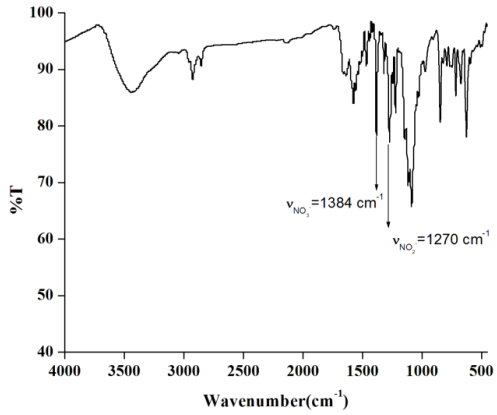

Figure A4.10: FT-IR spectrum of complex **5.1** after reaction with 1equivalent of $NaNO_2$ in acetonitrile in KBr pellet.

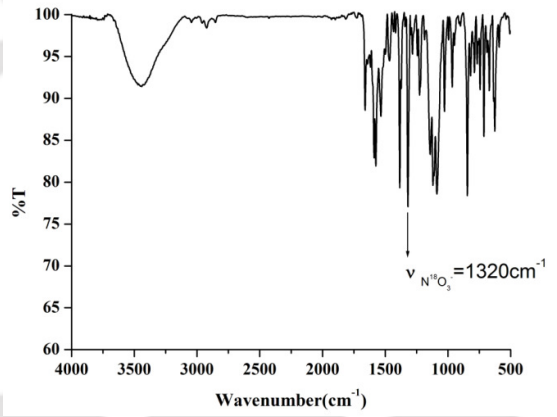

Figure A4.11: FT-IR spectrum of complex **5.1** after reaction with $NaNO_2$ in (H_2O^{18}) in KBr pellet.

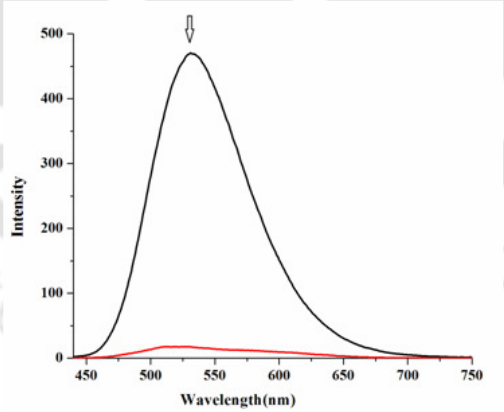

Figure A4.12: Fluorescence responses ($\lambda_{ex,}$ 425 nm) for 20 μM solution of free **PYAC** (black line) and after addition of 20 μM $Cu(ClO_4)_2.6H_2O$ (red line) in acetonitrile.

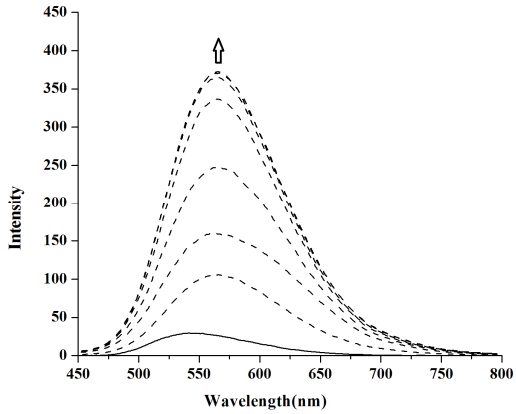

Figure A4.13: Fluorescence enhancement ($\lambda_{ex,}$ 425 nm) by addition of $NaNO_2$ (0.5eq) with 10 µM complex **5.1** in acetonitrile.

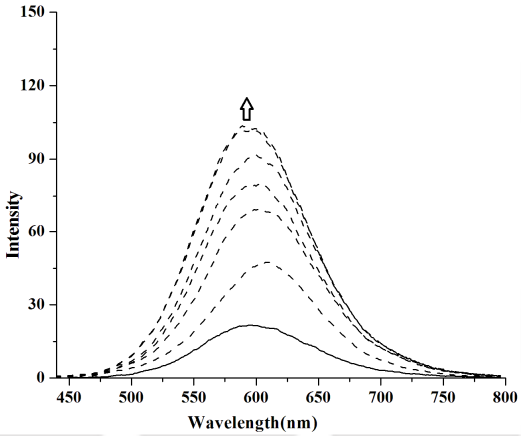

Figure A4.14: Fluorescence enhancement (λ_{ex} 425 nm) by addition of $NaNO_2$ (0.5eq) with 10 µM complex **5.1** in methanol/water.

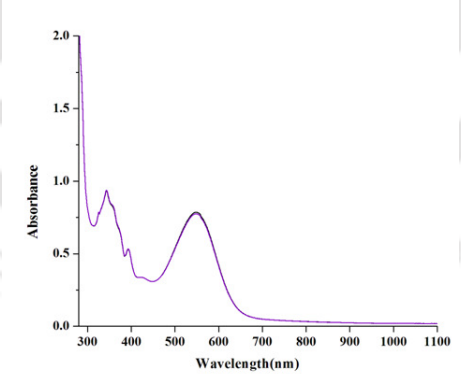

Figure A4.15: UV-visible spectra of complex **5.1** with addition of 1 equivalent of $NaNO_3$ in acetonitrile.

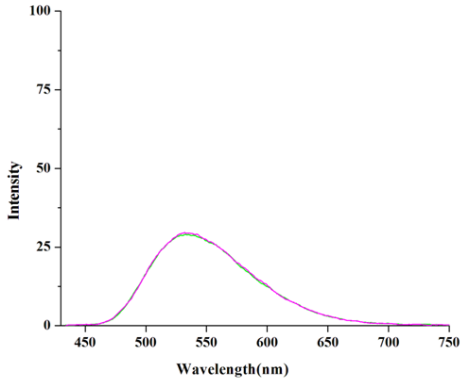

Figure A4.16: Fluorescence enhancement of the complex **5.1** after addition of 1 equivalent $NaNO_3$ in acetonitrile (λ_{ex} 425nm).

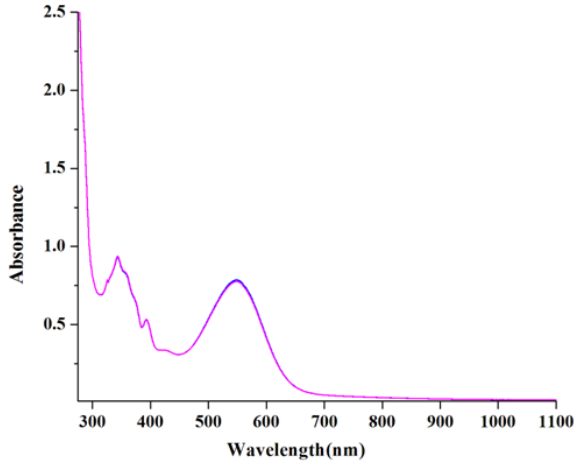

Figure A4.17: UV-visible spectra of complex **5.1** after addition of 1 equivalent of Na_2SO_4 in acetonitrile.

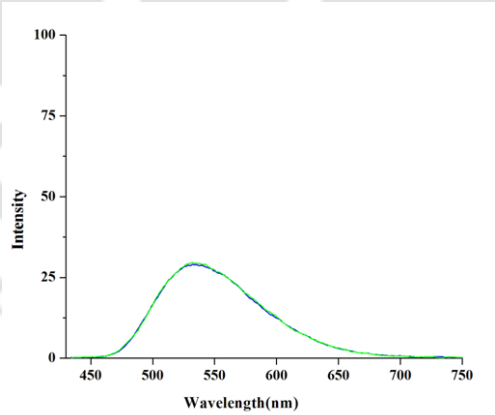

Figure A4.18: Fluorescence enhancement of complex **5.1** after addition of 1 equivalent Na_2SO_4 in acetonitrile (λ_{ex} 425nm).

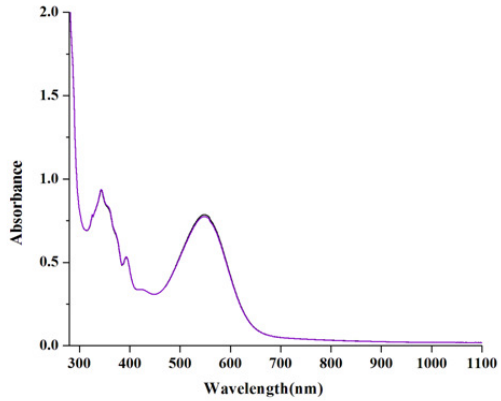

Figure A4.19: UV-visible spectra of complex **5.1** after addition of 1 equivalent of KH_2PO_4 in acetonitrile.

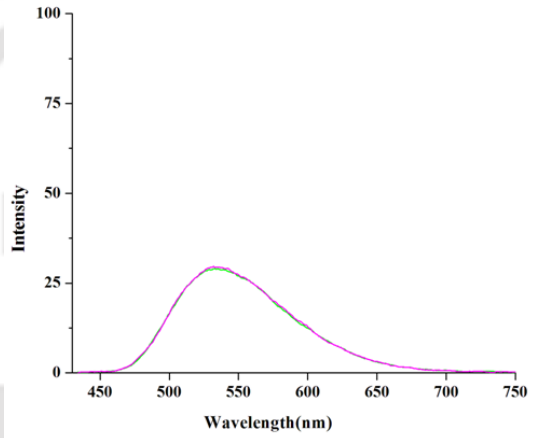

Figure A4.20: Fluorescence enhancement of complex **5.1** after addition of 1 equivalent KH_2PO_4 in acetonitrile (λ_{ex} 425nm).

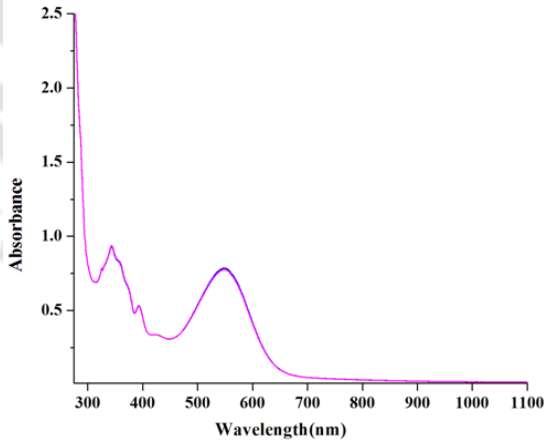

Figure A4.21: UV-visible spectra of complex **5.1** after addition of 1 equivalent of Na_2CO_3 in acetonitrile.

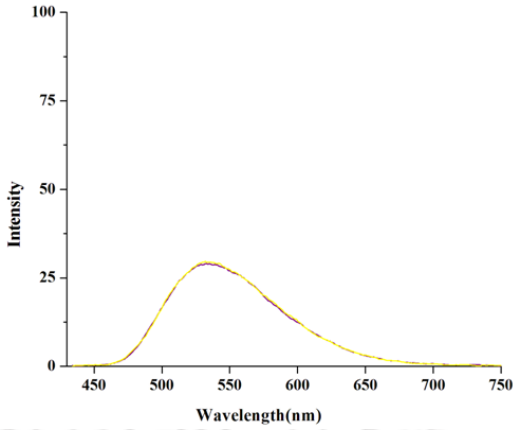

Figure A4.22: Fluorescence enhancement of the complex **5.1** after addition of Na_2CO_3in acetonitrile (λ_{ex} 425nm).

List of Publications

1. **Aromatic C-nitrosation by a copper(II)-nitrosyl complex**
   Rout, **K**.**C**.; Mondal, B. *Dalton Trans.* **2015**, *44*, 1829.

2. **Copper(II) complex as a selective turn on fluorosensor for nitric oxide and its intracellular application**
   Rout, **K**.**C**.; Mondal, B. *Inorg. Chim. Acta* **2015**, *xx*, xxxx.

3. **Copper(II) complex as selective turn-on fluorescent probe for nitrite ion**
   Rout, **K**.**C**.; Mondal, B. *Inorg. Chim. Acta* (under revision).

4. **Selective chromogenic and fluorogenic probe for nitric oxide from dark background**
   Rout, **K**.**C**.; Mondal, B. (Communicated).